

## Evolution of hot corinos and organics in Solar-type protostars

E. Bianchi<sup>1</sup>, C. Ceccarelli<sup>1, 2</sup>, C. Codella<sup>3, 1</sup>, B. Lefloch<sup>1, 2</sup>

<sup>1</sup>*Univ. Grenoble Alpes, IPAG, F-38000 Grenoble, France*

<sup>2</sup>*CNRS, IPAG, F-38000 Grenoble, France*

<sup>2</sup>*INAF-Osservatorio Astrofisico di Arcetri, L.go E. Fermi 5, 50125 Firenze, Italy*

The measurement of the abundance of both deuterated molecules and interstellar Complex Organic Molecules (iCOMs; C-bearing molecules containing at least six atoms) is a crucial step in understanding the possible formation of pre-biotic molecules in the interstellar medium and their delivery onto planetary systems around Sun-like stars. In addition, the deuterium fractionation can be used as fossil record of the physical conditions at the moment of the icy water and organics formation. Hot corinos are the typical laboratories where to study both iCOMs and deuterium fractionation. Indeed hot corinos are the inner 100 au envelopes around Sun-like protostars which are heated at temperatures larger than 100 K and where the dust mantles products enrich the gas chemical composition and trigger subsequent chemical gas-phase reactions.

In this talk, observations of iCOMs and deuterated species in Class 0 and Class I hot corinos will be presented. They are obtained using single-dish telescopes as the IRAM-30m as well as the new generation interferometers NOEMA and ALMA, in the framework of the large programs ASAI [1], SOLIS [2] and FAUST (PI:Yamamoto). The current observations contribute to fill in the gap between prestellar cores and protoplanetary disks, showing how the gas chemical content is modified during the early evolutionary stages of Sun-like star forming regions [3, 4]. In order to understand the possible heritage of iCOMs in our Solar System, the measurements are also compared to the recent observations of cometary material. Finally, iCOMs observations on Solar System spatial scales provide a precious tool to probe also the kinematics of the inner protostellar jet/disk system, tracing the interface between the infalling envelope and the self-gravitating rotating disk.

### References

- [1] Lefloch B., Bachiller R., Ceccarelli C., et al., 2018, MNRAS, 477, 4792
- [2] Ceccarelli C., Caselli P., Fontani F., et al., 2017, ApJ, 850, 176
- [3] Bianchi E., Codella C., Ceccarelli C., et al., 2017, MNRAS, 467, 3011
- [4] Bianchi E., Codella C., Ceccarelli C., et al., 2018, MNRAS, in press.

## Innermost Envelope Structure of B335 Traced by Complex Organic Molecules

M. Imai<sup>1</sup>, Y. Oya<sup>1</sup>, N. Sakai<sup>2</sup>, A. López-Sepulcre<sup>3</sup>, Y. Watanabe<sup>4</sup>, and S. Yamamoto<sup>1</sup>

<sup>1</sup>Department of Physics, University of Tokyo, Japan

<sup>2</sup>The Institute of Physical and Chemical Research, Japan

<sup>3</sup>Universite de Grenoble Alpes, IPAG, France

<sup>4</sup>Division of Physics, University of Tsukuba, Japan

B335 is an isolated low-mass protostellar source (Class 0) without influences of other star-forming regions. We have been studying the chemical characteristics of this source as a testbed of chemical evolution of a protostellar core. With ALMA, we found a hot corino in the closest vicinity ( $r \sim 10$  au) of the protostar by detecting various complex organic molecules (COMs) such as  $\text{HCOOCH}_3$  and  $\text{CH}_3\text{OCH}_3$ . B335 also shows an association of abundant carbon-chain molecules at a larger ( $r \sim 1000$  au) scale, which is a typical feature of warm carbon-chain chemistry (WCCC). Thus B335 has a hybrid (hot corino chemistry and WCCC) chemical character[1].

Recently, we explored the structure of the innermost envelope of this source, where hot corino chemistry is seen, at an angular resolution of  $0.1''$  (10 au) with ALMA. Using the emission lines of COMs, a very tiny rotation structure is resolved in this source for the first time. The radius of the centrifugal barrier is estimated to be 3 au, which is smaller by more than an order of magnitude than those of other protostellar sources. This result shows that the COM lines can be used as a powerful tracer of the closest vicinity of the protostar without influences of surrounding gas. Interestingly, the direction of the velocity gradient is different among molecular species (Figure 1). This feature is explained as rotating motion with infall motion rather than the Keplerian motion. The different velocity gradient may reflect the different distribution of COMs at a few au scale.

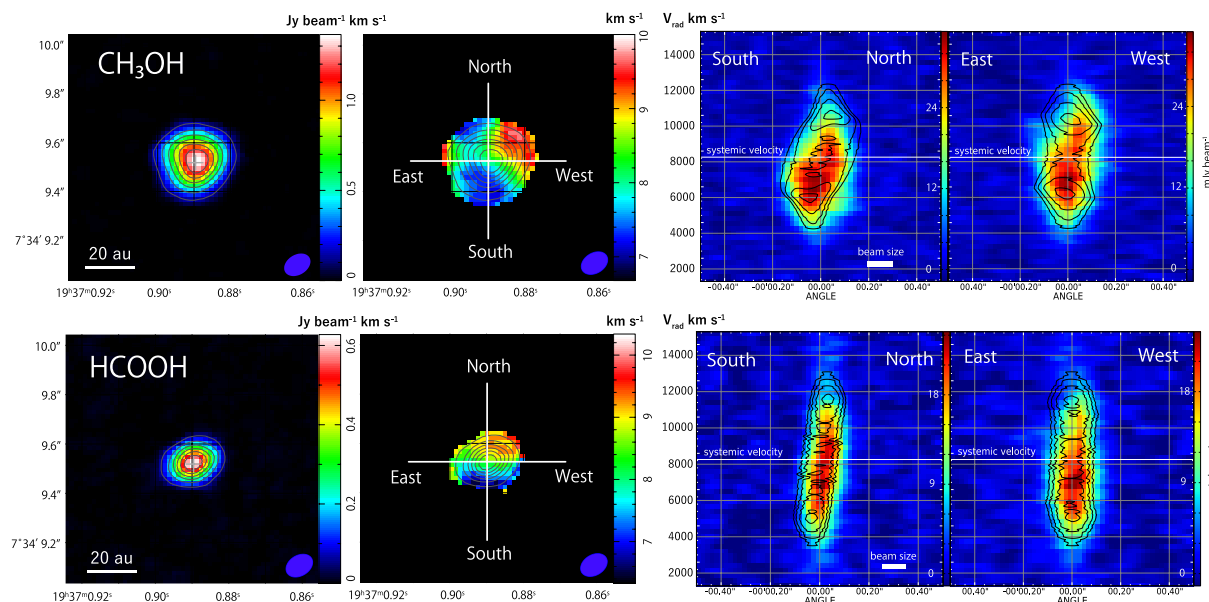


Figure 1: (left two panels) The moment 0 maps (left) and the moment 1 maps (right) of the  $\text{CH}_3\text{OH}$  and  $\text{HCOOH}$  emission. (right two panels) PV diagrams along the south-north (disk) and east-west directions, where the results of the infalling and rotating envelope model are overlaid in contours.

## References

- [1] M. Imai, N. Sakai, Y. Oya, et al. 2016, ApJ, 830, L37

## Elias 29: a Class I Low-Mass Protostellar Source Rich in S-bearing Species

Y. Oya,<sup>1</sup> N. Sakai,<sup>2</sup> A. López-Sepulcre,<sup>3</sup> C. Ceccarelli,<sup>3</sup> B. Lefloch,<sup>3</sup> and S. Yamamoto<sup>1</sup>

<sup>1</sup>*Department of Physics, The University of Tokyo, Japan*

<sup>2</sup>*RIKEN Cluster for Pioneering Research, Japan*

<sup>3</sup>*Université Grenoble Alpes, IPAG, France*

In the star-formation process, the chemical evolution from the interstellar space to planets is of interest as well as the physical evolution. So far, the chemical composition of the envelope gas is known to show significant diversity among sources; two distinct cases are hot corinos rich in saturated complex organic molecules (COMs) and warm carbon-chain chemistry (WCCC) sources rich in unsaturated carbon-chain molecules [1]. However, it is still important to study chemical compositions of low-mass protostellar sources under various environmental conditions in order to reveal a whole picture of chemical diversity.

Elias 29 (WL15) is a Class I low-mass protostellar source in the L1688 dark cloud in Ophiuchus. It is known to be strongly irradiated by the nearby bright star HD147889. We observed Elias 29 in the CS, SO, SO<sub>2</sub>, SiO, COM, and carbon-chain molecular lines with ALMA (Cycle 2). We found that both of COMs and carbon-chain molecules are faint. CS is also faint around the protostar, while it traces a southern ridge apart from the protostar. On the other hand, the SO and SO<sub>2</sub> lines are bright near the protostar, and show a velocity gradient perpendicular to the outflow blowing along the east-west direction [2]. This velocity gradient likely represents the rotation motion around the protostar (Fig. 1).

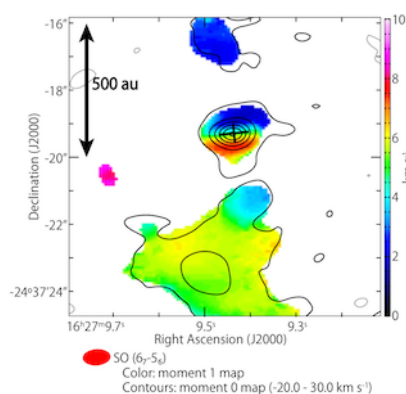


Figure 1: Moment 1 map of the SO line (6<sub>7</sub>-5<sub>6</sub>). SO traces the rotating motion around the protostar shown by a black cross.

The chemical characteristics of Elias 29 is quite peculiar; only the SO and SO<sub>2</sub> lines are prominent.

This can be explained qualitatively by the relatively high dust temperature (~20 K; [3]) of the parent core of Elias 29 caused by strong external irradiation. For this reason, CO does not deplete onto dust grains, which prevents formation of COMs on dust grains. Similarly, the S atom does not deplete onto dust grain, either, and is subject to the gas phase reaction to form SO and SO<sub>2</sub>.

So far, hot corino chemistry and WCCC provide an apparent 'axis' of chemical diversity, which would be caused by the different duration time of the starless core phase. However, the above result suggests that sulfur chemistry can be another important 'axis' of the diversity caused by the different temperature condition. More systematic studies are awaited.

### References

- [1] Sakai, N., & Yamamoto, S. 2013, *Chemical Reviews*, 113, 8981
- [2] Ceccarelli, C., Boogert, A.C.A., Tielens, A.G.G.M., et al. 2002, *A&A*, 395, 863
- [3] Rocha, W.R.M., & Pilling, S. 2018, *MNRAS*, 478, 5190

## Feeding the young protoplanetary disk: cold gas flows to the young disks

D. Harsono<sup>1</sup>, A. Hacar<sup>1</sup>, N. M. Murillo<sup>1</sup>, M. Persson<sup>2</sup>, M. L. R. van 't Hoff<sup>1</sup>, J. J. Tobin<sup>3</sup>,  
M. N. Drozdovskaya<sup>4</sup>, C. Walsh<sup>5</sup>, J. K. Jørgensen<sup>6</sup>, E. F. van Dishoeck<sup>1,7</sup>, C. Brinch<sup>8</sup>

<sup>1</sup> *Leiden Observatory, Leiden University, The Netherlands*

<sup>2</sup> *Chalmers University of Technology, Sweden*

<sup>3</sup> *National Radio Astronomy Observatory, Virginia, U. S. A.*

<sup>4</sup> *Center for Space and Habitability, University of Bern, Switzerland*

<sup>5</sup> *School of Physics and Astronomy, University of Leeds, U. K.*

<sup>6</sup> *StarPlan & Niels Bohr Institute, University of Copenhagen, Denmark*

<sup>7</sup> *Max-Planck-Institut für extraterrestrische Physik, Garching, Germany*

<sup>8</sup> *National Food Institute, Technical University of Denmark, Denmark*

Stars and protoplanetary disks form out of collapsing cold and dense cores. In the earliest stages of star formation, the infalling protostellar envelope is still feeding the growing accretion disk. The paths of the infalling gas and dust determine the pristinity of the material that will be inherited by the protoplanetary disk [1, 2]. Passively heated protostellar envelopes tend to be too cold for CO gas to be an efficient tracer of the infalling velocity structure. Therefore, cold gas tracers such as DCO<sup>+</sup>, N<sub>2</sub>H<sup>+</sup>, N<sub>2</sub>D<sup>+</sup> and DCN reveal the infalling structure [3]. While hot molecular lines can trace the shocked gas on disk surfaces, cold gas lines trace the infalling flow that feeds into the cold outer part of young disks. These molecular lines were observed with ALMA toward two Class I protostars to unravel the kinematics in the vicinity of the young protoplanetary disks. I will present our results on the cold gas inventory and kinematics of these systems. The combination of radiative transfer and chemical models [3,4] are used to study the cold physico-chemical structure at the disk-envelope interface. These data will eventually reveal whether or not pristine material is inherited by the planet-forming disks.

### References

- [1] Pontoppidan et al. 2014, PPVI
- [2] Drozdovskaya et al. 2014, MNRAS 445, 913
- [3] Murillo et al. 2015, A&A 579, 114
- [4] van 't Hoff et al. 2017, A&A 599, 101

# A Hungry Baby Star Eating a Space Hamburger and Spitting Spinning Bullets

Chin-Fei Lee<sup>1</sup>

<sup>1</sup>*ASIAA/NTU, Taiwan*

Please use this layout (Times New Roman 12 pt font size and single line spacing (12 pt) as given above for the title, authors (underline the name of the author presenting the contribution) and institution.

The forming process of Sun-like stars in the early phase is still not well understood. In particular, how the central protostars (baby stars) being fed is unclear. In addition, supersonic jets are often seen emanating from the central baby stars, but their role in star formation is still under debate. With the unprecedented power of the Atacama Large Millimeter/submillimeter Array (ALMA), the largest ground-based radio telescope ever built, we now start to unveil the mystery of star formation in the early phase. Recently, we have observed a very young nearby protostellar system HH 212 at unprecedented angular resolution and sensitivity with ALMA. We have resolved its accretion disk and supersonic jet for the first time in star formation. The disk is resolved for the first time in the vertical direction, showing a dark lane sandwiched between two bright features, appearing as a hamburger in space. More importantly, the structure and physical properties of the disk can be used to set the strong constraints on current accretion disk model for the feeding process. The jet is highly collimated and consists of a train of fast-moving bullets ejected from the innermost part of the disk. Interestingly, the bullets are found to be spinning convincingly for the first time. Therefore, the jet can indeed carry away the excess angular momentum from the innermost disk, allowing the disk material there to feed the central baby stars. In summary, our ALMA observations have unveiled for the first time the detailed growing process of a hungry baby star in the early phase, showing it spitting a chain of spinning bullets when eating a space hamburger.

## New Approaches to Large Molecular Synthesis in the Interstellar Medium

E. Herbst<sup>1</sup>

<sup>1</sup>*Departments of Chemistry and Astronomy, University of Virginia, USA*

Organic molecules with six or more atoms have been observed in many regions of space, in particular in the so-called interstellar medium (ISM), which consists mainly of clouds of gas and dust, parts of which are collapsing to form new generations of stars and planets. These organic molecules come in three groups: (1) so-called carbon-chain species, which are very unsaturated (hydrogen-poor) molecules with a linear or near linear structure; (2) COMs (complex organic molecules), which are more standard molecules, often found in an organic laboratory in the form of liquids, whereas they are found in space in their gaseous forms; (3) fullerenes and polycyclic aromatic hydrocarbons.

Until recently it was thought that the synthesis of the first two classes of molecules was well understood, with the chemistry dependent upon differing physical conditions: carbon-chain species are located in very cold clouds (10 K) while COMs are located in warming regions which eventually form stars and planets. The chemistry in cold regions was thought to be dominated by ion-neutral processes in the gas, while the chemistry in warming regions was thought to occur mainly on dust grains followed by near total desorption into the gas at temperatures over 100 K or so [1].

This simple picture is now known to be false. COMs are now also found in cold regions, and carbon-chain molecules are also found in warming regions. This talk will be concerned with the problem of producing COMs in cold regions, for which a number of new chemical mechanisms have been proposed, both in the gas and on the surfaces of dust grains. We will concentrate on a newly considered grain mechanism: radiolysis caused by high energy cosmic rays (mainly protons traveling near the speed of light) bombarding the ice mantles of cold dust grains [2,3].

### References

- [1] Herbst, E., & von Dishoeck, E. F. 2009, ARAA , 47, 427
- [2] Shingledecker, C. N., & Herbst, E. 2018, PCCP, 20, 5359
- [3] Shingledecker, C. N., Tennis, J., Le Gal, R., & Herbst, E. 2018, ApJ, 861:20

## Formation Process of Interstellar Glycine

T. Suzuki,<sup>1</sup> L. Majumdar,<sup>2</sup> M. Ohishi,<sup>3</sup> M. Saito<sup>3</sup>, T. Hiroita<sup>3</sup>, and V. Wakelam<sup>4</sup>

<sup>1</sup>*Astrobiology Center, Japan*

<sup>2</sup>*NASA Jet Propulsion Laboratory, America*

<sup>3</sup>*National Astronomical, Japan*

<sup>4</sup>*Bordeaux University, France*

The study of the chemical evolution of glycine in the interstellar medium is one of challenging topics in astrochemistry. We will present the chemical modeling of glycine in hot cores using the state-of-the-art three-phase chemical model NAUTILUS [1], which is focused on the latest glycine chemistry. For the formation process of glycine on the grain surface, we obtained consistent results with previous studies that glycine would be formed via the reactions of COOH with CH<sub>2</sub>NH<sub>2</sub>, which agrees with the previous modeling study [2]. However, we will report three important findings regarding the chemical evolution and the detectability of interstellar glycine.

First, with the experimentally obtained binding energy from the temperature programmed thermal desorption (TPD) experiment [3], a large proportion of glycine was destroyed through the grain surface reactions with NH or CH<sub>3</sub>O radicals before it fully evaporates. As a result, the formation process in the gas phase is more important than thermal evaporation from grains. If this is the case, NH<sub>2</sub>OH and CH<sub>3</sub>COOH rather than CH<sub>3</sub>NH<sub>2</sub> and CH<sub>2</sub>NH would be the essential precursors to the gas phase glycine. Secondly, since the gas phase glycine will be quickly destroyed by positive ions or radicals, early evolutionary phase of the hot cores would be the preferable target for the future glycine surveys. Thirdly, we suggest the possibility that the suprathreshold hydrogen atoms can strongly accelerate the formation of COOH radicals from CO<sub>2</sub>, resulting in the dramatic increase of formation rate of glycine on grains. The efficiency of this process should be investigated in detail by theoretical and experimental studies in the future.

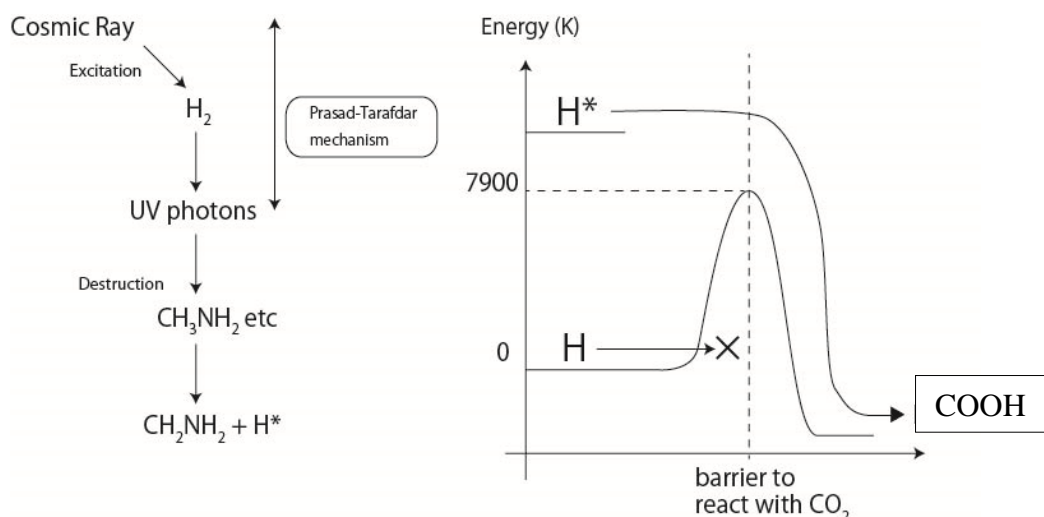


Figure 1: The chemistry of the suprathreshold hydrogen atoms.

### References

- [1] M. Ruaud, V. Wakelam, & F. Hersant, 2016, MNRAS, 459, 3756
- [2] R. T. Garrod, 2013, ApJ 765, 60.
- [3] G. Tzvetkov, M.G. Ramsey, F.P. Netzer, 2004, Chemical Physics Letters, 397, 392

**Effect of Dust Distribution on Chemical Structure in the TW Hya Disk**

H. Nomura,<sup>1</sup> T. Tsukagohi,<sup>2</sup> K. Ryohei,<sup>2</sup> T. Muto,<sup>3</sup> E. Akiyama,<sup>4</sup> Y. Aikawa,<sup>5</sup> S. Okuzumi,<sup>1</sup>  
K.D. Kanagawa,<sup>5</sup> S. Ida,<sup>1</sup> C. Walsh,<sup>6</sup> T.J. Millar<sup>7</sup>

<sup>1</sup>*Tokyo Institute of Technology*, <sup>2</sup>*NAOJ*, <sup>3</sup>*Kogakuin University*, <sup>4</sup>*Hokkaido University*,  
<sup>5</sup>*The University of Tokyo*, <sup>6</sup>*University of Leeds*, <sup>7</sup>*Queen's University Belfast*

Protoplanetary disks are the natal place of planets, and as a first step of planet formation, dust grains are thought to grow through collisional sticking, and then settle towards the disk midplane, drift radially and sometimes azimuthally to be piled up, depending on the gas distribution. In this work, we have modeled the physical and chemical structure of the TW Hya disk, based on the high spatial resolution observations of dust emission and molecular lines by ALMA. The observations of dust emission indicate the concentration of dust grains in the inner region of the disk [1][2], which will affect the UV radiation field, gas temperature, and then molecular line emission profiles. The result of our model calculations suggests that the flat distribution of  $^{13}\text{CO}$ ,  $\text{C}^{18}\text{O}$  and CN line emission can be explained as a result of shielding of UV radiation in the inner region of the disk where dust grains are accumulated. In addition, the observed CN line is relatively strong compared with the  $^{13}\text{CO}$  and  $\text{C}^{18}\text{O}$  lines. This can be explained as a result of depletion of CO gas or depletion of elemental abundance of oxygen in gas. Further observations of molecular lines, such as the  $\text{HCO}^+$  line, could be a clue to distinguish the origin of the possible depletion of gaseous species in the disk.

**References**

- [1] H. Nomura, T. Tsukagohi, K. Ryohei et al. 2016, ApJL, 819, L7.
- [2] T. Tsukagohi, H. Nomura, T. Muto et al. 2016, ApJL, 819, L7.



## Exploiting neutron scattering to understand the structure of amorphous solid water (ASW) in interstellar environments

H.J.Fraser,<sup>1</sup> S.Gaertner,<sup>2</sup> T.Headen,<sup>2</sup> T.Youngs,<sup>2</sup> and D.Bowron<sup>2</sup>

<sup>1</sup>*School of Physical Sciences, Open University, UK*

<sup>2</sup>*ISIS Neutron Source, Rutherford Appleton Laboratory, Harwell, UK*

Amorphous Solid Water (ASW) is the most common form of condensed matter in star and planet forming regions. As such, this porous, amorphous, metastable material is the key medium governing chemical reactivity in the solid-state in space, forming the “birthplace” of complex organic materials that are the precursors to life, as well as acting as a gas reservoir for volatiles that may otherwise be key coolants in the astronomical environments. In addition the physical properties of ASW impact on the earliest stages of planet formation, where the structure and amorphicity of the water ice impacts the sticking properties of nano- to cm-sized dust grains.

However, all these chemical and physical behaviors are dependent on the nano- and meso-scale structure of ASW. Alas, ASW is non-conducting and likely to change structure as soon as it is probed – so both direct (TEM STM AFM) and indirect (volumetric analysis, TPD RAIRS) methods of “seeing” the ASW structure still cannot reveal how the structure forms, or changes as a function of time or temperature. In the last few years we have been pioneering the use of neutron scattering methods to non-invasively reveal the nano-scale and meso-scale structure of ASW under pressure and temperature conditions akin to those in star and planet forming regions. Our results have shown that ASW has a significant diffusive interface [1] at the surface, and identified the mechanism for the onset of the glass transition at around 120 – 136 K [2]. Now our work is focused on identifying the pore size, shape and density in the ices as a function of time and temperature during growth and thermal processing (see Figure 1), and linking this back to our understanding of ice observations at the very onset of star-formation [3].

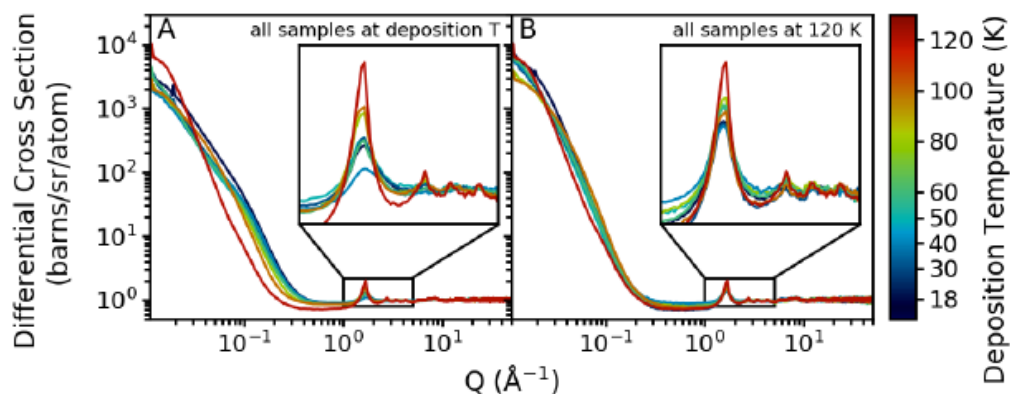


Figure 1: Example neutron scattering data for ASW, showing in (A) the neutron scattering data for ASW immediately after deposition, indicating that both the meso- and nano-scale structure of the ices changes as a function of surface deposition temperature and (B) comparing the neutron scattering data of all deposited samples once heated to 120 K, showing the metastable nature of the ASW, and that the resultant structure is dependent on the thermal pathway.

### References

- [1] Gaertner S et al (2017) ApJ 848 96
- [2] Hill et al (2016) Phys Rev Lett 21 215501
- [3] Noble JA et al (2017) MNRAS 467 4753

## Emergent ferroelectric proton ordering in crystalline ice grown on surface-modified Pt(111) substrates

N. Aiga,<sup>1</sup> T. Sugimoto,<sup>1,2</sup>, K. Watanabe<sup>3</sup> and Y. Matsumoto<sup>4</sup>

<sup>1</sup>*Institute for Molecular Science, Japan*

<sup>2</sup>*JST PRESTO, Japan*

<sup>3</sup>*Kyoto University, Japan*

<sup>4</sup>*Toyota Physical and Chemical Research Institute, Japan*

Crystalline ice is a ubiquitous solid substance in nature and has more than fifteen polymorphs depending on temperature and pressure [1]. The thermodynamically stable phase under ambient pressure and temperature is hexagonal ice: ice Ih. Ice Ih is paraelectric and has disordered configuration of protons (orientation of water molecules) under the Bernal-Fowler-Pauling ice rules [Figure 1(a)]. It was suggested that the proton ordered ferroelectric phase of ice Ih, i.e. ice XI [Figure 1(b)], can stably exist below  $T_c \sim 72$  K [2]; this implies that ferroelectric ice exists on cold interstellar space and planets such as Uranus and Neptune [3], and would play important roles in chemical and physical processes [4].

Recently, using sum-frequency generation (SFG) spectroscopy, we have demonstrated that hexagonal crystalline ice grown on Pt(111) has extremely high- $T_c$  ( $T_c \sim 170$  K) ferroelectric proton ordering [Figure 2] [5,6]. It was also shown that configurational anisotropy and protolysis driven by the electrostatics at the heterointerface are key factors in stimulating novel exotic ferroelectric proton ordering [5]. Because ice in space typically exists in direct contact with mineral surfaces, our concept of heterointerface-induced increase in  $T_c$  for the ferroelectric proton ordering suggests the existence of ferroelectric ice over a much vaster region in space than ever expected from  $T_c \sim 72$  K for ferroelectric bulk ice XI [3].

To give more insight into the emergent ferroelectricity in ice, we have conducted SFG spectroscopy of crystalline ice grown on CO- and O-precured Pt(111) substrates [7]. New unique features were observed in the growth process of ferroelectric ice and its thermodynamic stability, which will be discussed in details in our presentation.

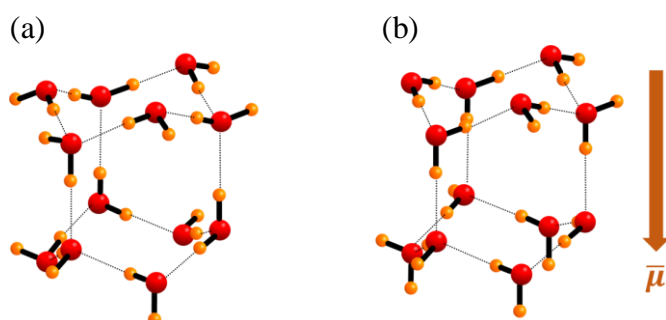


Figure 1 (a) Proton-disordered paraelectric ice Ih.  
(b) Proton-ordered ferroelectric ice XI.

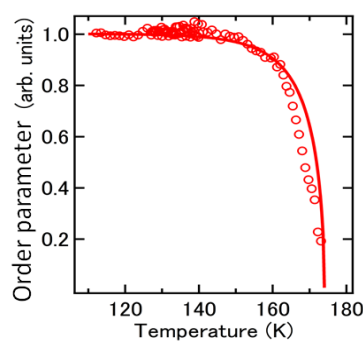


Figure 2 Temperature dependence of ferroelectric order parameter of ice/Pt(111).

### References

- [1] V. F. Petrenko and R. W. Whitworth, *Physics of Ice* (Oxford University Press, New York, 1999).
- [2] Y. Tajima, T. Matsuo, and H. Suga, *Nature* **299**, 810 (1982).
- [3] H. Fukazawa, A. Hoshikawa, Y. Ishii, B. C. Chakoumakos, and J. A. Fernandez-Baca, *Astrophys. J. Lett.* **652**, L57 (2006).
- [4] H. Wang, R. C. Bell, M. J. Iedema, A. A. Tsekouras, and J. P. Cowin, *Astrophys. J.* **620**, 1027 (2005).
- [5] T. Sugimoto, N. Aiga, Y. Otsuki, K. Watanabe, and Y. Matsumoto, *Nat. Phys.* **12**, 1063 (2016).
- [6] N. Aiga, T. Sugimoto, Y. Otsuki, K. Watanabe, and Y. Matsumoto, *Phys. Rev. B* **97**, 075410 (2018).
- [7] N. Aiga, T. Sugimoto, K. Watanabe, and Y. Matsumoto, in preparation.

**Methanol band strength changes due to density variations**

M. Á. Satorre,<sup>1</sup> G. Molpeceres,<sup>2</sup> R. Luna,<sup>1</sup> J. Ortigoso,<sup>2</sup> M. Domingo,<sup>1</sup> R. Escribano,<sup>2</sup>  
C. Santonja,<sup>1</sup> and B. Maté<sup>2</sup>

<sup>1</sup>*Centro de Tecnologías Físicas, Universitat Politècnica de València, Spain*

<sup>2</sup>*Instituto de Estructura de la Materia, IEM-CSIC, Spain*

Infrared band strengths are affected by ice density. Up to now no density values were available for temperatures covering from amorphous to crystalline ices. This presentation will show new experiments where density was measured at different temperatures from 20 K to 130 K. Ices were grown by vapour background deposition in two high vacuum chambers in the same conditions. Densities were measured via a cryogenic quartz crystal microbalance (mass deposited per surface unit) and laser interferometry (thickness). Absorbance infrared spectra of methanol ices of different thickness were recorded to obtain optical constants using an iterative minimization procedure. Infrared band strengths were determined from infrared spectra and ice densities.

Solid methanol densities measured at eight temperatures vary between 0.64 g cm<sup>3</sup> at 20 K and 0.84 g cm<sup>3</sup> at 130 K. The visible refractive index at 633 nm grows from 1.26 to 1.35 in that temperature range. New infrared optical constants and band strengths are given from 650 to 5000 cm<sup>-1</sup> (15.4–2.0 μm) at the same eight temperatures. The study was made on ices directly grown at the indicated temperatures, and amorphous and crystalline phases have been recognized. Our optical constants differ from those previously reported in the literature for an ice grown at 10 K and subsequently warmed. The disagreement is due to different ice morphologies. The new infrared band strengths agree with previous literature data when the correct densities are considered.

## Microwave spectroscopy of prebiotic molecules

H. Ozeki

*Department of Environmental Science, Faculty of Science, Toho University, Japan*

Among molecules so far detected in interstellar media (ISM), some are configuring the part of chemical synthesis pathway toward building block of life. Existence of such “prebiotic” molecules in ISM has drawn much attention to many researchers for a long time. For example, various kinds of formation mechanism of glycine, the simplest amino acid, have been proposed. Chemical models developed recently have taken into account reactions of the prebiotic molecules to tell the abundance and the distribution of these species.[1] Guided with the theoretical works, plenty of observational studies have been reported, leading to an identification of new interstellar molecule. Spectroscopic information such as molecular constants, permanent dipole moment, partition function, spectral line shape parameters, are prerequisite for this purpose. Most of them are derived from high-resolution molecular spectroscopy in the microwave region.[2]-[5]

Laboratory spectroscopy of “new” molecule demands both an accurate prediction of molecular structure and an efficient production of the molecule under investigation. State-of-the-art theoretical calculations provide molecular rotational constants with an accuracy of one percent level. Standardized way for efficient production of unstable molecules in the laboratory condition is hard to be established, thus we need to consider individually for each case. Recent progress on laboratory spectroscopy of prebiotic molecules are reviewed from the above-mentioned standpoints.

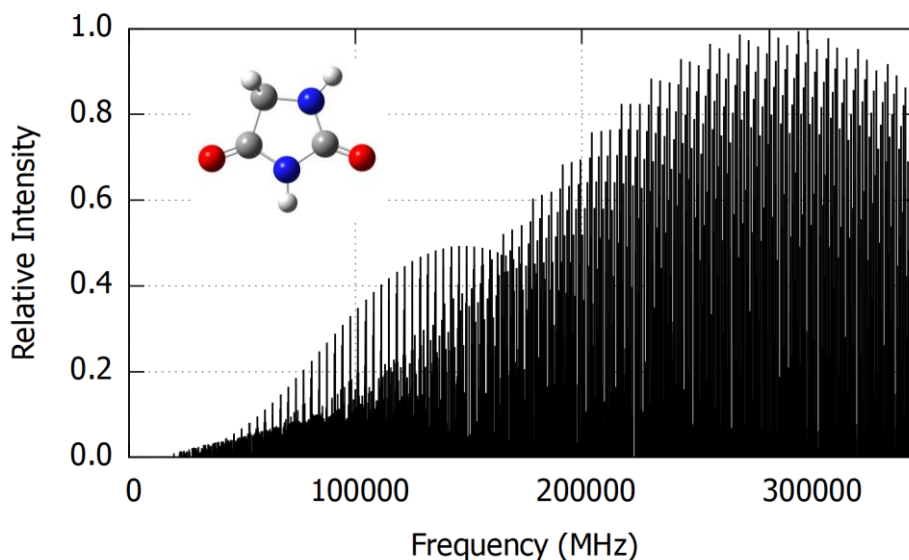


Figure 1: Spectral intensity distribution of Hydantoin, a possible precursor of glycine, at 100 K [4].

### References

- [1] *for example*, R. T. Garrod *ApJ* **765**, 60 (2013).
- [2] Y. Motoki, Y. Tsunoda, H. Ozeki, and K. Kobayashi, *ApJS*, **209**, 23 (2013).
- [3] Y. Motoki, F. Isobe, H. Ozeki, and K. Kobayashi, *A&A* **566**, A28 (2014).
- [4] C. D. Esposti, L. Dore, M. Melosso, K. Kobayashi, C. Fujita, and H. Ozeki, *ApJS* **230**, 26 (2017).
- [5] H. Ozeki, R. Miyahara, H. Ihara, S. Todaka, K. Kobayashi, and M. Ohishi, *A&A* **600**, A44 (2017).

## Infrared spectra of protonated and hydrogenated corannulene, $C_{20}H_{11}^+$ and $C_{20}H_{11}$ , in solid *para*-hydrogen and their relationship to interstellar unidentified infrared bands

Pavithraa Sundararajan,<sup>1</sup> Masashi Tsuge,<sup>1,2</sup> Masaaki Baba,<sup>3</sup> and Yuan-Pern Lee<sup>1,4,5</sup>

<sup>1</sup>*Department of Applied Chemistry, National Chiao Tung University, Taiwan.*

<sup>2</sup>*Institute of Low Temperature Science, Hokkaido University, Japan.*

<sup>3</sup>*Division of Chemistry, Graduate School of Science, Kyoto University, Japan.*

<sup>4</sup>*Center for Emergent Functional Matter Science, National Chiao Tung University, Taiwan*

<sup>5</sup>*Institute of Molecular Sciences, Academia Sinica, Taiwan.*

Polycyclic aromatic hydrocarbons (PAH) and their derivatives, including protonated and cationic species, are suspected to be carriers of the unidentified infrared (UIR) emission bands observed from the galactic and extra-galactic sources. We extended our investigations of infrared (IR) spectra of protonated planar PAH to a non-planar PAH, corannulene ( $C_{20}H_{10}$ ), which is regarded as a fragment of a fullerene,  $C_{60}$ . The protonated corannulene  $C_{20}H_{11}^+$  was produced on bombarding a mixture of corannulene and *para*-hydrogen (*p*- $H_2$ ) with electrons during deposition at 3.2 K. During maintenance of the electron-bombarded matrix in darkness the intensities of IR lines of protonated corannulene decreased because of neutralization by electrons that was slowly released from the trapped sites. The observed lines were classified into two groups according to their responses to secondary irradiation at 365 nm. Eighteen lines in one group are assigned to the lowest-energy species among five possible isomers, *hub*- $C_{20}H_{11}^+$ , and seventeen in another group to *rim*- $C_{20}H_{11}^+$ , the species of second lowest energy. Spectral assignments were derived based on a comparison of the observed spectra with those predicted with the B3PW91/6-311++G(2d,2p) method [1]. The observed IR spectrum of *hub*- $C_{20}H_{11}^+$  resembles several bands of the Class-A UIR bands.

We also report the IR spectra of hydrogenated corannulene ( $C_{20}H_{11}$ ) in solid *p*- $H_2$ . The hydrogenated corannulene were also generated from electron bombardment of a mixture of corannulene and *p*- $H_2$  during deposition of a matrix at 3.2 K. The features that increased with time after maintaining the matrix in darkness for a long period are assigned to the most stable isomers of hydrogenated corannulene, *hub*- $C_{20}H_{11}$  and *rim*- $C_{20}H_{11}$ , according to behavior of secondary photolysis and comparison with the vibrational wavenumbers and IR intensities predicted with the B3PW91/6-311++G(2d,2p) method. In an alternate method in which we produced hydrogenated corannulene by UV irradiation of a matrix  $C_{20}H_{10}/Cl_2/p$ - $H_2$ , followed by IR irradiation to promote the reaction  $Cl + H_2$  to form H atoms to react with corannulene. In this case we observed all three isomers, *hub*-, *rim*-, and *spoke*- $C_{20}H_{11}$ . This indicates that most *hub*- $C_{20}H_{11}$  and *rim*- $C_{20}H_{11}$  produced during electron bombardment might be from neutralization of protonated corannulene, because only *hub*- and *rim*- $C_{20}H_{11}^+$  were produced in these experiments.

### References

- [1] P. Sundararajan, M. Tsuge, M. Baba & Y.-P. Lee, 2018, ACS Earth Space Chem.  
DOI: 10.1021/acsearthspacechem.8b00089.

## Identification of the carriers of the unidentified infrared bands observed in classical novae

I. Endo,<sup>1</sup> I. Sakon,<sup>1</sup> A. L. Helton,<sup>2</sup> R. M. Lau,<sup>3</sup> S. Kimura,<sup>4</sup> S. Wada,<sup>4</sup> N. Ogawa,<sup>5</sup>  
N. Ohkouchi,<sup>5</sup> Y. Kebukawa,<sup>6</sup> and T. Onaka<sup>1</sup>

<sup>1</sup>University of Tokyo, Japan, <sup>2</sup>SOFIA Science Center, USA, <sup>3</sup>Jet Propulsion Laboratory, California Institute of Technology, USA, <sup>4</sup>The University of Electro-Communications, Japan, <sup>5</sup>Japan Agency for Marine-Earth Science and Technology, Japan, <sup>6</sup>Yokohama National University, Japan

The unidentified infrared (UIR) bands have been observed ubiquitously in various astrophysical environments. The bands consist of a series of emission features arising from aromatic and/or aliphatic C-C and C-H bonds in the mid-infrared wavelength range [1], and therefore, their carriers are considered as being related to interstellar organics. The polycyclic aromatic hydrocarbon (PAH) hypothesis is commonly used to interpret the behavior of the observed UIR bands, however, our knowledge on the true carriers of the UIR bands is still limited. Recently, the imaginary dust particle named Mixed Aromatic Aliphatic Organic Nanoparticles [2], which contain hetero atoms in addition to conventional hydrocarbon models, have recently been suggested as a more realistic interpretation of the carriers. The challenges toward identifying the carriers of the UIR bands are still ongoing. Past studies have shown that the UIR bands observed around novae are somewhat different from those observed in other astrophysical environment; predominantly characterized by the presence of broad 8 $\mu$ m feature [3]. Here we report the success of synthesizing laboratory organics ‘Quenched Nitrogen-included Carbonaceous Composite (QNCC)’ whose infrared properties are remarkably similar to the UIR bands observed in classical novae. QNCC is produced by rapidly cooling the plasma gas produced from nitrogen gas and hydrocarbons via 2.45 GHz microwave discharge. We found that N/C ratio (atom) of the QNCC is 4-5% based on the measurement with EA/IRMS. X-ray Absorption Near Edge Structure (XANES) analysis of NCC indicates that amine structure is contained in the QNCC. We concluded that the broad feature at 8 $\mu$ m is arising from amine structures in addition to aromatic C-C structures. This result suggests that, in addition to the classical hydrocarbon models, nitrogen inclusion should be the key for the better understanding of the carriers of the UIR bands.

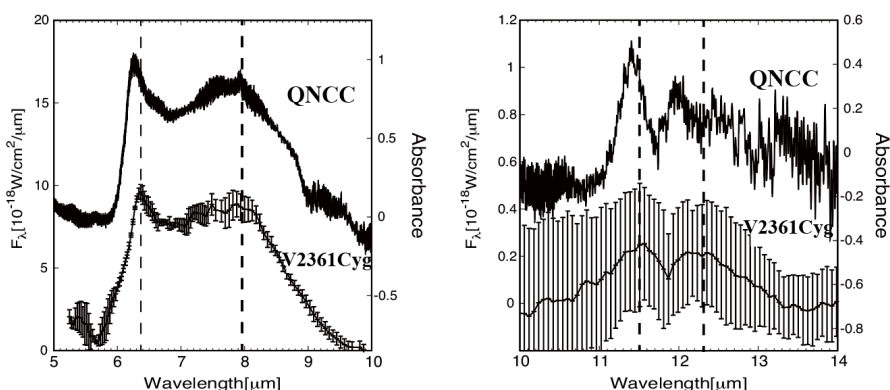


Figure 1: Comparison of the infrared absorption spectrum of QNCC with the UIR bands observed at a classical nova V2361 Cyg on 116 days after the outburst

### References

- [1] L. J. Allamandola, et al. 1989, ApJS, 71, 773
- [2] S. Kwok, & Y. Zhang, 2011, Nature 479, 80
- [3] A. L. Helton, A. Evans, E. C. Woodward, & D. R. Gehrz, 2010, EAS Pub. Ser., 46, 407

## Tracing the Evolution of Ice and Organics from Interstellar Ice Grains to Evolved Solar System Icy Bodies

Murthy S. Gudipati

*Science Division, NASA Jet Propulsion Laboratory, California Institute of Technology, 4800 Oak Grove Drive, Pasadena, CA 91109, USA*

*Murthy.Gudipati@JPL.NASA.GOV*

Understanding the evolution of interstellar ice grains from Dense-Molecular-Cloud (DMC) stage to an evolved Solar System like ours over 4.6+ billion years through various stages will provide necessary information to address the Origin of Life on Earth [Owen 2008].

The overarching research goal at the “Ice Spectroscopy Laboratory (ISL)” that I lead at the Jet Propulsion Laboratory is to understand how ice and organics co-exist and co-evolve from the DMC stage to comets [Altwegg, Balsiger et al. 2016], surfaces and interiors of icy bodies in our Solar System. In our laboratory, we study from radiation processing of interstellar ice grains containing simple organics to MeV electron bombardment of Europa’s surface using laboratory analogs. In order to understand the physics and chemistry of these ices, we developed spectroscopic techniques such as laser-ablation mass spectrometry [Henderson and Gudipati 2015] in addition to conventional infrared, ultraviolet, and laser-spectroscopy.

It is important to determine “tracer species” [Radhakrishnan, Gudipati et al. 2018] that can be followed along the path of the evolution of interstellar ice grains into a fully evolved Solar System. It is expected that comets originated from Oort Cloud preserve the primordial material, while short-period comets originating from Kuiper Belt may be thermally processed to some extent, hence depleted in super-volatiles such as N<sub>2</sub>, CO, O<sub>2</sub>, etc.

This presentation discusses an overview of the research we conducted at ISL over the past decade and summarizes outstanding questions.

Acknowledgments: The research presented here was funded by NASA Research and Analysis Programs such as Solar System Workings, Rosetta Mission (US), and was carried out at the Jet Propulsion Laboratory, California Institute of Technology, under a contract with the National Aeronautics and Space Administration (NASA).

### References

- Altwegg, K., Balsiger, H., et al. (2016). "Prebiotic chemicals-amino acid and phosphorus-in the coma of comet 67p/churyumov-gerasimenko." *Science Advances* **2**(5).
- Henderson, B. L. and Gudipati, M. S. (2015). "Direct detection of complex organic products in ultraviolet (Iy alpha) and electron-irradiated astrophysical and cometary ice analogs using two-step laser ablation and ionization mass spectrometry." *ApJ* **800**(1): 66.
- Owen, T. (2008). *The contributions of comets to planets, atmospheres, and life: Insights from cassini-huygens, galileo, giotto, and inner planet missions*, Springer.
- Radhakrishnan, S., Gudipati, M. S., et al. (2018). "Photochemical processes in CO<sub>2</sub> /H<sub>2</sub>O ice mixtures with trapped pyrene, a model polycyclic aromatic hydrocarbon." *The Astrophysical Journal* **864**(2): 151.

## Utilizing tunable vacuum ultraviolet light and resonance enhanced multiphoton ionization for isomer specific detection of polycyclic aromatic hydrocarbons from astrophysical ice analogues

M. J. Abplanalp,<sup>1</sup> R. Frigge,<sup>1</sup> and R. I. Kaiser<sup>1</sup>

<sup>1</sup>*Department of Chemistry, University of Hawaii at Manoa, Honolulu, HI, USA*

More than 200 molecules have been detected in the interstellar medium (ISM), but no polycyclic aromatic hydrocarbons (PAHs)—organic molecules consisting of fused aromatic rings—have been observed spectroscopically in the gas phase of the ISM. PAHs have been proposed to be the parent for up to 20 % of the interstellar carbon budget though, and have been linked to the astrobiological evolution of the ISM as well as possible nucleation sites for carbonaceous interstellar grains. Although many attempts have been made to study complex ice mixtures there is still a lack of understanding of the chemical complexity from individual ice constituents such as acetylene. Acetylene has been detected in the ISM, but not within ice mantles. However, the gas-phase abundance of acetylene was only able to be accounted for by models when sublimation from icy grain mantles was included. Furthermore, the processing of methane ice, a known ISM ice constituent, results in the formation of acetylene as a product. Also, acetylene ice has been firmly identified as an ice on the surface of Titan. We will discuss the results of processing pure acetylene ices at 5 K with energetic electrons, simulating secondary electrons formed via penetration of galactic cosmic rays through ISM ices. The ices were monitored in-situ via Fourier transform infrared spectroscopy (FTIR) and during heating via mass spectrometry utilizing a quadrupole mass spectrometer with an electron impact ionization source as well as with a reflectron time-of-flight mass spectrometer coupled to a tunable photoionization source (PI-ReTOF-MS) used to do single photon ionization (SPI) as well as resonance enhanced multiphoton ionization experiments (REMPI) allowing for a comprehensive analysis of the products formed in the acetylene ice. The FTIR analysis detected several small hydrocarbon products while the extremely sensitive SPI-ReTOF-MS analysis identified products with general formulae:  $C_nH_{2n+2}$ ,  $C_nH_{2n}$ ,  $C_nH_{2n-2}$ ,  $C_nH_{2n-4}$ ,  $C_nH_{2n-6}$ ,  $C_nH_{2n-8}$ ,  $C_nH_{2n-10}$ ,  $C_nH_{2n-12}$ ,  $C_nH_{2n-14}$ , and  $C_nH_{2n-16}$ . These SPI studies at 10.49 eV revealed ion signals that might belong to aromatic molecules like benzene ( $C_6H_6$ ;  $m/z = 78$ ), and PAHs like naphthalene ( $C_{10}H_8$ ;  $m/z = 128$ ) as well as phenanthrene or anthracene ( $C_{14}H_{10}$ ;  $m/z = 178$ ) subliming from the irradiated ice. However, to confidently determine which isomers these signals belonged to SPI cannot be used as not enough information is known about the other isomers' ionization energies, and instead REMPI was exploited. These REMPI experiments were able to confirm several astrochemically interesting molecules and PAHs. With the proof that tunable photoionization is an extremely useful and important tool for furthering our understanding of astrochemistry a new instrument coupled to a synchrotron is currently being assembled (Hefei-Shanghai-Hawaii Center for Astrochemistry).

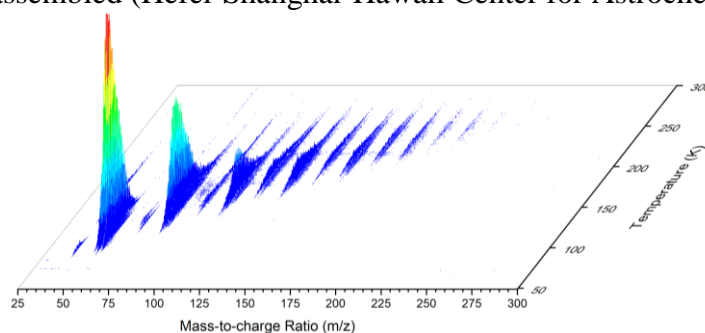


Figure 1: PI-ReTOF-MS data reporting the temperature dependent mass spectra from irradiated acetylene ice at a photoionization energy of 10.49 eV.



## **An experimental study of the UV-induced photo-isomerization of interstellar molecules**

Y. Nakano, R. Uesugi, H. Ueta, T. Hirayama

<sup>1</sup>*Department of Physics, Rikkyo University*

Molecules of the same composition with different structures (e.g. HCCH and HHCC) are called isomers. Many of polyatomic molecules among nearly 200 species already discovered in interstellar space by astronomical observations are suggested to have isomers. As different isomers show different chemical properties and behaviors in the interstellar space, transitions between different isomers sometimes play a crucial role in characterizing the chemical environment of the clouds. Probing the astronomical objects in terms of the abundance ratio of isomers may also provide a detailed information on their chemical conditions, such as the gas temperature, flux and polarizability of radiation, isotope enrichment factors and so on.

We have started a new experimental study on the isomerization of interstellar molecular ions with a focus on those induced by a UV radiation above the ionization limit of hydrogen. The experiment is based on three parts; one is the preparation of isolated molecular ions in the gas phase and this will be done by electro-spray, electron-discharge, and gas-jet ionization methods depending on the species. The second part is the generation of monochromatic UV radiation with a substantial intensity. A dedicated UV beamline for this experiment is under development in the laser plasma light source facility in Rikkyo University. As the last part, the molecular structure has to be identified, although this is not usually straightforward since the isomers have the same mass and velocities. The low-temperature ion-mobility spectrometry (IMS) method will be used to separate the isomers during the time they drift through a cold tube filled with a helium gas. Figure 1 shows the the present view of the drift-tube apparatus in the laboratory. The status of the experimental developments and the basic concepts of the research will be presented.



Figure1: Photograph of the IMS apparatus.

## Time-independent approach for fine-structure calculations in electronic spectra

Karolis Šarka<sup>1,‡</sup>, Shinkoh Nanbu<sup>1</sup>

<sup>1</sup>*Department of Materials and Life Sciences, Sophia University, Japan*

<sup>‡</sup> E-mail to: [ksarka@eagle.sophia.ac.jp](mailto:ksarka@eagle.sophia.ac.jp)

Extraterrestrial and interstellar bodies contain molecules that are either unstable, or require experimental conditions hiding the fine-structure through thermal or collision broadening. For diatomic molecules, we can perform the quantum-exact calculations of spectra based on time-independent Schrödinger equation and R-matrix propagation of time-independent wavefunctions across the global potential energy curves for all discrete vibrational and rotational states and a combination of R-matrix and S-matrix theories for the continuum region.

We present the fine-structure spectra for sulfur dimer and its isotopologues[1] – a part of Archean Earth, Venus, Io, and other extraterrestrial atmospheres. The mass-independent isotopic fractionation for molecules with low density-of-states can be evaluated in the fine-structure spectra as a result of the anharmonicity of the potential curves. The potential energy curves and transition dipole moments are calculated at MRCI-F12/aug-cc-pVQZ level at full valence active space; absorption spectra are calculated for two lowest electronic states with an allowed transition from the ground state ( $X^3\Sigma_g^-$ ) –  $B'^3\Pi_u$  and  $B^3\Sigma_u^-$ .

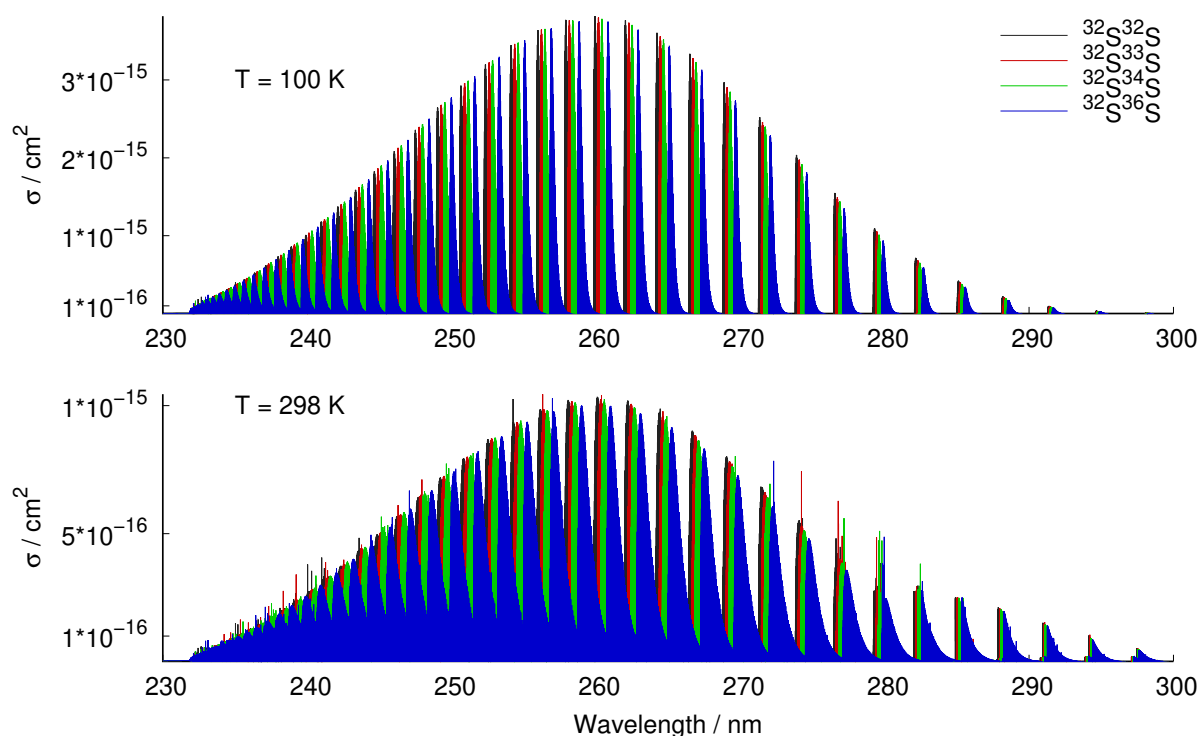


**Figure 1:** Fine-structure spectra of  $S_2$  and its isotopologues for excitation to  $B^3\Sigma_u^-$  state.

## References

- [1] Karolis Šarka, Sebastian O Danielache, Alexey Kondorskiy, and Shinkoh Nanbu. Theoretical study of electronic properties and isotope effects in the uv absorption spectrum of disulfur. *Chemical Physics*, 516:108–115, 2019.

## Thermal and photo-induced desorption processes from molecular ices relevant to the interstellar medium

M. Bertin,<sup>1</sup> X. Michaut,<sup>1</sup> R. Dupuy,<sup>1</sup> G. Féraud,<sup>1</sup> L. Philippe,<sup>1</sup> and J.-H. Fillion<sup>1</sup>

<sup>1</sup>LERMA – Sorbonne Université / Obs. De Paris, Paris - France

In the colder regions ( $\sim 10 - 100$  K) of space, the matter is predominantly molecular, physisorbed at the surface of micrometer-size dust grains. These icy mantles are the main reservoir of molecules: they can act as catalysts for further chemical complexity, and enrich the gas phase by means of desorption processes. Constraining the desorption is a key parameter in the astrochemical models since it may control dramatically the gas-to-ice abundances ratio. Depending on the temperature of the grains, both thermal and on-thermal desorption processes are at play, and each of these processes needs to be quantified.

I will present experimental approaches that are used to constrain the efficiency of both thermal and photoinduced desorption from model molecular ices. Thermal desorption from cold ice is studied by the TPD method, from which multi-heating rate experiments can provide both adsorption energies and exponential prefactors,<sup>1,2</sup> the latter being usually arbitrary chosen by empiric formula whose validity can be debated for big and tightly bounded molecules. The UV photodesorption is studied using the tunable UV output of synchrotron facility at SOLEIL, opening up the possibility to extract both absolute efficiencies in the 7 – 14 eV range, and bringing valuable information on the underlying mechanisms of desorption by the identification of the first absorption steps within the ice.<sup>3</sup> Some perspective of these works will also be given, in particular concerning the role of higher photon energies (soft X-rays) in the photodesorption from molecular ices.<sup>4</sup>

### References

- [1] Doronin et al. 2015, J Chem Phys 143, 084703
- [2] Bertin et al. 2017, A&A 598, A18
- [3] e.g. Bertin et al. 2016 ApJ 817, L12 ; Dupuy et al. 2017, A&A 603, A63
- [4] Dupuy et al. 2018, Nat. Astron. 2, 796

**Photo-desorption of circumstellar nitrogen-bearing ice analogs**

A. Ciaravella,<sup>1</sup> Y.-J. Chen,<sup>2</sup> C. Cecchi-Pestellini,<sup>1</sup> C.-H. Huang,<sup>2</sup>  
A. Jimenez-Escobar,<sup>2</sup> G.M. Munoz Caro,<sup>3</sup> and N.-E. Sie<sup>2</sup>

<sup>1</sup>*INAF - Osservatorio Astronomico di Palermo,  
P.zza Parlamento 1, 90134 Palermo, Italy*

<sup>2</sup>*Department of Physics, National Central University,  
Jhongli City, Taoyuan County 32054, Taiwan*

<sup>3</sup>*Centro de Astrobiología (INTA-CSIC),  
Carretera de Ajalvir, km 4, Torrejón de Ardoz, 28850 Madrid, Spain*

We study the photo-desorption occurring in H<sub>2</sub>O:CO:NH<sub>3</sub> ice mixtures irradiated with monochromatic (550 and 900 eV) and broad band (250-1250 eV) soft X-rays generated at the National Synchrotron Radiation Research Center (NSRRC, Hsinchu, Taiwan). We detect many masses photo-desorbing, from atomic hydrogen ( $m/z = 1$ ) to complex species with  $m/z = 69$  (e.g., C<sub>3</sub>H<sub>3</sub>NO, C<sub>4</sub>H<sub>5</sub>O, C<sub>4</sub>H<sub>7</sub>N), supporting the enrichment of the gas phase.

At low number of absorbed photons, substrate-mediated exciton-promoted desorption dominates the photo-desorption yield inducing the release of weakly bound (to the surface of the ice) species; as the number of weakly bound species declines, the photo-desorption yield decrease about one order of magnitude, until porosity effects, reducing the surface/volume ratio, produce a further drop of the yield.

We derive an upper limit to the CO photo-desorption yield, that in our experiments varies from 1.4 to 0.007 molecule photons<sup>-1</sup> in the range  $\sim 10^{15}$ - $10^{20}$  absorbed photons cm<sup>-2</sup>. We apply these findings to a protoplanetary disk model irradiated by a central T Tauri star.

## Formation of complex organic molecules on cold surfaces

F. Dulieu<sup>1</sup>, T. Nguyen<sup>1</sup>, E. Congiu<sup>1</sup>, S. Baouche<sup>1</sup>, A. Sow<sup>1</sup>, M. Minissale<sup>1,2</sup>

<sup>1</sup> *LERMA, Université de Cergy-Pontoise, Sorbonne Université, Observatoire de Paris, PSL University, CNRS, France*

<sup>2</sup> *PIIM, Aix-Marseille Université, Marseille, France*

Interstellar Complex Organic Molecules (iCOMs) are considered as the building blocks of more complex pre-biotic compounds. In particular, formamide (NH<sub>2</sub>CHO), widely observed in different astrophysical media, is thought to be the starting point of some emblematic metabolic and genetic species [1]. Formamide formation through gas phase route exists [2, 3], even if it is still debated, but solid-state chemistry should also be a vector of the molecular complexity observed in later phases of the matter evolution, such as in comets and meteorites.

Our group aims at understanding how the molecular complexity may increase on cold surfaces, from atoms or molecules, without the help of others external energetic agents (photons, electrons, ions...). During the last few years we have developed a new experimental facility (named VENUS) to study the different non-energetic pathways of solid-state astrochemistry.

During my presentation I will show how we can constrain the penetration depth of H and O through molecular ices (e. g. H<sub>2</sub>O, NO, H<sub>2</sub>CO). Penetration actually occurs at a negligible rate in comparison with other surface processes (diffusion and self reaction) (Minissale et al, submitted). Thus, I will present evidence that formamide can also be formed very efficiently following solid-state chemical pathways (Dulieu et al, in prep.).

Finally, I will give few examples of how we can nowadays determine the chemical networks (including the evaluation of barriers, and type of reaction) of specific chemical solid state systems, such like the hydrogenation of NO (Nguyen et al, in prep.), combining complete sets of experiments with state-of-the-art calculations of quantum chemistry.

[1] Saladino, R. et al., 2012. Formamide and the origin of life. *Physics of life reviews*, 9(1), pp.84–104.

[2] Barone, V. et al., 2015. Gas-phase formation of the prebiotic molecule formamide: insights from new quantum computations. *Monthly Notices of the Royal Astronomical Society: Letters*, 453(1).

[3] Codella, C. et al., 2017. Seeds of Life in Space (SOLIS) - II. Formamide in protostellar shocks: Evidence for gas-phase formation. *Astronomy & Astrophysics*, 605, p.L3.

## A Complete Quantification of Photon-induced Desorption Processes: Morphology effect on CO<sub>2</sub> ice

Ni-En Sie<sup>1</sup>, R. Martín-Doménech<sup>2</sup>, G. M. Muñoz Caro<sup>2</sup>, Yu-Jung Chen<sup>1</sup>

<sup>1</sup>*Department of Physics, National Central University, Taoyuan 32001, Taiwan*

<sup>2</sup>*Centro de Astrobiología, INTA-CSIC, Torrejón de Ardoz, Madrid 28850, Spain*

According to literature[1], different deposition temperatures of CO<sub>2</sub> ice lead to distinct structures of CO<sub>2</sub>, which possesses an amorphous structure below 35 K and a crystalline structure at temperatures higher than 35 K[2]. In Öberg et al. 2009, the photodesorption yield of CO<sub>2</sub> ice depends on its morphology. For the purpose of investigating the relationship between the photodesorption yield of CO<sub>2</sub> ice and its morphology, the CO<sub>2</sub> ice was deposited at 16, 30, 40, 50, and 60 K respectively, and all of these ices were irradiated with vacuum ultraviolet (VUV) photons at 16 K. In this work, we will introduce a novel method to quantify the photodesorption yield of CO<sub>2</sub> ices by a calibrated quadrupole mass spectrometer (QMS). The experimental results show that the photodesorption yields of CO<sub>2</sub> ices deposited at different temperatures mentioned above are almost the same, meaning that the photodesorption yield of CO<sub>2</sub> ice is irrelevant to its morphology, which is inconsistent with previous works[1, 3, 4].

### References

- [1] Öberg, K., E. van Dishoeck, and H. Linnartz, *Astronomy and Astrophysics*, 2009. **496**: p. 281-293.
- [2] Falk, M., *The Journal of chemical physics*, 1987. **86**(2): p. 560-564.
- [3] Yuan, C. and J.T. Yates Jr, *The Astrophysical Journal*, 2014. **780**.
- [4] Bahr, D.A. and R.A. Baragiola, *The Astrophysical Journal*, 2012. **761**(1): p. 36.

## Radical species on interstellar ices: some clues from a quantum mechanics/molecular mechanics study

W. M. C. Sameera,<sup>1</sup> Bethmini Senevirathne,<sup>2</sup> Madhuranga Rathnayake,<sup>3</sup> Muhsen Abood Al-Ibadi,<sup>4</sup> Ayane Miyazaki,<sup>1</sup> Stefan Andersson,<sup>5</sup> Gunnar Nyman,<sup>2</sup> Naoki Watanabe<sup>1</sup>

<sup>1</sup>*Institute of Low Temperature Science, Hokkaido University, Kita-ku North 19 West 8, Sapporo 060-0819, Japan.*

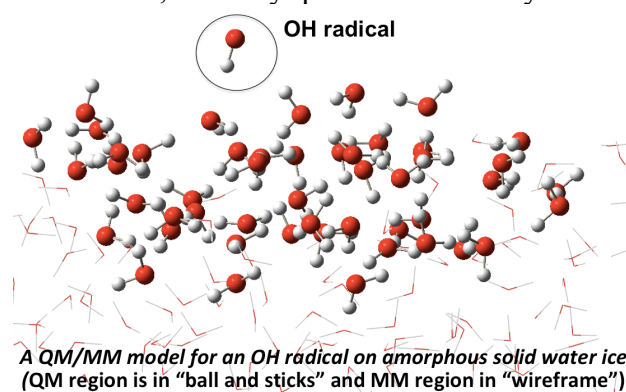
<sup>2</sup>*University of Gothenburg, Department of Chemistry and Molecular Biology, Kemigården 4, SE-412 96 Gothenburg, Sweden.*

<sup>3</sup>*ARC Centre of Excellence in Exciton Science, School of Chemistry, The University of Sydney, Sydney, New South Wales 2006, Australia.*

<sup>4</sup>*Department of Chemistry, Faculty of Science, University of Kufa, Alnajaf, Iraq.*

<sup>5</sup>*SINTEF, P.O. Box 4760 Torgarden, NO-7465 Trondheim, Norway.*

The origin of radical species in the interstellar medium (ISM) and mechanistic details of their reactions remain a mystery. The radical species in the ISM play an important role in the formation of more complex molecules or radicals. These chemical processes occur on the icy mantles of interstellar grains at very low temperatures (typically 10 K). Radicals may adsorb on ice, diffuse, and subsequently react with other species adsorbed at the ice.<sup>1,2</sup> The rates of these processes are difficult to characterize from experimental studies alone, whereby quantum chemistry becomes a critical tool.<sup>3,4,5</sup>



We have used quantum mechanics/molecular mechanics (QM/MM) methods to study OH, HCO, CH<sub>3</sub>, CH<sub>3</sub>O, SH, and O radicals binding on crystalline hexagonal water ice (I<sub>h</sub>) and amorphous solid water (ASW). Calculated binding energies of the radicals are sensitive to the number of dangling hydrogen (*d*-H) or dangling oxygen (*d*-O) at the binding sites. A range of strong binding energies was observed for each radical when the binding sites consist of *d*-Hs or *d*-Os, indicating that radical diffusion would be slow. In the absence of dangling atoms at the binding sites, the calculated binding energies are significantly weaker, allowing radicals to diffuse on the ice. Our study provides important insights into radical desorption and diffusion on interstellar ices.

### References

- [1] T. Hama & N. Watanabe, *Chem. Rev.* 2013, 113, 8783-8839.
- [2] N. Watanabe & A. Kouchi, *Prog. Surf. Sci.* 2008, 83, 439-489.
- [3] W. M. C. Sameera & F. Maseras, *J. Chem. Inf. Model*, 2018, 58, 1828-1835.
- [4] W. M. C. Sameera, B. Senevirathne, S. Andersson, F. Maseras & G. Nyman, *J. Phys. Chem. C*, 2017, 121, 15223-15232.
- [5] D. Sharma, W. M. C Sameera, S. Andersson, G. Nyman & M. J. Paterson, *ChemPhysChem*, 2016, 17, 4079-4089.

## Newly discovered interstellar molecules

M. Agúndez,<sup>1</sup> N. Marcelino,<sup>1</sup> J. Cernicharo,<sup>1</sup> E. Roueff,<sup>2</sup> and M. Tafalla<sup>3</sup>

<sup>1</sup>*Instituto de Física Fundamental, CSIC, Madrid, Spain*

<sup>2</sup>*LERMA, Observatoire de Paris, France*

<sup>3</sup>*Observatorio Astronómico Nacional, Madrid, Spain*

The continuous improvement in the sensitivity of radiotelescopes is allowing to unveil the chemical composition of molecular clouds with an unprecedented level of detail. In the current year we have discovered six new interstellar molecules, all of them observed in the dense core L483 thanks to the sensitivity of a 3 mm line survey carried out with the IRAM 30m telescope. Some of them have been also observed in other dense cores. The discovered species are the cation  $\text{NS}^+$ , which seems to be ubiquitous in assorted types of interstellar environments [1], the radical HCS and its metastable isomer HSC, which provide new observational constraints on the chemistry of sulfur in dark clouds [2], the radical NCO and the ion  $\text{H}_2\text{NCO}^+$ , which are key precursors in the synthesis of the widespread HNCO molecule and its related isomers [3], and CNCN, a metastable isomer of the non polar and thus radio invisible molecule cyanogen (NCCN), a species which is the simplest member of the family of dicyanopolynes and is inferred to be fairly abundant in interstellar clouds [4]. All these discoveries have provided a wealth of observational constraints for chemical models and ultimately are allowing to better understand the chemical richness and the chemical processes at work in dense interstellar clouds.

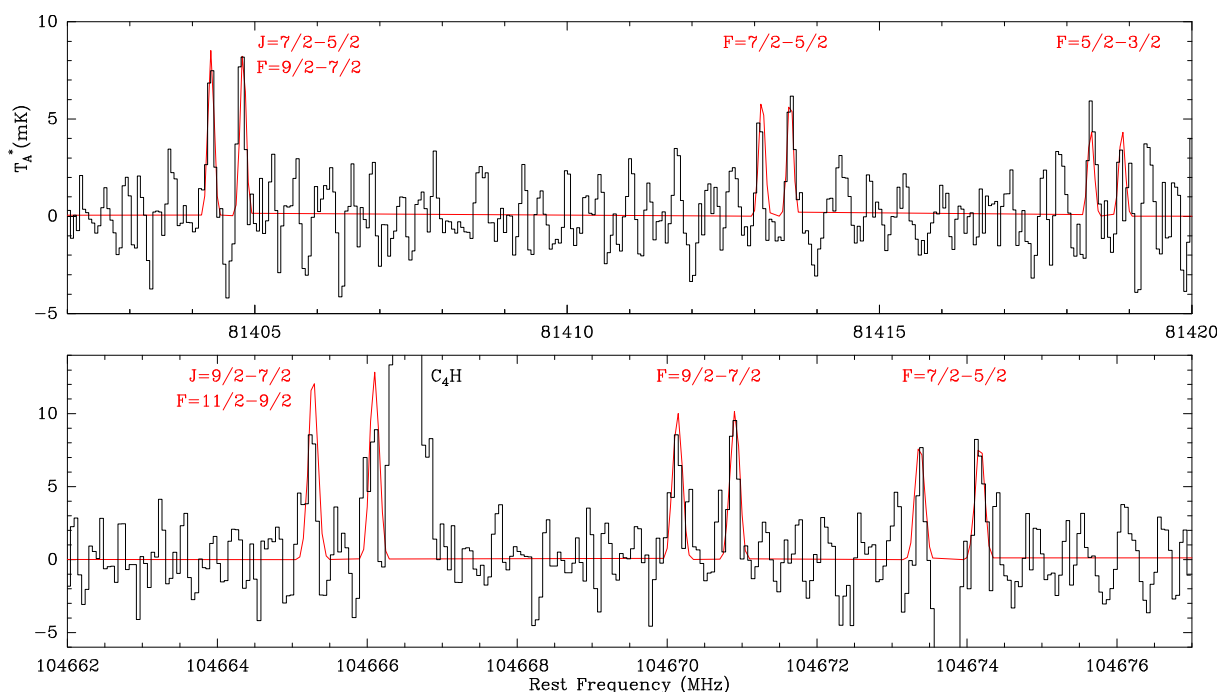


Figure 1: As an example we show the weak lines observed towards L483 with the IRAM 30m telescope that led to the detection of the NCO radical [3].

### References

- [1] J. Cernicharo, B. Lefloch, M. Agúndez, et al. 2018, ApJ, 853, L22
- [2] M. Agúndez, N. Marcelino, J. Cernicharo, and M. Tafalla 2018, A&A, 611, L1
- [3] N. Marcelino, M. Agúndez, J. Cernicharo, et al. 2018, A&A, 612, L10
- [4] M. Agúndez, N. Marcelino, and J. Cernicharo 2018, ApJ, 861, L22



## ALMA Observations of the Spatial Distribution of three C<sub>2</sub>H<sub>4</sub>O<sub>2</sub> Isomers towards Sgr B2(N)

C. Xue,<sup>1</sup> A. J. Remijan,<sup>2</sup> A. M. Burkhardt,<sup>3</sup> and E. Herbst<sup>1,3</sup>

<sup>1</sup>*Department of Chemistry, University of Virginia, United States*

<sup>2</sup>*National Radio Astronomy Observatory, United States*

<sup>3</sup>*Department of Astronomy, University of Virginia, United States*

The C<sub>2</sub>H<sub>4</sub>O<sub>2</sub> isomeric triplet found in the interstellar medium consists of glycolaldehyde (CH<sub>2</sub>OHCHO), acetic acid (CH<sub>3</sub>COOH), and methyl formate (HCOOCH<sub>3</sub>), the mechanisms of synthesis of which may involve both gas-phase and grain-surface processes [1]. Using the ALMA Band 3 observations [2], we report the discovery of previously undetected transitions of the C<sub>2</sub>H<sub>4</sub>O<sub>2</sub> isomers with the high spatial-resolution sub-millimeter maps of CH<sub>2</sub>OHCHO, CH<sub>3</sub>COOH, and HCOOCH<sub>3</sub>. HCOOCH<sub>3</sub> and CH<sub>2</sub>OHCHO each display two different velocity components at 64 km s<sup>-1</sup> and 73 km s<sup>-1</sup> respectively, while only one velocity component of CH<sub>3</sub>COOH at 64 km s<sup>-1</sup> is resolved. Moreover, the distribution of HCOOCH<sub>3</sub> is extended and offset from the continuum emission, unlike CH<sub>2</sub>OHCHO and CH<sub>3</sub>COOH, of which the low-velocity component we find to be concentrated toward the continuum emission peak of Sgr B2(N). The difference in the morphology of the three isomers indicates that the three isomers might have different formation mechanisms.

### References

- [1] J. M. Hollis, F. J. Lovas & P. R. Jewell, 2000, ApJ, 540, L107
- [2] A. Belloche, H. S. P. Müller, R. T. Garrod, & K. M. Menten, 2016, A&A, 587, A91

## Detection of absorption lines of CH<sub>3</sub>CN in envelope of Sagittarius B2 (M)

M. Araki,<sup>1</sup> S. Takano,<sup>2</sup> Y. Minami,<sup>1</sup> T. Oyama,<sup>1</sup> N. Kuze,<sup>3</sup> K. Kamegai,<sup>4</sup> and K. Tsukiyama<sup>1</sup>

<sup>1</sup> Faculty of Science Division I, Tokyo University of Science, Japan

<sup>2</sup> College of Engineering, Nihon University, Japan

<sup>3</sup> Faculty of Science and Technology, Sophia University, Japan

<sup>4</sup> Astronomy Data Center, National Astronomical Observatory of Japan, Japan

Detections of organic molecules in diffuse and translucent clouds is essential to reveal a history of organic molecules in space. Molecules in these clouds suffer more cooling by radiations and less heating by collisions. However, for acetonitrile CH<sub>3</sub>CN, a rotation around a molecular axis cannot be cooled by radiations, and then rotational populations are concentrated to  $J = K$  levels. Strong absorption lines from the levels can be produced. To simulate the lines, we formulated this rotational behavior as “Hot Axis Effect” [1]. In this work, to detect this molecule in diffuse and translucent clouds we searched for absorption lines of the  $J_K = 4_3-3_3$  transitions at 73.6 GHz toward the galactic center Sagittarius (Sgr) B2(M) and other sources by using Nobeyama 45 m telescope. As a result, the absorption lines having the velocity of 64 km s<sup>-1</sup> were detected toward Sgr B2(M). The excitation temperature of  $2.9 \pm 0.5$  K, the kinetic temperature of  $95 \pm 32$  K, and the column density of  $(1.34 \pm 0.15) \times 10^{14}$  cm<sup>-2</sup> were derived for this molecule. The kinetic temperature suggests that the 64 km s<sup>-1</sup> component is located in the envelope of Sgr B2(M). Thus, the envelope is thought to be a habitat of small complex organic molecules (COMs), which have been detected so far. We also found the similarity of abundances of small COMs between the envelope and the core of Sgr B2(M) and the variety of abundances of them among the envelope and other diffuse clouds.

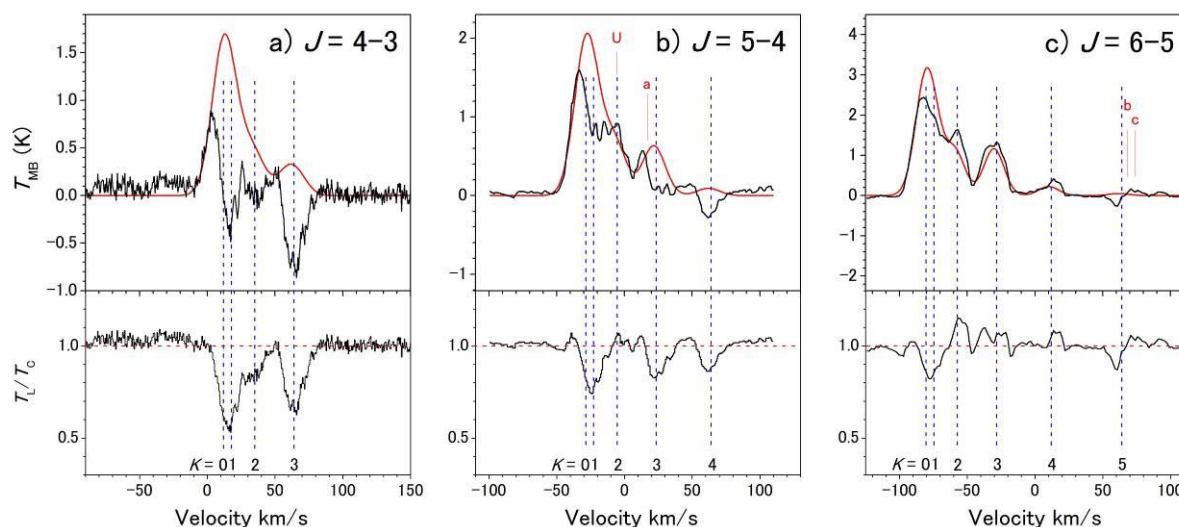


Figure 1: Absorption lines obtained by subtraction of emission lines for CH<sub>3</sub>CN toward Sgr B2(M). In the upper panels, the red lines are estimated emission profiles and solid lines are observed profiles. The velocities are based on the frequencies of the transitions from the  $J = K$  levels. The spectra of  $J = 5-4$  and  $6-5$  are from Belloche *et al.* [2]. The red bars marked by the alphabets show emission lines of other molecules.

### References

- [1] M. Araki *et al.*, 2014, *Astronomical Journal* 148, 87.
- [2] A. Belloche *et al.*, 2013, *A&A* 559, 47.

## ALMA observations of layered structures due to CO selective dissociation in the $\rho$ Ophiuchi A plane-parallel PDR

M. Yamagishi<sup>1</sup>, C. Hara<sup>2</sup>, R. Kawabe<sup>3</sup>, F. Nakamura<sup>3</sup>, T. Kamazaki<sup>3</sup>, Y. Shimajiri<sup>4</sup>, T. Takekoshi<sup>5</sup>, H. Nomura<sup>6</sup>, S. Takakuwa<sup>7</sup>, and J. Di Francesco<sup>8</sup>

<sup>1</sup>*Institute of Space and Astronautical Science, Japan Aerospace Exploration Agency, Japan*

<sup>2</sup>*Graduate School of Science, The University of Tokyo, Japan*

<sup>3</sup>*National Astronomical Observatory of Japan, National Institutes of Natural Sciences, Japan*

<sup>4</sup>*Institute of Astronomy, The University of Tokyo, Japan*

<sup>5</sup>*Laboratoire AIM, CEA/DSM-CNRS-Universit e Paris Diderot, IRFU/Service d'Astrophysique, CEA Saclay, France*

<sup>6</sup>*Department of Earth and Planetary Sciences, Tokyo Institute of Technology, Japan*

<sup>7</sup>*Department of Physics and Astronomy, Graduate School of Science and Engineering, Kagoshima University, Japan*

<sup>8</sup>*NRC Herzberg Astronomy and Astrophysics Research Centre, Canada*

One of the outstanding issues in current PDR study is that there is no unified understandings about the PDR spatial structure. An important approach to examine the PDR spatial structure is observation of CO selective dissociation with high spatial resolution. A plane-parallel PDR is expected to make CO layered structures due to selective dissociation at the PDR interface from more- to less-abundant isotopologues as a function of distance from the excitation star, while a clumpy PDR is difficult to make such layered structures. We analyzed  $^{12}\text{CO}(2-1)$ ,  $^{13}\text{CO}(2-1)$ ,  $\text{C}^{18}\text{O}(2-1)$ , and 1.3 mm continuum maps of the  $\rho$  Ophiuchi A PDR obtained with ALMA. Layered structures of the three CO isotopologues with an angular separation of  $10'' = 6.6 \times 10^{-3} \text{ pc} = 1400 \text{ au}$  are clearly detected around the excitation star. We estimated the spatial variations of  $X(^{13}\text{CO})/X(\text{C}^{18}\text{O})$  abundance ratios, and found that the abundance ratio is as high as 40 near the emission front, and decreases to the typical value in the solar system of 5.5 in a small angular scale of  $4'' = 2.6 \times 10^{-3} \text{ pc} = 560 \text{ au}$ . We also found that the  $I(^{12}\text{CO}(2-1))/I(^{13}\text{CO}(2-1))$  intensity ratio is very high ( $>27$ ) in the Class II young stellar object, GY-51, located in the PDR. The enhancement of the ratios indicates that the UV radiation significantly affects the CO isotopologues via selective dissociation in the overall  $\rho$  Ophiuchi A PDR, and that the  $\rho$  Ophiuchi A PDR has a plane-parallel structure.

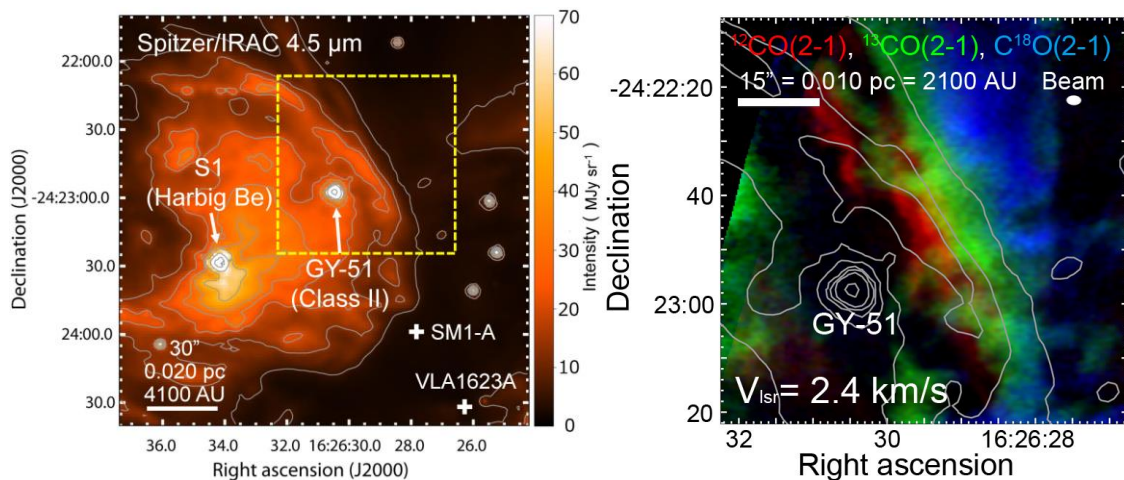


Figure 1: (left) Spitzer/IRAC 4.5  $\mu\text{m}$  map of  $\rho$  Oph A. The yellow dashed box indicates the target area in the present study. (right) Color-composite maps of (red)  $^{12}\text{CO}(2-1)$ , (green)  $^{13}\text{CO}(2-1)$ , and (blue)  $\text{C}^{18}\text{O}(2-1)$  emissions at  $V_{\text{lsr}}=2.4 \text{ km/s}$ . Contours are the same as in the left panel.

## Deuteration in the initial condition of the high-mass star formation

S. Feng,<sup>1</sup> P. Caselli,<sup>2</sup> K. Wang<sup>3</sup>, O. Sipilae<sup>2</sup>, H. Beuther<sup>4</sup>, and Y. Lin<sup>5</sup>

<sup>1</sup>*NAOJ, JP*

<sup>2</sup>*MPE, Germany*

<sup>3</sup>*ESO, Germany*

<sup>4</sup>*MPIA, Germany*

<sup>2</sup>*MPIfR, Germany*

Knowledge of the initial chemical conditions of high-mass star-forming regions (HMSFRs) is important for understanding how such stars form. Deuteration is a key process since it allows us to probe the earliest stages of star formation.

Using IRAM-30 m telescope, we carried an imaging line survey at 1.3 mm–4.3 mm towards the darkest, coldest southern end of the filament G28.34+0.06 [1, 2]. This region covers a pair of high-mass clumps P1 and S, which are 2 pc-apart on the projection plane of the sky, and their kinematical features indicate different evolutionary stages. (1) Analysing the profiles of key physical and chemical parameters, we studied the deuteration of six species ( $\text{NH}_2\text{D}$ ,  $\text{N}_2\text{H}^+$ , HCN, HNC,  $\text{HCO}^+$ , and  $\text{CH}_3\text{OH}$ ), and unveiled the chemical gradient from the more evolved protostellar clump P1 to the extremely young protostellar clump S. (2) At a spatial resolution of 0.8 pc, we found the deuteration of  $\text{N}_2\text{H}^+$ ,  $\text{HCO}^+$ , and HNC are more efficient in the cold environment. In particular,  $\text{HCO}^+$  and HNC shows higher deuteration than previous studies towards the dark clouds by a factor of 1–2 magnitude. In contrast, deuteration of  $\text{NH}_3$  and  $\text{CH}_3\text{OH}$  show clear enhancement towards the location between P1 and S, where CO has the largest depletion ( $\sim 250$ ). (3) Supported by our gas-grain model [3], the variations in deuteration of different species result in their different gas-grain forming paths.

This comparable chemical study towards a pair of young HMSFRs in the same natal cloud excludes the impacts from the environmental difference, illustrates the potential of taking the deuteration efficiency of species with different gas-grain forming paths as a tool in diagnosing the evolutionary stage of a HMSFR. The result of this pilot study will be ground by observations on a larger sample of source pairs in the similar dark clouds [4].

### Reference

- [1] Wang, K., Zhang, Q., Wu, Y., & Zhang, H. 2011, ApJ, 735, 64
- [2] Feng, S., Beuther, H., Zhang, Q., et al. 2016a, A&A, 592, A21
- [3] Sipilae, O., et al. 2015, A&A, 578, A55
- [4] Feng et al. in prep. (IRAM-30m project ID: 115-17)

**An experimental study of the gas-phase ion-neutral reaction  
by merged-beam collisions**

R. Nagaoka<sup>1</sup>, S Iida<sup>1,2</sup>, M. Iizawa<sup>1</sup>, S. Kuma<sup>3</sup>, T Azuma<sup>2,3</sup>, Y. Nakano<sup>1,3</sup>

<sup>1</sup>*Department of Physics, Rikkyo University, Japan*

<sup>1</sup>*Department of Physics, Tokyo Metropolitan University, Japan*

<sup>1</sup>*AMO Physics Laboratory, RIKEN, Japan*

The gas-phase reaction in the low-temperature interstellar clouds is predominated by ion-neutral reactions without reaction barrier. While the understanding of the interstellar chemical reaction has dramatically progressed by the radio astronomical observations and the large-scale reaction network calculations, experimental studies are still limited due to the technical difficulties in controlling the cold collision of ions and neutrals.

Merging beams is one of the promising approach to access such processes, in which energetic particle beams are merged in a collinear configuration and the particles collide with each other in extremely low relative velocities corresponding to the thermal energies below 100 K (Figure 1 (Left)). As well as translational collision energies, internal temperature of the molecules are also important that dictates the chemical reaction processes. Cryogenic ion storage rings are suitable apparatus to realize the precise control of both translational and internal degree of freedom in the gas-phase collision experiments. An in-ring merged-beam experiment is being carried out at RIKEN Cryogenic Electrostatic ring (RICE) [1], using the rovibrationally cooled molecular ion beam and the neutral atomic beams. Preparation of the cold molecular beam is already tested in the RICE and the experimental developments in the neutral beam production are ongoing. The neutral beams are produced by a laser-induced photo-detachment of negative ion beams, for which a duoplasmatron and Cs sputter ions sources have been installed, after the acceleration and focusing/defocusing by electrostatic field. Figure 1 (Right) shows the photograph of the photo-detachment chamber, in which a high-power cw diode laser (808nm, 5 kW) is irradiating the negative ion beam through a fused silica window. The effective laser intensity is to be enhanced by a multi-pass optics installed inside the vacuum chamber.

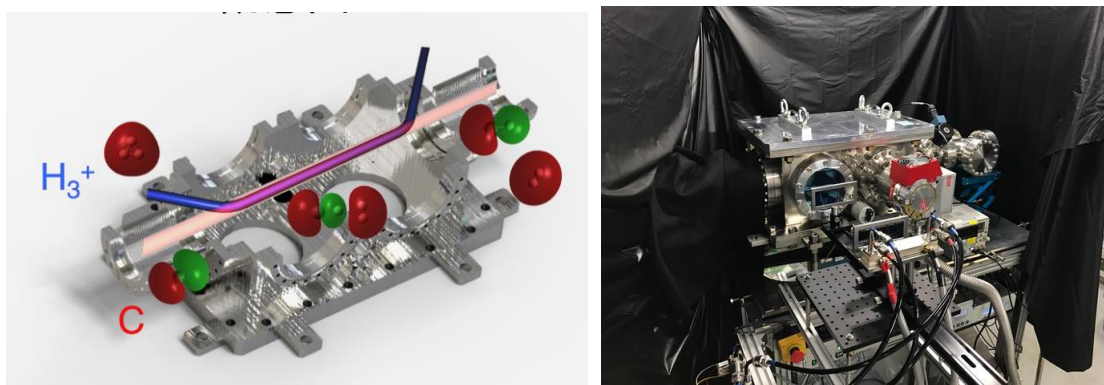


Figure 1: (Left) Schematic image of merged beam collisions. (Right) Photograph of the vacuum chamber for photo detachment of negative ion beams.

## References

- [1] Y. Nakano, et al., Rev. Sci. Instrum. 88, 033110 (2017).

## Reactivity of cationic pentane and its growth reaction

Y. Matsuda<sup>1</sup>

<sup>1</sup>*Department of Chemistry, Graduate School of Science, Tohoku University, Japan*

In an interstellar chemistry, radical cations are ones of important species, because they are highly reactive. We have studied structures and ionization-induced reactions of monomers and clusters of radical cations in the gas phase by use of mass spectrometry, infrared spectroscopy, and theoretical calculations. Recently, we have investigated the reactivity of radical cations of alkanes. Through this, extremely high proton donor abilities of CH bonds of cationic alkanes have been elucidated, although neutral alkanes are typically aprotic.[1]

Figure 1 shows the structure of the di-hydrated cluster of cationic pentane. As seen in the figure, a proton of cationic pentane is transferred to the water moiety and is shared intermolecularly. No energy barrier in this proton transfer reaction is indicated by theoretical calculation. These results demonstrate the high proton donor ability of CH bonds in cationic pentane. The mechanism of its high proton donor ability is analyzed by infrared spectroscopy of cationic pentane monomer.[2]

Furthermore, we have determined the structure of cationic pentane dimer. Figure 2 shows the structure of cationic pentane dimer. The dimer cation are formed by the intermolecular semi-covalent bond type interaction between the hydrogen atoms. In the mass spectrum of the pentane dimer, the H<sub>2</sub>-loss fragment cation ( $m/z=142$ ) as well as the pentane dimer ( $m/z=144$ ) is observed. In this H<sub>2</sub>-loss fragment cation, the carbon atoms which lost the hydrogen atoms form the intermolecular hemibond. This hemibond formation would be a key for hydrocarbon growths.

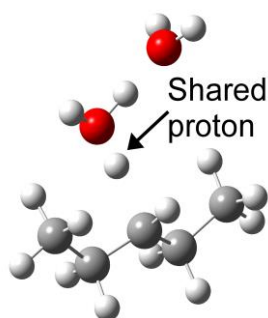


Figure 1: Structure of cationic pentane-(H<sub>2</sub>O)<sub>2</sub> cluster.

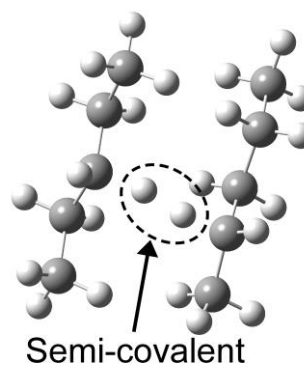


Figure 2: Structure of cationic pentane dimer.

### References

- [1] T. Endo, Y. Matsuda, A. Fujii, *J. Phys. Chem. Lett.* 8, 4716 (2017).
- [2] M. Xie, Y. Matsuda, and A. Fujii, *J. Phys. Chem. A.* 120, 6351 (2016).

## Solar wind charge exchange and related atomic processes in laboratory

N. Numadate, Y. Yamada, T. Ohna, and H. Tanuma

*Department of Physics, Tokyo Metropolitan University, Japan*

The soft X-ray emission observed with the ROSAT all-sky survey in the 1990s found an intensity fluctuating in cycles of a few days duration [1]. It was difficult to understand this phenomenon before the mechanism of the soft X-ray emissions from comets has been revealed. In 1996, the ROSAT also observed the soft X-ray emission from the comet C/Hyakutake 1996 B2 approaching to Earth [2]. According to Cravens' suggestion, it has been recognized that the soft X-ray emission stems from charge exchange collisions between the solar wind ions and the neutrals among the comet, and this phenomenon is called "Solar Wind Charge eXchange" (SWCX) [3]. In analogy to this, it was proposed that the soft X-ray background radiation with fluctuating intensity is due to a charge-exchange of the highly charged ions in the solar wind with thin neutral matter within the heliosphere [4].

In order to analyze soft X-ray emission spectra observed with X-ray observatory satellites quantitatively, accurate emission cross sections in collisions of multiply charged ions with neutral atoms are required by astrophysicists. We have a 14.25 GHz electron cyclotron resonance ion source (ECRIS) which can produce various multiply charged ions (for example, bare, H-like, and He-like ions of C, N, and O atoms *etc.*) and beam lines for collision experiments between multiply charged ions and neutral gases with solar wind speed of 300-800 km/s which corresponds to a kinetic energy range of 0.5-3.3 keV/u.

Using this multiply charged ion beam facility, we have been performing the following experiments in this decade:

- 1) Total charge exchange cross sections:
- 2) Emission spectra and emission cross sections [5, 6]:
- 3) Observation of forbidden transitions following charge exchange collisions [7, 8]:
- 4) Soft X-ray emissions from inner-shell excited Li-like ions [9]:

We will show our recent results on atomic collision experiments with multiply charged ions in the workshop.

### References

- [1] S. L. Snowden, *et al.*, 1994, ApJ, 424, 714.
- [2] C. M. Lisse, *et al.*, 1996, *Science*, 274, 205.
- [3] T. E. Cravens, 2000, ApJ, 532, L153.
- [4] R. Fujimoto, *et al.*, 2007, PASJ, 59, S133.
- [5] T. Kanda, *et al.*, 2011, Phys. Scr. T144, 014025.
- [6] H. Shimaya, *et al.*, 2013, Phys. Scr. T156, 014002.
- [7] N. Numadate, *et al.*, 2014, Rev. Sci. Instrum. 85, 103119.
- [8] N. Numadate, *et al.*, 2017, Nucl. Instrum. Meth. B, 408 114.
- [9] N. Numadate and H. Tanuma, *submitted to PRA*.

## Laser Spectroscopic Study of CaH B ( $v=3, 5$ and $7$ ) -X ( $v=0$ ) bands

Kyohei Watanabe<sup>1</sup>, Iori Tani<sup>1</sup>, Kaori Kobayashi<sup>1</sup>,  
Fusakazu Matsushima<sup>1</sup>, Yoshiki Moriwaki<sup>1</sup> and Stephen C. Ross<sup>2</sup>

<sup>1</sup>*Department of Physics/ University of Toyama, Japan*

<sup>2</sup>*Department of Physics/ University of New Brunswick, Canada*

The electronic transitions of Calcium monohydride (CaH) have been found in the sunspot and M dwarf stars [1], and they are used to investigate the luminosity and surface gravity of those stars. Therefore, many spectroscopic studies have been carried out so far. The first laboratory spectroscopy of CaH was carried out in 1925 on the  $C^2\Sigma^+ - X^2\Sigma^+$  transitions in the near-UV region [2]. Recently, high precise measurements of CaH were reported [3, 4]. In addition to the astronomical interests, CaH draw a structural interest for its avoided crossing between the  $B^2\Sigma^+$  and  $D^2\Sigma^+$  electronic states and the resultant double minimum potential. We are interested in their interactions with other electronic states and the rotational and vibrational structure near the potential barrier. In our previous work, we found interaction between the B state and the D state by non-adiabatic effect as energy shifts in vibrational levels [5]. In this work, we measured the region between  $v=2$  and  $9$  and tried to bridge the gap.

We investigated the region from  $19100\text{ cm}^{-1}$  to  $21000\text{ cm}^{-1}$  by laser-induced fluorescence and observed three vibrational bands. We assigned those bands to the B ( $v=3, 5$  and  $7$ ) - X ( $v=0$ ) transitions. The rotational constants,  $B$ , of the  $v=5$  and  $7$  state is about  $2/3$  of those of the  $v=0 - 3$ . This indicate that  $v=5$  and  $7$  states lies above the potential barrier. Local perturbations were also observed in the rotational of the B ( $v=3$ ) state. In this talk, we report on the assignments of these newly observed vibrational levels and discuss the observed perturbations.

### References

- [1] C. M. Olmsted, *Astrophys. J.* 27, 66 (1908).
- [2] Robert S. Mulliken, *Phys. Rev.* 25, 509 (1925).
- [3] A. Shayesteh, et al., *J. Mol. Struct.* 288, 46 (2013).
- [4] R. S. Ram et al., *J. Mol. Spectrosc.* 266, 86 (2011).
- [5] K. Watanabe et al., *Chem. Phys. Lett.* 657, 1 (2016).



## Millimeter-wave Spectroscopy of Thiophene

Yotaro Ichikawa and Kaori Kobayashi

*Department of Physics, University of Toyama, Japan*

Hetero five-membered ring molecules may be potential candidates of interstellar molecules. Thiophene( $C_4H_4S$ ) is one of this kind of rings that contains sulfur atom. Kretschmer and colleagues reported the results of rotational spectroscopy of  $^{32}S$ -,  $^{33}S$ -, and  $^{34}S$ - thiophene isotopomers in 1993[1]. Up to 30 GHz was covered in their study. Also in 2008, Although the infrared spectra of the  $\nu_{14}$  and  $\nu_8$  vibration bands using synchrotron radiation was reported[2,3], it is still not enough to have rotational transition frequencies in the millimeter-wave region. In this paper, we extend frequency range and provide accurate rest frequencies.

In this research, we used our conventional source-modulation microwave spectrometer and measured in the 50 to 100 GHz. An example is shown in the Figure. Prediction was carried out based on the previous study [3]. Assignment and analysis using SPFIT and SPCAT suites [4] are in progress. We will report our current status.



Figure: An example of millimeter-wave spectrum in the 942 GHz region.

### References

- [1] U. Kretschmer, W. Stahl, and H. Dreizler, *Z. Naturforsch.* 48a, 733-736 (1993)
- [2] Jennifer van Wijngaarden, Samantha J Van Nest, Cody W van Dijk, Dennis Tokaryk. 259 (2010) 56–59
- [3] J. van Wijngaarden, D. W. Tokaryk, 251 (2008) 365–368
- [4] H. M. Pickett, R. L. Poynter, E. A. Cohen, M. L. Delitsky, J. C. Pearson, and H. S. P. Muller, *J. Quant. Spectrosc. & Rad. Transfer* 60, 883-890 (1998).

## High-resolution spectrum of methyl formate in the microwave and far infrared region

Akio Itoh, Kaori Kobayashi, Department of Physics, University of Toyama, Toyama, Japan;  
Nobukimi Ohashi, Kanazawa University, Kanazawa, Japan;

Dennis W. Tokaryk, Department of Physics, University of New Brunswick, Fredericton, NB,  
Canada;

Brant E. Billingham, EFD, Canadian Light Source Inc., Saskatoon, Saskatchewan, Canada.

Methyl formate molecule ( $\text{HCOOCH}_3$ ) is a molecule with a high spectral density that is commonly found in the high mass star forming regions. Recently it has been observed in a very young low mass star formation region. We succeeded in assigning rotational spectra up to the second torsional excited state of using microwave spectroscopy. Based on this result [1], unidentified lines in the interstellar space were successfully assigned to this state [2]. There are other low-lying vibrational modes, COC deformation and skeletal torsion. Observation of this molecule even in the vibrational excited states are highly expected. To assign these states, we have been working on the microwave and far-infrared spectroscopy. So far, our assigned rotational spectra in the microwave region was confirmed to be due to the excited COC deformation by combining the data in the far-infrared region. We will report our current status.

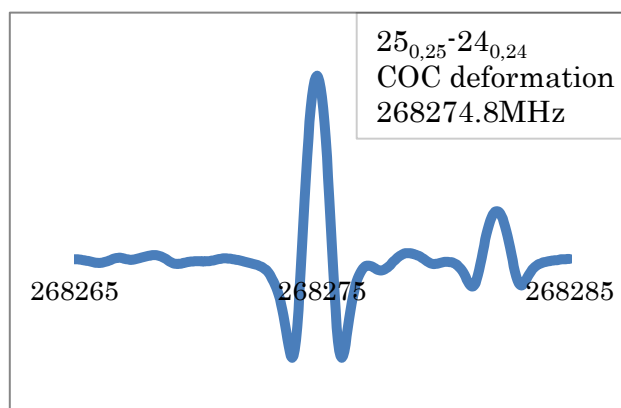


Figure : An example of microwave spectrum in the 268 GHz region.

### References

- [1] K. Kobayashi, K. Ogata, S. Tsunekawa, S. Takano. 2007, ApJ, 657, L17.
- [2] S. Takano, Y. Sakai, S. Kakimoto, M. Sasaki, K. Kobayashi. 2012, PASJ. 64. 89.

## Absorption spectroscopy of the electronic transition of thiophenoxy radical

H. Sato, M. Negishi, M. Araki, T. Oyama and K. Tsukiyama

Department of Chemistry, Tokyo University of Science, Japan

Diffuse Interstellar Bands (DIBs) are absorption bands by molecular cloud between the earth and stars. Several hundreds of bands have been detected, but no bands have been assigned except for the five ones of  $C_{60}^+$ . Recently benzonitrile  $C_6H_5CN$  was firstly discovered in a dark cloud by radio observations. Hence, we focus on the thiophenoxy radical  $C_6H_5S$  as a candidate of DIBs. To compare DIBs with the thiophenoxy radical, the strongest peaks of this radical need to be measured in a laboratory. Shibuya *et al.* reported fluorescence excitation spectra of the  ${}^2A_2-X{}^2B_1$  electronic transition of this radical [1]. From their spectra, it was mentioned that the origin band produces the strongest peak. However, Araki *et al.* observed absorption spectrum of phenoxy radical  $C_6H_5O$  and found that the vibronic bands are stronger than the origin band [2]. The fact suggests that intensities of higher vibronic bands of the thiophenoxy radical are lost by radiationless transitions in the fluorescence excitation spectra. Thus, absorption lines of vibronic bands of the thiophenoxy radical were expected to be stronger than that of the origin band. We observed the high-resolution absorption spectrum of  $C_6H_5S$  by cavity ring down spectroscopy in the resolution of  $0.005 \text{ \AA}$  in a laboratory. The radical was produced by pulsed discharge with a hollow cathode using a gas mixture of thiophenol  $C_6H_5SH$  and helium in a cell. The absorption bands were measured in the  $4721\text{--}5168 \text{ \AA}$  region as shown in Figure 1. The observed strong bands were assigned to the  $6a$  and  $6b$  mode based on the previous works [3-5] and our quantum chemical calculation (B3LYP/6-311++G(d,p)). We found that the strongest band in the  ${}^2A_2-X{}^2B_1$  electronic transition of this radical is the  $6a_0^26b_0^1$  vibronic band. This band may appear as DIB if sufficient amount of this radical exists in interstellar medium.

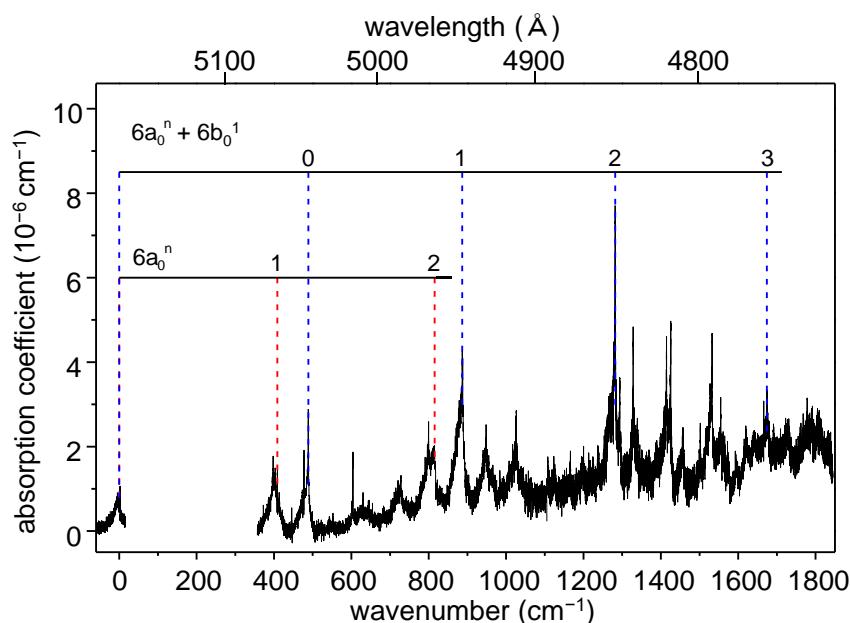


Figure 1: Absorption spectrum of the  ${}^2A_2-X{}^2B_1$  electronic transition of thiophenoxy radical

### References

- [1] K. Shibuya *et al.*, 1988, Chem. Phys. 121, 237. [2] M. Araki *et al.*, 2015, AJ 150, 113. [3] J. Spanget-Larsen *et al.*, 2001, J. Am. Chem. Soc. 123, 11253. [4] M. Araki *et al.*, 2014, AJ 148, 87. [5] M. Fukushima *et al.*, 2005, SPSJ, Proceedings, Spring, 125.

## Infrared relaxation in Hydrogenated Amorphous Carbon Chemical Analogues

G. Molpeceres,<sup>1</sup> B. Maté,<sup>1</sup> J. Ortigoso<sup>1</sup> and H.A Galué<sup>2</sup>

<sup>1</sup>Departamento de Física Molecular, IEM-CSIC., *Spain*

<sup>2</sup>Department of Physics and Astronomy, Vrije Universiteit, *Netherlands*

For the past 30 years, Polycyclic Aromatic Hydrocarbons (PAHs) have been able to reproduce the Unidentified Infrared Emission (UIE) emission bands, a set of spectroscopic features found between 11.2 and 6.2  $\mu\text{m}$  and at 3.3  $\mu\text{m}$  in the mid IR, corresponding to aromatic C=C stretchings and bendings and C-H bendings, respectively [1,2]. The so-called PAH hypothesis is able to account for the general appearance of the bands explaining them as a combination of PAHs molecules in different oxidation states [1]. One of the main advantages of PAH molecules is that they can undergo transient heating to effective temperatures of 1000K upon absorption of a single UV photon, relaxing afterwards. With the years, refinements of the classical theory have been developed and successfully applied to the fitting of astronomical sources [3,4]. Several criticisms arise from the classical PAH hypothesis, being the most important one that no single PAH molecule has been positively identified in the Interstellar Medium (ISM) [5]. Among the years, several alternatives have been postulated like considering small solid particles as candidates for carriers of such band and assuming that isolated aromatic domains within these particles may suffer transient heating by UV photons [6,7]. The present work is devoted to the simulation of the UV absorption and IR emission spectra of a series of randomly packed hydrogenated amorphous carbon (HAC) chemical analogues [8] using ab initio methods. We have employed CASTEP [9] for the calculation of the vibrational properties and the optical constants in the ultraviolet and visible range. The calculation of the emission curves has been done implementing a canonical photocooldown emission model from the literature [4 and references therein]. We show that the IR photo-cooldown of our randomly packed amorphous analogs is consistent with the spectral characteristics of the interstellar UIE bands, offering a reconciling scenario between the PAH hypothesis and the mixed aliphatic-aromatic amorphous solid interpretations.

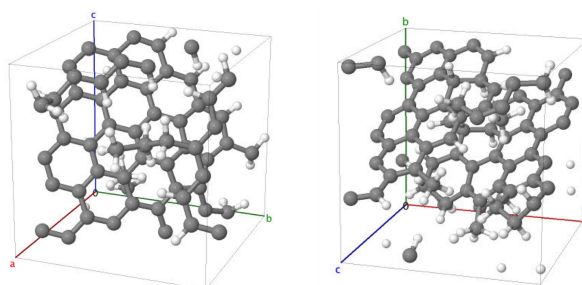


Figure 1: Examples of the packed structures simulated in this work.

### References

- [1] Allamandola, L.J, Tielens, A.G.G.M and Barker, J.R 1985 ApJ Letters, 290, p. L25-L28.
- [2] Tielens, A. G. G. M. 2008. Annual Review of Astronomy and Astrophysics, 46(1).
- [3] Rosenberg, M.J.F, Berné, O. and Boersma, C. 2014 A&A 566, L4.
- [4] Galué, H.A., Díaz Leines, G. 2017 PRL 119, 171102.
- [5] Kwok, S. and Zhang, Y. 2013 ApJ, 771, 5.
- [6] Scott, A., Duley, W. and Jahani.H 1997 ApJ 2, L175-L177
- [7] Kwok, S. and Zhang, Y. 2011 Nature, 479, 80-83.
- [8] Molpeceres, G., Timón, V, Jiménez-Redondo, M., et al 2017 PCCP, 19, 1352-1360
- [9] Clark, S. J., Segall, M. D., Pickard, C. J., et al. 2005 Z. Kristallogr, 220, 567-570.

## IR spectroscopy and energetic processing of methyl isocyanate ice

V. J. Herrero, B. Maté, G. Molpeceres, V. Timón, I. Tanarro,  
R. Escribano and R. J. Peláez

*Instituto de Estructura de la Materia (IEM-CSIC), Serrano 121-123, 28006 Madrid, Spain*

Methyl isocyanate was recently detected in the interstellar medium [1-2] (the reported detection on comet 67P/CG [3] could not be confirmed[4]). Although it was usually neglected in astrochemical networks, this new evidence fosters new studies on this species. We present here our work on the IR spectra and on the energetic processing of ices of this molecule.

We have recorded in our lab the IR spectra of amorphous  $\text{CH}_3\text{NCO}$  and  $\text{CD}_3\text{NCO}$  obtained by vapor deposition at 20 K. The most intense band corresponds to the NCO asymmetric stretching ( $\nu_a\text{-NCO}$ ). It has a characteristic quadruplet structure, usually attributed to the interaction with the  $\text{CH}_3$  torsion.  $\text{CD}_3\text{NCO}$  was used to help the spectral assignment. We have also measured the band strengths for the absorptions of  $\text{CH}_3\text{NCO}$  in ice at 20 K.

Since no X-ray structure for crystalline  $\text{CH}_3\text{NCO}$  had been reported, we put forward a tentative theoretical structure, derived taking as a starting point the crystal of isocyanic acid. We have predicted a spectrum for the proposed structure, and compared it with our experimental observation [5] (see Fig. 1).

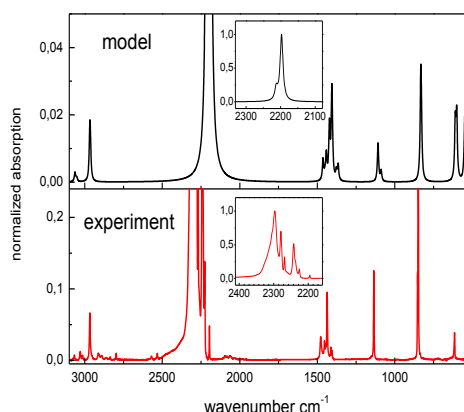


**Fig. 1.** Comparison of theoretical spectrum of the crystal with experiment.

We have studied the stability of  $\text{CH}_3\text{NCO}$  under heating, UV irradiation with a  $\text{D}_2$  lamp (UV photons  $\approx 10.3\text{-}6.9$  eV), and cosmic ray bombardment, simulated with high energy electrons (5 keV) [6]. The samples were either pure  $\text{CH}_3\text{NCO}$  or  $\text{CH}_3\text{NCO}$  diluted in  $\text{H}_2\text{O}$ . Heating of the ices leads to variations in the  $\nu_a\text{-NCO}$  band profile but not to an appreciable depletion of  $\text{CH}_3\text{NCO}$  until  $\text{H}_2\text{O}$  sublimation (beyond  $T=150$  K) and thus rules out hydrolysis in the ice. UV irradiation and electron bombardment at 20 K lead to the destruction of  $\text{CH}_3\text{NCO}$  and to the formation of  $\text{CO}$ ,  $\text{CO}_2$  and  $\text{OCN}^-$  ions in the processed ices.

These results indicate that the lifetime of hypothetical  $\text{CH}_3\text{NCO}$  present in the ice mantles of dust grains in a typical dense cloud might be longer than the cloud's lifetime.

The sample was kindly provided by J.-C. Guillemin. We are grateful to J. Cernicharo for suggesting the topic and continuous support. This work was funded by the European Union (ERC-2013-Syg 610256 NANOCOSMOS) and by the Spanish MINECO (FIS2016-C3-1P). Computer calculations were carried out at Trueno and Cesga.

### References

- [1] Halfen, D. T., Ilyushin, V.V., & Ziurys, L. M. 2015, ApJ, 812, L5
- [2] Cernicharo, J., Kisiel, Z., Tercero, B. et al. 2016, A&A, 587, L4
- [3] Goesmann, F., Rosenbauer, H., Brederhöft, J. H. et al. 2015, Sci, 349, aab0689
- [4] Altwegg, K., Balsiger, H., Berthelier, J. J., et al. 2017, MNRAS, 469, S130
- [5] B. Maté et al. MNRAS 2017, 470, 4222.
- [6] B. Maté et al. 2018, A&A, 861:61

## Direct Optical Measurements of $C_3H_4^+$ and $C_3H_3^+$ Cations in Solid Ar

Meng-Yeh Lin,<sup>1</sup> Meng-Chen Liu,<sup>1</sup> Chih-Hao Chin,<sup>1</sup> Tzu-Ping Huang,<sup>1</sup> and Yu-Jong Wu<sup>1,2</sup>

<sup>1</sup>*National Synchrotron Radiation Research Center, Taiwan*

<sup>2</sup>*Department of Applied Chemistry, National Chiao Tung University, Taiwan*

*E-mail: yjwu@nsrrc.org.tw*

$C_3H_4^+$  and  $C_3H_3^+$  ions are important in many diverse applications and fields, such as flame and combustion processes, and planetary and interstellar chemistry. They are commonly observed fragments in the combustion of hydrocarbons and are proposed as reactants in the synthesis of cumulenenic and cyclic hydrocarbons in interstellar medium through ion–molecule reactions.  $C_3H_3^+$  ions have also been detected in the tail of Halley’s comet.

We produced allene cations ( $H_2C_3H_2^+$ ) in solid Ar via electron bombardment (200 eV) of an allene/Ar matrix sample during matrix deposition. Subsequently, we irradiated the matrix sample with 365-nm light, which resulted in isomerization from allene cations to propyne cations ( $H_3C_3H^+$ ) in the solid Ar. The IR absorption features of the both cations were recorded and assigned based on the theoretical prediction, D-isotopic substitution, and photochemical behaviors [1]. In the meanwhile, we also recorded UV absorption spectra of this sample and an intense vibrationally resolved progression in the spectral region of 266–237 nm was assigned to the  $A^2E \leftarrow X^2E$  electronic transition of allene cations, and the torsional mode is dominant in this progression. Moreover, although the strong absorption of neutral allene appeared in the spectral region at wavelengths shorter than 225 nm, the weak absorption of allene cations corresponding to the  $B^2A_1 \leftarrow X^2E$  transition was extracted from the difference spectrum recorded after photolysis at 385 nm [2].

In separate experiments, we subjected propyne/Ar matrix samples to electron bombardment at 200 or 2000 eV, followed by deposition at 8 K. Allene cations also were found to be dominant for low-energy bombardment, similar to the case in previous allene experiments. This suggests that the loss of H atoms from the two precursors might be inhibited due to the rapid excess energy quenching after bombardment. In contrast, several H-degradation species including propargyl cations ( $H_2C_3H^+$ ) were formed in the high-energy bombardment experiment [3]. This study confirmed the assignment of the  $\nu_5$  mode at  $1140.6\text{ cm}^{-1}$  which was reported discrepantly in previous IRPD [4] and VMI-PE [5] measurements. In addition, the IR absorption of the  $\nu_{11}$  mode was observed for the first time. The “true” experimental relative IR intensities of the observed vibrational modes of the cation were also determined.

### References

- [1] M.-C. Liu, S.-C. Chen, T.-P. Huang, C.-H. Chen, H.-F. Chen, & Y.-J. Wu, *J. Phys. Chem. Lett.* **6**, 3185-3189 (2015).
- [2] C.-H. Chin, M.-Y. Lin, T.-P. Huang, & Y.-J. Wu, *Spectrochim. Acta A* **196**, 233-237 (2018).
- [3] C.-H. Chin, M.-Y. Lin, T.-P. Huang, P.-Z. Wu, & Y.-J. Wu, *Sci. Rep.* (2018) accepted
- [4] A. M. Ricks, G. E. Douberly, P. v. R. Schleyer, & M. A. Duncan, *J. Chem. Phys.* **132**, 051101 (2010).
- [5] H. Gao, Z. Lu, L. Yang, J. Zhou, & C. Y. Ng, *J. Chem. Phys.* **137**, 161101 (2012).

## The Temperature Dependent VUV Spectra Shifts of CO Ices

Y.-J. Chen,<sup>1</sup> G. M. Muñoz Caro,<sup>2</sup> and D. Field<sup>2</sup>

<sup>1</sup>*Department of Physics, National Central University, Taiwan*

<sup>2</sup>*Centro de Astrobiología (CSIC-INTA), Spain*

<sup>3</sup>*Department of Physics and Astronomy, University of Aarhus, Denmark*

Ice photodesorption has been considered as a non-thermal process, which contributes the abundance of gas-phase molecules toward the cold interstellar regions. In this work VUV absorption spectra of carbon monoxide ices were measured to evaluate the possible link between the structure and the photodesorption yield of carbon monoxide ice[1]. The temperature dependent VUV spectral shifts (few hundred wavenumbers) were observed that can be reproduced by a simple electrostatic model base on Stark effect on a hole and electron residing several nm wavenumbers apart, identifying the presence of Wannier-Mott excitons[2]. The spontelectric effect in CO simultaneously explains the long-standing enigma of the sensitivity of vacuum ultraviolet spectra to the deposition temperature.

### References

- [1] G. M. Muñoz Caro, Y.-J. Chen, S. Aparicio et al., *A&A*, 589, A19, 2016
- [2] Y.-J. Chen, G. M. Muñoz Caro, S. Aparicio et al., *Phys. Rev. Lett.*, 119, 157703, 2017

## Process of Methanol Desorption due to Hydrogen Atom Exposure of Solid Methanol at Low Temperature

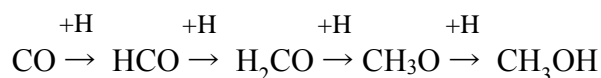
Y. Yarnall,<sup>1,2</sup> H. Hidaka,<sup>1</sup> R. Escribano<sup>3</sup>, W. M. C. Sameera<sup>1</sup>, Y. Oba<sup>1</sup>, M. Tsuge<sup>1</sup>, T. Hama<sup>1</sup>, A. Kouchi<sup>1</sup>, and N. Watanabe<sup>1</sup>

<sup>1</sup> *Institute of Low Temperature Science, Hokkaido University, Sapporo, Hokkaido, Japan.*

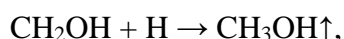
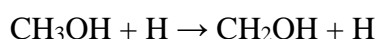
<sup>2</sup> *Chemistry and Biochemistry, George Mason University, Fairfax, VA, United States.*

<sup>3</sup> *Instituto de Estructura de la Materia, CSIC, Serrano 123, 28006 Madrid, Spain.*

Molecular clouds (MCs) are cold (~10K) and dark (small UV flux) objects and are the place for the ‘early phase of chemical evolution’ in space [1]. In such an environment, non-thermal chemical reactions involving atom tunneling on interstellar grains is one of the most important processes for chemical evolution [7]. Methanol (CH<sub>3</sub>OH), a precursor of complex organic molecule, is one of the abundant molecules which has been found in both gas and solid phases of MCs. Methanol can be formed by the successive hydrogen atom addition to carbon monoxide via H<sub>2</sub>CO formation on a grain surface, called CO hydrogenation [2, 4].



Reaction network calculation cannot reproduce the amount of gaseous CH<sub>3</sub>OH observed by only the chemistry of gas-phase reactions [5]. Thus, to explain the abundance of gaseous methanol, the desorption of solid CH<sub>3</sub>OH has been theoretically suggested as one of the candidates for supplying gaseous CH<sub>3</sub>OH [5, 6]. Chemical desorption which is triggered by releasing the heat of reaction during CH<sub>3</sub>OH formation on a grain surface would be a major desorption process because other desorption, thermal and photo desorption, cannot work efficiently in the MC’s environment. Recently, Chuang *et al.* (2018) had conducted experiments for studying chemical desorption occurred during the sequential reactions of CO hydrogenation and reported the desorbed amount as the amount of total carbon loss [3]. We focus on the chemical desorption of only methanol by the following reactions,



and conducted the experiments of H atoms exposure of solid methanol on amorphous solid water (ASW) at 10K. In this presentation, we show an evidence of the methanol desorption by the chemical desorption process and discuss problems that we must consider when applying experimental results to the reaction network calculation in MCs.

### References

- [1] A. G. G. M. Tielens, 2015, *Reviews of Modern Physics* 85, p. 1021–1081.
- [2] H. Hidaka, N. Watanabe, T. Shiraki, A. Nagaoka, & A. Kouchi, 2004, *ApJ* 614, p. 1124–1131.
- [3] K.-J. Chuang, G. Fedoseev, D. Qasim, S. Ioppolo, E.F.van Dishoeck, & H. Linnartz, 2018, *ApJ* 853, p. 102.
- [4] N. Watanabe and A Kouchi, 2002, *ApJ* 571, L173–L176.
- [5] R.T. Garrod, I.H. Park, P. Caselli, & E. Herbst, 2006, *RSC133*, p. 51-62.
- [6] R.T. Garrod, V Wakelam, & E. Herbst, 2007, *A&A* 467, p. 1103-1115.
- [7] T. Hama, & N. Watanabe, 2013, *Chemical Reviews*, p. 8783-8839.



## Formamide production during dust grain impacts

C. Cecchi-Pestellini,<sup>1</sup> G. Cassone,<sup>2</sup> A. Ciaravella<sup>1</sup>

<sup>1</sup>*INAF - Osservatorio Astronomico di Palermo,  
P.za Parlamento 1, 90134 Palermo, Italy*

<sup>2</sup>*Institute of Biophysics of the Czech Academy of Sciences,  
Královopolská 135, 61265 Brno, Czech Republic*

Thus far, amino acids have not been identified in the ISM. However, a few species with the peptide moiety have been detected (e.g., formamide, NH<sub>2</sub>CHO), perhaps the most important for proteins. The role played by formamide in the emergence of terrestrial life is one of the hottest subjects of contemporary research on the origins of life (e.g. Saladino et al. 2015 and Becker et al. 2016). While formamide is readily formed in interstellar ice analogs (e.g., Jones et al. 2011, and references therein), its gas-phase synthesis has also been suggested (Kahane et al. 2013; Barone et al. 2015). Possible support for this new chemical scenario may come from the observations of formamide emission in a shocked region around a solar-type protostar (Codella et al. 2017). However, Quénard et al. (2018) have shown that either gas-phase formation or grain surface synthesis may dominate depending on the physical conditions of the source. Consequently, both formation routes may possibly co-exist. This makes dust-related chemistry a very lively area of current research.

Here we report on a study, based on the multi-scale shock-compression technique combined with ab initio molecular dynamics approaches, where the shock-wave-driven chemistry of mutually colliding isocyanic acid (HNCO) containing icy grains has been simulated by first principles. At the shock-wave velocity threshold triggering the chemical transformation of the sample (7 km/s), formamide is the first synthesized species, thus being the springboard for the further complexification of the system. Also, upon increasing the shock impact velocity, formamide is formed in progressively larger amounts. More interestingly, at the highest velocity considered (10 km/s), impacts drive the production of diverse carbon-carbon bonded species. In addition to glycine, the building block of alanine (i.e., ethanimine) and one of the major components of a plethora of amino acids including, e.g., asparagine, cysteine, and leucine (i.e., vinylamine), have been detected after shock compression.

Conversion from chemical simplicity to chemical complexity can thus occur very rapidly within the transient events following catastrophic impacts.

### References

- Barone, V., Latouche, C., Skouteris, D., et al. 2015, MNRAS, 453, L31  
 Becker, S., Thoma, I., Deutsch, A., et al. 2016, Sci, 352, 833  
 Codella, C., Ceccarelli, C., Caselli, P., et al. 2017, A&A, 605, L3  
 Kahane, C., Ceccarelli, C., Faure, A., & Caux, E. 2013, ApJL, 763, L38  
 Quénard, D., Jiménez-Serra, I., Viti, S., Holdship, J., & Coutens, A. 2018, MNRAS, 474, 2796  
 Saladino, R., Carota, E., Botta, G., et al. 2015, PNAS, 112, E2746

## The Origin of Life and the Crystallization of Aspartic Acid in Water

Tu Lee\*, Yu Kun Lin

*Department of Chemical and Materials Engineering, National Central University, 300  
Jhong-Da Road, Jhong-Li City 320, Taiwan, R.O.C.*

The unusual molecular complexation of the enantiomers of aspartic acid in water was discovered and proven by a solubility test, solution freezing point, crystallization kinetics, and the incubation time change. The transformation of a “conglomerate solution” (CS) to a “racemic compound solution” (RCS) was dependent on both temperature and time. The CS was the solution phase which produced conglomerate crystals, and the RCS was the solution phase which gave a racemic compound. Fourier transformed infrared spectroscopy and powder X-ray diffraction were used to characterize aspartic acid solids crystallized from those complex solution phases and to distinguish conglomerate crystals from a racemic compound. We found that it took more than 36 h at 25 °C and 5 h at 45 °C just to complete the solution phase transformation of the CS of aspartic acid to the RCS of aspartic acid. However, the presence of an equimolar of succinic acid could hinder the solution phase transformation of the CS of aspartic acid to the RCS of aspartic acid for up to at least 8 h at 60 °C. This leeway of hours had provided an opportunity for the thermodynamically stable racemic aspartic acid to convert into the metastable conglomerate in water first by either a rapid acid-base reaction or the addition of an antisolvent with the temperature drop, without being concerned by its back conversion later to a racemic compound thermodynamically for quite some time. As a result, enantioseparation of aspartic acid by preferential crystallization in a large scale would have been very common and easy to occur on the primitive earth.

### Reference

[1] Lee, T.; Lin, Y. K. The origin of life and the crystallization of aspartic acid in water. *Cryst. Growth Des.* **2010**, *10*(4), 1652-1660.

## Phosphorescence of hydrogen-capped polyenes in solid neon at 20 K

T. Wakabayashi,<sup>1</sup> K. Ozaki,<sup>1</sup> R. Sata,<sup>1</sup> H. Suzuki,<sup>1</sup> Y. Morisawa,<sup>1</sup> and U. Szczepaniak<sup>2</sup>

<sup>1</sup>Department of Chemistry, School of Science and Engineering, Kindai University, Japan

<sup>2</sup>Institute of Physical Chemistry, Polish Academy of Sciences, Poland

Linear carbon chain molecules are highly reactive and thought to be reaction intermediates converted to carbon nanostructures such as fullerenes, nanotubes, and graphene. Terminated by hydrogen or chemically inert moieties such as a cyano-group, the carbon chain molecules acquire intrinsic stability to be isolated in solutions at ambient temperature. We have developed a method to produce, isolate, and concentrate in solutions a series of hydrogen-end-capped molecules, namely polyynes  $\text{H}(\text{C}\equiv\text{C})_n\text{H}$  ( $n = 4-8$ ), to characterize them by UV absorption, IR absorption [1], and resonance Raman spectroscopy [2]. Formation mechanism of cyanopolyynes,  $\text{H}(\text{C}\equiv\text{C})_n\text{C}\equiv\text{N}$  ( $n = 3-6$ ), was also investigated by NMR spectroscopy using  $^{13}\text{C}$  isotope-enriched samples [3]. Recently, phosphorescence spectra were reported for cyanopolyynes through  $\text{HC}_5\text{N}$  to  $\text{HC}_9\text{N}$  in solid rare-gas matrices [4-6]. In the present work, size-separated polyynes were co-condensed with the solvent molecules of hexane at 20 K in vacuum and subjected to phosphorescence spectroscopy.

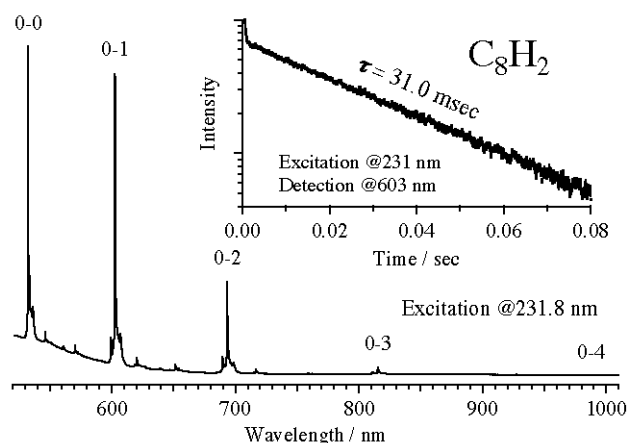


Figure 1: Phosphorescence spectrum of  $\text{C}_8\text{H}_2$  in solid hexane at 20 K. Peaks in vibrational progression of the symmetric stretching  $\nu_2$  mode of the  $sp$ -carbon chain ( $\sim 2190\text{ cm}^{-1}$ ) are conspicuous at 532, 603, 694, 815, and 988 nm for  $0-\nu$  bands ( $\nu = 0-4$ ). Inset shows phosphorescence lifetime of  $\sim 31.0\text{ ms}$  for the  $a^3\text{C}_g^+ \rightarrow \text{X}^1\text{C}_g^+$  transition of  $\text{C}_8\text{H}_2$  at 20 K.

### References

- [1] Y. Wada *et al.* *Chem. Phys. Lett.* **541**, 54-59, (2012).
- [2] T. Wakabayashi *et al.* *Chem. Phys. Lett.* **433**, 296-300, (2007).
- [3] T. Wakabayashi *et al.* *Carbon* **50**, 47-56, (2012).
- [4] M. Turowski *et al.* *J. Chem. Phys.* **133**, 074310 (2010).
- [5] I. Couturier-Tamburelli *et al.* *J. Chem. Phys.* **140** (2014) 044329.
- [6] U. Szczepaniak *et al.* *J. Phys. Chem. A* **121**, 7374 (2017).

## Variation of carbon isotopic composition with formation of clathrate hydrate

T. Inoue, A. Kinjo, R. Netsu and T. Ikeda-Fukazawa

*Department of Applied Chemistry, Meiji University, Japan*

In interstellar molecular clouds, various molecules such as H<sub>2</sub>O, CO, CO<sub>2</sub>, CH<sub>3</sub>OH, H<sub>2</sub>CO, and NH<sub>3</sub> are condensed onto dust grains. Water exists as amorphous ice on the dust grains and is transformed into various structures depending on thermal conditions and compositions of coexisting molecules. From the results using transmission electron microscopy and Fourier transformed infrared (IR) spectroscopy, it was found that the vapor deposited amorphous ice including CH<sub>3</sub>OH and CO<sub>2</sub> is transformed into clathrate hydrate at around 120 K [1]. This suggests that the cometary ice exists as clathrate hydrate. Clathrate hydrates are inclusion compounds consisting of water molecules and a variety of guest molecules. From infrared astronomical observation, it was found that the <sup>12</sup>C/<sup>13</sup>C isotopic ratio of comets is larger than that of interstellar matter [2]. To investigate the effect of clathrate hydrate formation on <sup>12</sup>C/<sup>13</sup>C isotopic ratio, IR spectra of vapor deposited amorphous ice including <sup>12</sup>CO<sub>2</sub> and <sup>13</sup>CO<sub>2</sub> were measured. Using the spectra, the variation process of <sup>12</sup>CO<sub>2</sub>/<sup>13</sup>CO<sub>2</sub> ratio during warming was analyzed.

Amorphous ice including <sup>12</sup>CO<sub>2</sub> and <sup>13</sup>CO<sub>2</sub> was prepared with vapor deposition of mixture of <sup>12</sup>CO<sub>2</sub>, <sup>13</sup>CO<sub>2</sub> gases and distilled and degassed water on a substrate of oxygen-free copper at 43 K. In the gas mixture, the <sup>12</sup>C/<sup>13</sup>C isotopic ratios were 4–92, and (<sup>12</sup>CO<sub>2</sub> + <sup>13</sup>CO<sub>2</sub>)/H<sub>2</sub>O ratio was 1. The total pressure in the vacuum chamber was kept at about  $5.0 \times 10^{-5}$  Pa during the deposition. After the deposition of amorphous ice, the substrate was warmed to 180 K at a rate of 1–4 K/min. The IR spectra were measured using a spectrometer (Shimadzu IRPrestage-21) at 2 K intervals during warming. To analyze the sublimation behaviors, the temperature programmed desorption (TPD) curves were also measured using quadrupole mass spectrometer (Pfeiffer QME220) during warming.

The results show that the wave number of the O–H stretching modes of H<sub>2</sub>O, <sup>12</sup>C=O asymmetric stretching mode of <sup>12</sup>CO<sub>2</sub>, and <sup>13</sup>C=O asymmetric stretching modes of <sup>13</sup>CO<sub>2</sub> during the warming significantly change at  $100 \pm 10$  K. The wave number of newly appeared peak at this temperature was close to that of <sup>12</sup>C=O asymmetric stretching mode of <sup>12</sup>CO<sub>2</sub> in clathrate hydrate. Furthermore, a gas release was also observed at this temperature from the TPD curves. These results indicate the formation of CO<sub>2</sub> clathrate hydrate at  $100 \pm 10$  K. From the analyses of integrated intensities of <sup>12</sup>CO<sub>2</sub> and <sup>13</sup>CO<sub>2</sub> peaks, it was found that the <sup>12</sup>CO<sub>2</sub>/<sup>13</sup>CO<sub>2</sub> ratio increases at around 100 K. These results suggest that the formation of clathrate hydrate from amorphous ice with warming can be a cause of <sup>12</sup>C condensation. Furthermore, it was found that the changing rate of <sup>12</sup>CO<sub>2</sub>/<sup>13</sup>CO<sub>2</sub> with formation of clathrate hydrate depends on initial <sup>12</sup>C/<sup>13</sup>C ratio in amorphous ice. The present results have important implications for water states and their role in materials' evolution in the universe.

### References

- [1] D. Blake, L. Allamandola, S. Sandford, D. Hudgins, F. Freund, 1991, *Science* 254, 548
- [2] V. Vanysek, J. Rahe, 1978, *The Moon and the Planets* 18, 441
- [3] F. Fleyfel, J. P. Devlin, 1991, *J. Phys. Chem.* 95, 3811

## Effects of defects on structure of amorphous ice

A. Yoshimura and T. Ikeda-Fukazawa

*Department of Applied Chemistry, Meiji University, Japan*

In interstellar molecular clouds, various molecules (e.g., H<sub>2</sub>O, NH<sub>3</sub>, CO, CO<sub>2</sub>, and so on) are formed from elements such as H, C, O, and N [1]. Most of H<sub>2</sub>O in interstellar molecular clouds exists as a thin shell of amorphous ice around dust grain. The molecules, which are adsorbed or included in amorphous ice, undergo chemical evolutions to organic molecules through various reaction processes. The photochemical reaction caused by ultraviolet (UV) photon irradiation is one of the dominant reaction processes [2]. Thus, the variation in structure of amorphous ice with UV-irradiation is an important factor to understand the processes of molecular evolutions. Recently, Tachibana *et al.* [3] found that the viscosity of the UV-irradiated amorphous ice decreases at around 50 K, and becomes a lower value than that at the glass transition temperature. The defects formed by UV-irradiation are expected as a cause of the decrease in viscosity. To investigate the effects of defects on the structure of amorphous ice, the molecular dynamics (MD) calculations of amorphous ice including OH and OH<sup>-</sup> were performed.

The MD calculations were performed using an atom-atom potential model with MXDORTO program [4]. We used an interatomic potential model (KAWAMURA potential model) for the potential parameters of water molecule [5]. The potential parameters of OH and OH<sup>-</sup> were determined by constraining molecular structure to reproduce the energy surfaces obtained from molecular orbital calculations. The amorphous ice was prepared by quenching of a liquid phase consisting of 360 water molecules from 290 K to 10 K [5]. The system including OH (or OH<sup>-</sup>) with 5% in concentration was prepared by replacing 18 H<sub>2</sub>O molecules with 18 OH (or 18 OH<sup>-</sup>) at 10 K. To equilibrate fundamental cell, the MD code was run for 2 ns at 10 K. Then, the system was warmed to 90 K with  $2.5 \times 10^{-5}$  K/fs in rate. The viscosity of amorphous ice was estimated using Stokes–Einstein relation.

The result shows that the density of amorphous ice including OH with 5% in concentration is lower than that of pure amorphous ice, whereas that including OH<sup>-</sup> is higher. For the viscosity, the amorphous ices including OH and OH<sup>-</sup> have lower and higher values in comparison with that of pure amorphous ice, respectively. In order to investigate the mechanisms of the variations in density and viscosity with formation of defects, the local structures around the defects were analysed. The results show that the mean coordination number of OH is 1.29, while that of OH<sup>-</sup> is 4.35. For H<sub>2</sub>O, the coordination numbers for both of the states are close to the value of pure amorphous ice. This indicates that the variations in density and viscosity are resulted from the local structures around the defects. The density of amorphous ice decreases as the coordination number decreases. The enhancement of thermal vibrations of OH due to the release from restrictions of surrounded molecules can be a cause of decrease in viscosity.

### References

- [1] J. M. Greenberg and J. I. Hage, *Astrophys. J.* **361**, 260 (1990).
- [2] F. J. Ciesla and S. A. Sandford, *Science* **336**, 452 (2012).
- [3] S. Tachibana *et al.*, *Sci. Adv.* **3**, eaao2538 (2017).
- [4] K. Kawamura, MXDORTO, Japan Chemistry Program Exchange, #29 (1990).
- [5] Y. Kumagai and T. Ikeda-Fukazawa, *Chem. Phys. Lett.* **678**, 154 (2017).

## Effects of Adsorbed H<sub>2</sub>O amorphous ice on Surface Structure of Forsterite Glass

A. Kubo, J. Nishizawa, and T. Ikeda-Fukazawa

*Department of Applied Chemistry, Meiji University, Japan*

Forsterite (Mg<sub>2</sub>SiO<sub>4</sub>) glass exists as dust grains in interstellar molecular clouds and young stellar objects [1]. In interstellar molecular clouds, elements such as hydrogen, oxygen, carbon, and nitrogen deposit on dust grains, and form various molecules (e.g., H<sub>2</sub>O, CO, CO<sub>2</sub>, NH<sub>3</sub>, CH<sub>4</sub>, H<sub>2</sub>CO, CH<sub>3</sub>OH, and so on) [2]. These molecules undergo chemical evolutions to organic molecules through various processes on the surface of dust grains [2]. The structure of forsterite glass is one of the important factors governing the chemical evolutions in interstellar molecular clouds. However, there are few studies for effects of molecular adsorption on the structure and properties of forsterite glass [3]. To investigate the adsorption process of H<sub>2</sub>O and the effect of adsorption on surface structure of forsterite glass, molecular dynamics (MD) calculations were performed.

The MD calculations were performed using an atom-atom potential model with MXDORTO program [4]. The potential parameters for forsterite were empirically determined by constraining the structure to reproduce the experimental results of density, thermal expansion coefficient, and bulk modulus [5]. For H<sub>2</sub>O, KAWAMURA potential model was used [6]. A fundamental orthorhombic cell consisting of 2400 Mg<sub>2</sub>SiO<sub>4</sub> with two-dimensional periodic boundary conditions was used. The glass structure was prepared by quenching the liquid phase from 3000 to 10 K with 2 K/fs in rate. The quenched glass was warmed to 300 K with the same rate, and 2682 H<sub>2</sub>O were adsorbed on the glass. Then, the system was quenched to 10 K with 2 K/fs, and structures were analyzed at 10 K. The MD code was run with NTV ensemble.

The result shows that the atomic displacement parameter (ADP) of each atomic species in forsterite (i.e., Mg, Si, and O) in the interface decreases with adsorption of H<sub>2</sub>O amorphous ice. For the forsterite glass without water adsorption, the ADP values of the surface layer were higher than those of internal part due to existence of dangling bonds in the surface layer. To investigate the mechanisms of ADP decrease observed in the interface with amorphous ice, the coordination number of the magnesium atoms was analyzed. The result shows that the coordination number in the interface layer increases with adsorption of H<sub>2</sub>O amorphous ice, because new covalent bonds are formed with the adsorbed H<sub>2</sub>O molecules. The decrease in the ADP values observed in the interface is resulted from the variation of the coordination number. The mean Mg–O length of the newly formed covalent bonds is 0.256 nm, and is slightly longer than that in the MgO<sub>x</sub> units in the forsterite glass without water adsorption (i.e., 0.238 nm). Due to the formation of covalent bonds with H<sub>2</sub>O molecules, MgO<sub>x</sub>H<sub>2</sub> units exist as an intermediate state in the interface with forsterite glass and amorphous ice. The present results have important implications for the role of forsterite glass in chemical evolutions in the universe.

### References

- [1] J. P. Bradley, L. P. Keller, T. P. Snow, M. S. Hanner, G. J. Flynn, J. C. Geno, S. J. Clemett, D.E. Broenlee, J. E. Bowey, 1999, **Science** 285, 1716.
- [2] N. Watanabe, A. Kouchi, 2008, **Prog. Surf. Sci.** 83, 439.
- [3] J. A. Tangeman, B. L. Phillips, A. Navrotsky, J. K. R. Weber, A. D. Hixson, T. S. Key, 2001, **Geophys. Res. Lett** 28, 2517.
- [4] K. Kawamura, MXDORTO, 1990, **Japan Chemistry Program Exchange**, #029.
- [5] T. Ikeda-Fukazawa, 2016, **J. Soc. Inorg. Mater. Jpn** 23, 130.
- [6] Y. Kumagai, T. Ikeda-Fukazawa, 2017, **Chem. Phys. Lett** 678, 154.

## Structure and dynamics of amorphous ice including carbon dioxide

Y. Naoshima and T. Ikeda-Fukazawa

*Department of Applied Chemistry, Meiji University, Japan*

In interstellar molecular clouds, various elements such as hydrogen, oxygen, carbon, and nitrogen are condensed onto dust grains, and formed H<sub>2</sub>O amorphous ice and various molecules (e. g., CO<sub>2</sub>, NH<sub>3</sub>, CH<sub>4</sub>, H<sub>2</sub>CO, and so on). The various gas molecules, which are included in amorphous ice as impurities, undergo chemical evolutions to organic molecules through various processes [1]. Thus, the structure and properties of amorphous ice including gas molecules are important to understand the molecular evolutions of organic molecules [2]. To investigate the effects of included gas molecules on the structure and properties of amorphous ice, the molecular dynamics (MD) calculations of amorphous ice including CO<sub>2</sub> were performed.

We used an interatomic potential model (KAWAMURA potential model) for the MD simulations [3]. The amorphous ice was prepared by quenching of a liquid phase consisting of 368 water molecules and  $n$  CO<sub>2</sub> molecules ( $n = 0-64$ ) from 360 K to 200 K with 1.0 K/fs in cooling rate. After annealing at 200 K, the system was cooled to 60 K with 1.0 K/fs. The density of the system at 60 K depends on the time period of the annealing at 200 K, and was controlled to be 0.960 g/cm<sup>3</sup> in the present study. For the system with  $n > 4$ , CO<sub>2</sub> molecules formed a cluster before the quenching at 360 K. To prepare a system with isolated CO<sub>2</sub> molecules, pure amorphous ice was formed by quenching with the same procedure. Then,  $m$  H<sub>2</sub>O molecules were replaced with  $m$  CO<sub>2</sub> molecules ( $m=1-61$ ) at 60 K.

The results show that the density of H<sub>2</sub>O ice with a CO<sub>2</sub> cluster is larger than that of pure ice and the density increases with increase in  $n$ . On the other hand, the density of H<sub>2</sub>O ice with isolated CO<sub>2</sub> molecules decrease with increase in  $m$ . To investigate the mechanisms of the density changes in H<sub>2</sub>O ice, the vibrational densities of states of H<sub>2</sub>O were calculated. The results show that the frequency of O-H stretching mode with both of isolated CO<sub>2</sub> and CO<sub>2</sub> cluster is higher than that of pure amorphous H<sub>2</sub>O ice. This indicates that the included CO<sub>2</sub> has effect to weaken the strength of hydrogen bonds of surrounding H<sub>2</sub>O ice. The mean coordination number of H<sub>2</sub>O in amorphous ice including isolated CO<sub>2</sub> is smaller than that of pure amorphous H<sub>2</sub>O ice. On the other hand, the mean coordination number of H<sub>2</sub>O ice with CO<sub>2</sub> cluster is close to that of pure amorphous H<sub>2</sub>O ice except for the interface with CO<sub>2</sub> cluster. These results suggest that the isolated CO<sub>2</sub> has effects to decrease the density of H<sub>2</sub>O ice due to decreasing of hydrogen bonding number of H<sub>2</sub>O molecules, whereas the cluster CO<sub>2</sub> causes an increase in density by distortion of local structure of ice in the interface. From the results, we discuss the effects of carbon dioxide on structure and dynamics of amorphous ice.

### References

- [1] A. Kouchi, T. Yamamoto, T. Kuroda, J. M. Greenberg, 1994, *Astron. Astrophys.* 290, 1009.
- [2] Y. Kumagai, T. Ikeda-Fukazawa, 2017, *Chem. Phys. Lett.* 678, 153.
- [3] N. Kumagai, K. Kawamura, T. Yokokawa, 1994, *Mol. Simul.* 12, 177.

**Electron dynamics described by real-time TDHF/TDDFT calculation:  
Application to the dissociative recombination reaction**

T. Akama,<sup>1</sup> T. Koyama,<sup>2</sup> and T. Taketsugu<sup>1,2</sup>

<sup>1</sup>*Department of Chemistry, Faculty of Science, Hokkaido University, Japan*

<sup>2</sup>*Graduate School of Chemical Sciences and Engineering, Hokkaido University, Japan*

Electron dynamics is an ultrafast phenomenon occurring in attoseconds, which was recently observed by experiments and has attracted much attention. Electron dynamics is caused by change of external field of the intriguing system, such as light or collision of molecules and electrons. Therefore, electron dynamics should play an important role in reaction of interstellar matters which is sometimes concerned with electronically excited states. To elucidate mechanism of electron dynamics, theoretical calculation would be a powerful tool. Real-time propagation (RT) of time-dependent theories, such as time-dependent Hartree-Fock (TDHF) method and time-dependent density functional theory (TDDFT), have been applied to describing electron dynamics.

The dissociative recombination (DR) reaction is a combination of an electron and a positive molecular ion, followed by the dissociation into several neutral fragments ( $XY + e^- \rightarrow [XY]^* \rightarrow X + Y$ ). The DR reaction proceeds via the direct process or the indirect process. In the direct process, the molecular system directly hops to the dissociative excited state of neutral molecule after capturing an electron, while in the indirect process, this transition proceeds via Rydberg states. In the previous studies for DR reactions, AIMD calculation was performed for the direct process [1] and the indirect process [2,3], although the electron capture process was not considered explicitly.

In this study, we applied RT-TDHF/TDDFT calculation describing electron dynamics to the indirect process of the DR reaction. The electron capturing process ( $XY + e^- \rightarrow [XY]^*$ ) of the indirect process was approximately described by the electron dynamics calculation using RT-TDHF/TDDFT, starting with the initial condition that an electron added to the Rydberg orbital of the ground state of the cation. To analyze this calculation and obtain the distribution to the excited states (including Rydberg and dissociative states), Fourier transform analysis was applied to time evolution of polarization vector and density matrix elements.

## References

- [1] T. Taketsugu, A. Tajima, K. Ishii, & T. Hirano, 2004, ApJ 608, 323.
- [2] M. Kayanuma, T. Taketsugu, & K. Ishii, 2006, CPL 418, 511.
- [3] M. Kayanuma, T. Taketsugu, & K. Ishii, 2008, TCA 120, 191.



## Quantum chemical prediction of possible reactions of interstellar nucleobases

Y. Komatsu<sup>1,2,3</sup> and T. Suzuki<sup>1,2</sup>

<sup>1</sup>*NINS-Astrobiology Center, Japan*

<sup>2</sup>*Division of Optical and Infrared Astronomy,  
National Astronomical Observatory of Japan, Japan*

<sup>3</sup>*“Materials research by Information Integration” Initiative,  
National Institute for Materials Science, Japan*

Nucleobases, which generate the genetic code, i. e. ATCG, were detected from the Murchison meteorite [1]. To take the fact as well into consideration that glycine, the simplest amino acid, was detected both from Murchison meteorite and the comet 67P/C-G, life-related molecules can be constructed easily in an extra-terrestrial environment.

In this study, to estimate possible reactions of nucleobases in the ultracold environment and consider which are key components and where are suitable regions to proceed reactions of such complex molecules, we use the Global Reaction Route Mapping (GRRM) program [2] in order to discover complicated reaction networks, and focus especially on dissociation channels.

At first, we estimated rough profiles of reactions in vacuum with realistic computational costs. As a result, we found two key reaction paths toward pyrimidine from abundant interstellar molecules, HCN, C<sub>2</sub>H<sub>2</sub> (Figure 1). Both reactions have high reaction barriers, which indicate the difficulty in ultralow-temperature environment. To avoid the higher barriers, the formation of C<sub>2</sub>H<sub>2</sub>NCH with lower reaction barrier was evaluated. Key reactions on icy grain surface will be presented. In addition to pyrimidine, the estimated paths toward cytosine, thymine, uracil were also estimated and will be presented.

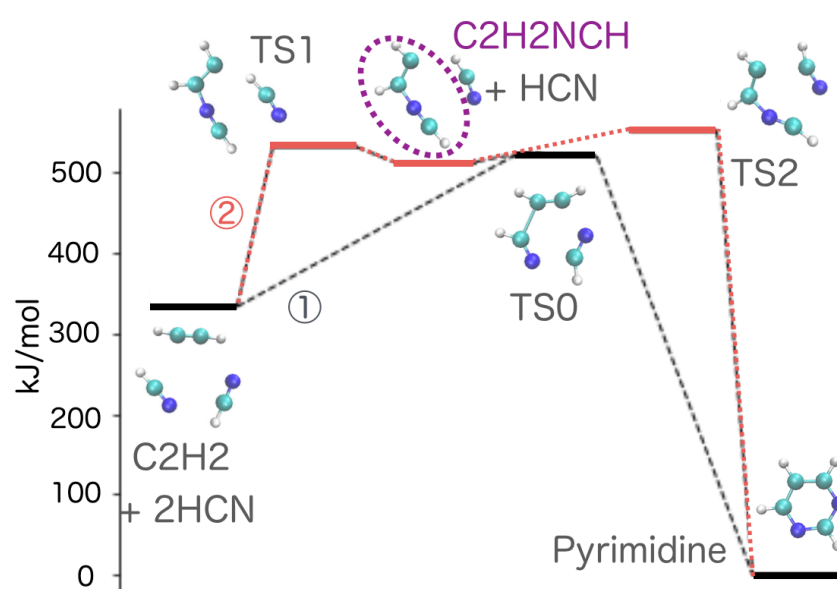


Figure 1: Two reaction paths toward pyrimidine were discovered. The potential energies for stable structures and transition states are shown. Each energy was evaluated at MP2/aug-cc-pVTZ level.

### References

- [1] Z. Martins et al., 2008, Earth and planetary science Letters 270, 130.
- [2] K. Ohno & S. Maeda, 2004, The Journal of Physical Chemistry A 110.28, 8933.

## A new path for H<sub>2</sub> formation supposed to occur in the CO rich ice-mantle

Tsuneo Hirano,<sup>1</sup> Yuriko Ono,<sup>2</sup> Haruka Aota,<sup>1</sup> Miki Uehara,<sup>1</sup> and Tetsuya Taketsugu<sup>2</sup>

<sup>1</sup> Department of Chemistry, Ochanomizu University, Japan

<sup>2</sup> Department of Chemistry, Faculty of Science, Hokkaido University, Japan

Low temperature surface or solid-phase radical reaction on interstellar dusts has been paid much attention for the understanding of chemical evolution of molecules in dark clouds. Several stationary points for reactions of CO with H atom yielding HCO and HOC were examined at the level of MR-SDCI/cc-pVTZ (Fig.1). Throughout the following exothermal reactions (1), (2), and (3), ice-mantle serves as the reaction-heat absorber in making the reaction facilitate.

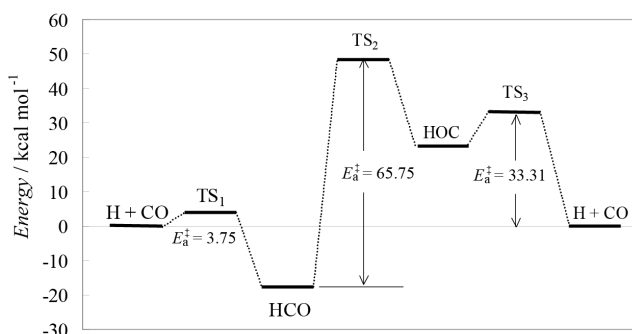
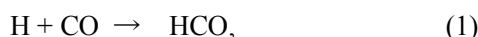


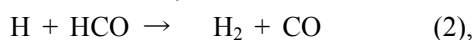
Fig. 1 Energy profile for the reactions between H and CO.

First, the reaction,



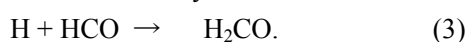
has a reaction barrier of ca. 3.75 kcal/mol. At the typical temperature of 15 K in the molecular cloud, the barrier in the reaction is too high, so that only tunneling reaction would be feasible between the reactants adsorbed on neighboring sites (Langmuir-Hinshelwood mechanism). Tunneling probability is calculated to be as small as  $1.7 \times 10^{-10}$ , but hydrogen atom trapped in a potential well on the ice-surface will repeat the collision with CO through  $ca 10^{13}$  oscillations/sec, resulting in the completion of tunneling in 3.2 msec.

The succeeding reaction with H atom, which approaches from (A) side in Fig. 2, results in hydrogen abstraction from HCO yielding H<sub>2</sub> and CO molecules,



as shown by successive red-arrow marks.

Alternatively, the approach from (B) side results in formaldehyde formation.



Both reactions (2) and (3) are calculated to be a down-hill reaction without activation energy barrier.

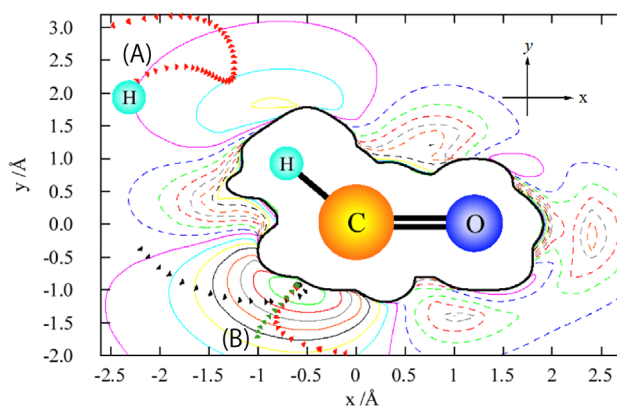


Fig. 2 2D potential energy surface around HCO.

Accordingly, combination of reactions (1) and (2) will make a H<sub>2</sub> production cycle. Here, CO behaves just like the catalyst in the cycle. This is another new reaction path for the H<sub>2</sub> production from H atoms in space through neutral reaction (*cf.* [1]).

[1] J. Takahashi, K. Masuda, and M. Nagaoka, *ApJ*, **520**,724 (1999).

## Theoretical study of the photodissociation reaction of sulfate ion in water solution

H. Soma<sup>1</sup>, A. Ohta<sup>1</sup>, O. Kobayashi<sup>2</sup>, and S. Nanbu<sup>1</sup>

<sup>1</sup>Department of Chemistry, Sophia University, Japan

<sup>2</sup>Department of Chemistry, Yokohama City University, Japan

Photolysis of  $\text{SO}_4^{2-}$  in water after excitation to the second and fourth excited states ( $S_2$  and  $S_4$ ) was studied by an on-the-fly *ab initio* molecular reaction dynamics (MRD) simulation based on Particle Mesh Ewald summation [1] with ONIOM model (PME-ONIOM [2]). SA-CASSCF /MIDI4\* basis set [3] was employed to describe the electronic structure of  $\text{SO}_4^{2-}$  (QM part); the water solution was treated at MM level. At the photoexcitation to  $S_2$ , the two different dissociation channels,  $\text{O}(^1\text{D}) + \text{SO}_3^{2-}(1^1\text{A}_1)$  and  $\text{O}(^2\text{P}) + \text{SO}_3^-(1^2\text{A}_1)$ , were found. But the vertical excitation energy was 9.96 eV, which means that the photolysis might not happen by solar-flux. On the other hand, we found dispersion function for basis set plays an important role to reduce the excitation energy by 5.30 eV. Therefore, on-the-fly *ab initio* MD are going to be executed at aug-cc-pVDZ basis set. We will discuss the result at that level.

**Table 1.** Vertical excitation energy that calculated by CASSCF method / eV

State	Basis function			
	MIDI4*	cc-pVDZ	cc-pVTZ	aug-cc-pVDZ
$S_1$	9.76	9.56	9.13	5.14
$S_2$	9.96	9.76	9.26	5.30
$S_3$	10.5	10.4	9.73	5.37
$S_4$	11.1	10.8	10.3	6.67

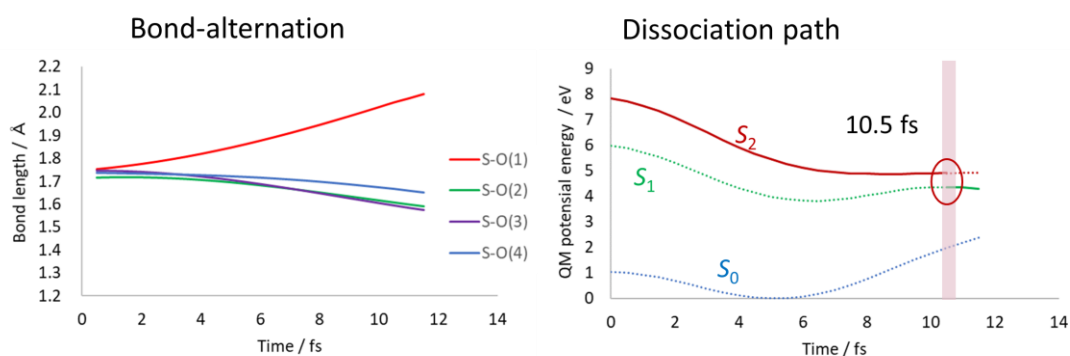


Figure 1: Result from photoexcitation to  $S_2$  by aug-cc-pVDZ

### References

- [1] L.W.Chung, W.M.C.Sameera, R.Ramozzi *et al.* *Chem. Rev.*, **115**, 5678-5796 (2015)
- [2] O. Kobayashi and S. Nanbu, *Chem. Phys.*, **461**, 47 (2015).
- [3] Y.Sakai, H.Tatewaki, S.Huzinaga, *J. Comput. Chem.*, **2**, 108 (1981).

## Methoxy radical on interstellar ices: a quantum mechanics/molecular mechanics study

W. M. C. Sameera,<sup>1</sup> Muhsen Abood Al-Ibadi,<sup>2</sup> Bethmini Senevirathne,<sup>3</sup> Stefan Andersson,<sup>4</sup> Gunnar Nyman,<sup>3</sup> Naoki Watanabe<sup>1</sup>

<sup>1</sup>*Institute of Low Temperature Science, Hokkaido University, Kita-ku North 19 West 8, Sapporo 060-0819, Japan.*

<sup>2</sup>*Department of Chemistry, Faculty of Science, University of Kufa, Alnajaf, Iraq.*

<sup>3</sup>*University of Gothenburg, Department of Chemistry and Molecular Biology, Kemigården 4, SE-412 96 Gothenburg, Sweden.*

<sup>4</sup>*SINTEF, P.O. Box 4760 Torgarden, NO-7465 Trondheim, Norway.*

The origin of the radical species in the interstellar medium (ISM), the mechanistic details of their formation, and their reactions are still not fully understood. These complex chemical processes are challenging to characterise from experimental studies. In this direction, theoretical and computational chemistry provides important contributions. The methoxy radical (CH<sub>3</sub>O) is a primary radical species in the ISM. The CH<sub>3</sub>O radical was observed in the cold and dense core Barnard-1b.[1] We have used a quantum mechanics/molecular mechanics (QM/MM) method to rationalise CH<sub>3</sub>O radical binding on crystalline hexagonal water ice (I<sub>h</sub>) and amorphous solid water (ASW).[2] In our QM/MM method,[3]-[6] the electronically important region (i.e. the binding site) is described by a quantum mechanical method, while a classical force field method is used for the remaining part. Therefore, our QM/MM approach provides accurate binding energies, and large ice clusters can be calculated at a low computational cost.

Depending on the dangling-hydrogen (*d*-H) or dangling-oxygen (*d*-O) at the binding site, a range of binding energies is observed. Computed averaged binding energies on I<sub>h</sub> and ASW are comparable, while I<sub>h</sub> with defects show relatively strong binding. Therefore, the distribution of *d*-Os and *d*-Hs on ice surfaces and the nature of the ice surface play a key role on the radical binding energies. Our study gives important insights about CH<sub>3</sub>O radical binding on interstellar ices.

### References

- [1] J. Cernicharo, N. Marcelino, E. Roueff, M. Gerin, A. Jiménez-Escobar, & G. M. Muñoz Caro, *The Astrophysical Journal Letters*, 759:L43 (4pp).
- [2] W. M. C. Sameera, Muhsen A. Al-Ibadi, B. Senevirathne, S. Andersson, G. Nyman, & N. Watanabe. (In preparation)
- [3] W. M. C. Sameera & F. Maseras, *J. Chem. Inf. Model*, 2018, 58, 1828-1835.
- [4] W. M. C. Sameera, B. Senevirathne, S. Andersson, F. Maseras, & G. Nyman, *J. Phys. Chem. C*, 2017, 121, 15223-15232.
- [5] D. Sharma, W. M. C Sameera, S. Andersson, G. Nyman, & M. J. Paterson, *ChemPhysChem*, 2016, 17, 4079-4089.
- [6] L. W. Chung, W. M. C. Sameera, R. Ramozzi, A. J. Page, M. Hatanaka, G. P. Petrova, T. V. Harris, X. Li, Z. Ke, F. Liu, H-B. Li, L. Ding, & K. Morokuma, *Chem. Rev.* 2015, 115, 5678-5796.

## Computational approach for detecting undetected interstellar molecules: CH<sub>2</sub>DOD and CHD<sub>2</sub>OD

Z. Awad<sup>1</sup> and A. Badawi<sup>2</sup>

<sup>1</sup>*Astronomy, Space Science and Meteorology Department, faculty of science, Cairo University, Egypt*

<sup>2</sup>*Zewail City of Science and Technology, Egypt*

Observations revealed that complex molecules (COMs) are very abundant in star forming regions (SFRs) either low-mass or massive. Methanol is believed to be the main driver of molecular complexity in the interstellar medium. Some deuterated forms of methanol; namely CH<sub>2</sub>DOD and CHD<sub>2</sub>OD, could play a role in the formation of deuterated COMs. We found that these undetected forms are detectable in SFRs (with abundances  $>10^{-12}n_H$ ). We ran theoretical models and computed the peak positions of the IR spectral lines of these species and compared them with experimentally predicted IR positions.

Our results are in agreement with experimental data. Given the calculated abundances of these undetected species and their spectral line positions, we recommend searches for these molecules in SFRs.

**On the detectability of undetected methanol forms in star forming regions**

Z. Awad<sup>1</sup> and A. Badawi<sup>2</sup>

<sup>1</sup>*Astronomy, Space Science and Meteorology Department, faculty of science, Cairo University, Egypt*

<sup>2</sup>*Zewail City of Science and Technology, Egypt*

The growing body of observed complex organic molecules (COMs), in particular deuterated isotopes, motivated us to revise the chemical networks used in modeling their chemistry. Methanol and its deuterated forms (all probable forms) are well-known parent molecules of more complex species. In this study, we are looking into the detectability of undetectable methanol forms and the impact of their inclusion in chemical models.

Our results showed that the undetectable forms of methanol such as CH<sub>2</sub>DOD and CHD<sub>2</sub>OD can be detected with abundances  $\sim \text{few} \times 10^{-11} n_{\text{H}}$  in cores around low-mass and massive star forming regions and their effect if added to chemical models without detection is minor. Therefore, we conclude that their inclusion in theoretical chemical models is safe.

**Fresh sublimates detected in a disk in outburst**

J.-E. Lee<sup>1</sup>, S. Lee<sup>1</sup>, G. Baek<sup>1</sup>, Y. Aikawa<sup>2</sup>, L. Cieza<sup>3</sup>, S.-Y. Yoon<sup>1</sup>, G. Herczeg<sup>4</sup>, and  
D. Johnstone<sup>5</sup>, S. Cassasus<sup>6</sup>

<sup>1</sup>*School of Space Research, Kyung Hee University, Korea*

<sup>2</sup>*Department of Astronomy, The University of Tokyo, Japan*

<sup>3</sup>*Facultad de Ingenier'ia y Ciencias, N'ucleo de Astronom'ia, Universidad Diego  
Portales, Chile*

<sup>4</sup>*Kavli Institute for Astronomy and Astrophysics, Peking University, China*

<sup>5</sup>*NRC Herzberg Astronomy and Astrophysics, Canada*

<sup>6</sup>*Departamento de Astronom'ia, Universidad de Chile, Chile*

Ices in protoplanetary disks are of special interest, since they are reservoirs of volatiles that could be incorporated to planetesimals (cometesimals) and eventually be delivered to planets. Chemical composition of ices in disks is, however, not easy to observe.

We observed a disk around FU ori star V883 Ori using ALMA. Previous work [1] found that the water snow line is located at the radius of  $\sim 40$  au; a warm region is extended compared with typical disks, since the disk is heated via the outburst accretion. The duration of the outburst ( $\sim 10^2$  years) in FU ors is much shorter than the chemical timescale of the gas-phase reactions (several  $10^4$  yrs). We thus expect to detect fresh sublimates, which could tell us the ice composition in the disk prior to outburst.

We detected various COM lines in the disk of V883 Ori. The high spatial resolution data shows that CH<sub>3</sub>OH emission is bright and originates in the water sublimation front. It suggests that the COMs we detected are fresh sublimates.

**References**

- [1] L. Cieza et al. 2016, Nature, 535, 258

## Chemistry in Star Forming Cores: WCCC vs Hot Corino

Y. Aikawa

*Department of Astronomy, The University of Tokyo, Japan*

Various complex organic species (COMs) and carbon chains are detected in low-mass protostellar cores. Cores with COMs are called hot corinos, while those with unsaturated carbon chains are called Warm Carbon Chain Chemistry (WCCC) sources. Hot corinos tend to be deficient in carbon chains, and WCCC sources tend to be deficient in COMs, although recent observations found that cores like B335 are reasonably bright both in COMs and carbon chain lines [1][2][3]. Theoretical models show that unsaturated carbon chains are formed via gas-phase reactions of sublimated  $\text{CH}_4$ , while many COMs are formed from  $\text{CH}_3\text{OH}$ , which in turn form via hydrogenation of CO (e.g. [4][5]). Deficiency of COMs (carbon chains) in WCCC sources (hot corinos) are thus considered to originate in chemistry in prestellar core stage; e.g. the cores evolve to be WCCC sources, if they start gravitational collapse before carbon is completely converted to CO.

In order to investigate the critical condition for the cores to be WCCC sources or hot corinos, we run three-phase chemical reaction network models in star-forming cores, varying the initial temperatures, visual extinction ( $A_V$ ), and duration of prestellar phase. Preliminary results show that the duration of the prestellar phase does not significantly affect the abundances of carbon chains and COMs. Both species are reduced, if the initial core is warmer than  $\sim 20$  K. While the low  $A_V$  is expected to enhance carbon chains and reduce COMs, both species become abundant in the model with the initial ambient  $A_V$  of 1 mag;  $\text{CH}_3\text{OH}$  and other COMs are formed via reactions such as  $\text{CH}_3 + \text{OH}$ . It is thus not straightforward to reproduce the deficiency of COMs (carbon chains) in WCCC sources (hot corinos).

### References

- [1] N. Sakai & S. Yamamoto 2013, Chemical Review, 113, 8981
- [2] M. Imai, N. Sakai, Y. Oya et al. 2016, ApJ 830, 37
- [3] Y. Oya, N. Sakai, Y. Watanabe et al. 2017, ApJ, 837, 174
- [4] R.T. Garrod & E. Herbst 2006, A&A, 457, 927
- [5] Y. Aikawa, V. Wakelam, R.T. Garrod & E. Herbst 2008, ApJ, 674, 984



## The effect of carbon grain destruction on the chemical structure of protoplanetary disks

Chen-En Wei,<sup>1</sup> Hideko Nomura,<sup>1</sup> Jeong-Eun Lee,<sup>2</sup> Wing-Huen Ip,<sup>3</sup> Catherine Walsh,<sup>4</sup> and T. J. Millar<sup>5</sup>

<sup>1</sup> Department of Earth and Planetary Sciences, Tokyo Institute of Technology, Japan

<sup>2</sup> Department of Astronomy and Space Science, Kyung Hee University, Republic of Korea

<sup>3</sup> Graduate Institute of Astronomy, National Central University, Taiwan

<sup>4</sup> School of Physics and Astronomy, University of Leeds, UK

<sup>5</sup> School of Mathematics and Physics, Queen's University Belfast, UK

The bulk composition of the Earth is dramatically carbon poor compared to that of the interstellar medium, and it extends to the asteroid belt (Figure 1). This indicates that carbonaceous component in grains must have been converted into the gas-phase in the inner regions of disks prior to planetary formation. We examine the effect of carbon grain destruction using a chemical reaction network, containing both gas-phase reactions and gas-grain interactions. When carbon grains are destroyed, the elemental abundance of the gas becomes carbon-rich and the abundances of carbon-bearing molecules, such as HCN and carbon-chain molecules, increase dramatically near the midplane, while oxygen-bearing molecules are depleted. We compare the results with the observed solid carbon fraction in the solar system. It shows a carbon depletion gradient with some quantitative discrepancies: the model shows a higher value at the position of asteroid belt and a lower value at the location of the Earth. In addition, using the obtained molecular abundances distributions, coupled with line radiative transfer calculations, it indicates that HCN,  $\text{H}^{13}\text{CN}$  and  $\text{c-C}_3\text{H}_2$  may be good tracers to examine the effect of carbon grain destruction in the protoplanetary disk by ALMA.

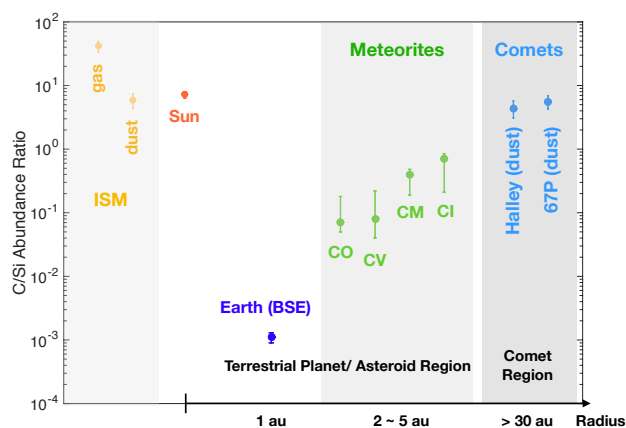


Figure 1: The carbon to silicon abundance ratio with error bars in the protosun [1], Earth, four classes of carbonaceous chondritic meteorites [2], cometary dust of Halley [3] and 67P/C-G [4], and ISM [2].

## References

- [1] Lodders, K. 2010, *Astrophysics and Space Science Proceedings*, 16, 379
- [2] Bergin, E. A., Blake, G. A., Ciesla, F., Hirschmann, M. M., & Li, J. 2015, *Proceedings of the National Academy of Science*, 112, 8965
- [3] Jessberger, E. K., Christoforidis, A., & Kissel, J. 1988, *Nature*, 332, 691
- [4] Bardyn, A., Baklouti, D., Cottin, H., et al. 2017, *MNRAS*, 469, S712

## Isotopic fractionation in interstellar clouds: Hydrogen, carbon, nitrogen, and oxygen

K. Furuya<sup>1</sup>

<sup>1</sup>*Center for Computational Sciences, University of Tsukuba*

The level of isotopic fractionation in molecules provides insights into their formation environments and how they formed. Radio observations toward star-forming regions have quantified the degree of isotopic fraction of abundant volatile elements (H, C, N, and O) in various molecules [e.g., 1, 2, 3]. Theoretical studies of isotopic fractionation are crucial to interpret the observations. The aim of this work is (i) to identify the major fractionation pathways of the abundant volatile elements, and (ii) to reveal (possible) correlations or anticorrelations of the isotope ratios among different elements.

In this poster, we present the results of our extended astrochemical models of molecular clouds, which includes isotopic fractionation of abundant volatile elements (H, C, N, and O). A set of isotopic exchange reactions, isotope selective photodissociation, and nuclear spin states of H<sub>2</sub> are considered. We find/confirm that hydrogen and carbon isotope fractionation are predominantly driven by isotope exchange reactions, while nitrogen and oxygen isotope fractionation are predominantly driven by isotope selective photodissociation. We show that different isotopes show different fractionation patterns.

### References

- [1] J. K. Jørgensen, H. S. P. Müller, H. Calcutt, et al. 2018, arxiv:1808.08753
- [2] M. V. Persson, J. K. Jørgensen, H. S. P. Müller, et al. 2018, A&A 610, A54
- [3] K. Furuya, Y. Watanabe, T. Sakai, Y. Aikawa, & S. Yamamoto, 2018, A&A 615, L16

## Water lines and multiple ring and gap structures of the protoplanetary disk around HD 163296 observed by ALMA

S. Notsu,<sup>1</sup> E. Akiyama,<sup>2</sup> A. Booth,<sup>3</sup> H. Nomura,<sup>4</sup> C. Walsh,<sup>3</sup> T. Hirota,<sup>5</sup> M. Honda<sup>6</sup>, T. Tsukagoshi,<sup>5</sup> T. J. Millar<sup>7</sup>

<sup>1</sup>*Department of Astronomy, Graduate School of Science, Kyoto University, Japan*

<sup>2</sup>*Institute for the Advancement of Higher Education, Hokkaido University, Japan*

<sup>3</sup>*School of Physics and Astronomy, University of Leeds, UK*

<sup>4</sup>*Department of Earth and Planetary Science, Tokyo Institute of Technology, Japan*

<sup>5</sup>*National Astronomical Observatory of Japan, Japan*

<sup>6</sup>*Department of Physics, School of Medicine, Kurume University, Japan*

<sup>7</sup>*School of Mathematics and Physics, Queen's University Belfast, UK*

Observationally locating the position of the H<sub>2</sub>O snowline in protoplanetary disks is crucial for understanding the planetesimal and planet formation processes, and the origin of water on the Earth. The velocity profiles of emission lines from disks are usually affected by Doppler shift due to Keplerian rotation. Therefore, the line profiles are sensitive to the radial distribution of the line-emitting regions. In our previous works (e.g., [1][2][3]), we calculated the chemical composition of the disks around a T Tauri star and a Herbig Ae star using chemical kinetics, and then the water line profiles to identify that lines with small Einstein A coefficients and relatively high upper state energies are dominated by emission from the hot midplane region inside the H<sub>2</sub>O snowline, and therefore through analyzing their line profiles the position of the H<sub>2</sub>O snowline can be located.

We got the upper limit fluxes of ortho-H<sub>2</sub>(16)O 321 GHz, para-H<sub>2</sub>(18)O 322 GHz, and HDO 335 GHz lines from the protoplanetary disk around the Herbig Ae star HD 163296, using ALMA [4]. These water lines are considered to be the candidate water lines to locate the position of the H<sub>2</sub>O snowline, on the basis of our previous model calculations [1][2][3]. We compared the upper limit fluxes with the values obtained by our model calculations with dust emission, and we constrained the H<sub>2</sub>O snowline position and the dust properties from the observations. Future observations of submillimeter water lines with longer observation time are required to clarify the position of the H<sub>2</sub>O snowline in the disk midplane.

We also detected multiple ring and gap patterns in the 0.9 mm (ALMA Band 7) dust continuum emission. The 0.9 mm dust continuum emission has an asymmetry in the long axis direction, although previous observation of the 1.3 mm (ALMA Band 6) dust continuum emission did not have it [5].

### References

- [1] S. Notsu, H. Nomura, D. Ishimoto et al., 2016, ApJ, 827, 113
- [2] S. Notsu, H. Nomura, D. Ishimoto et al., 2017, ApJ, 836, 118
- [3] S. Notsu, H. Nomura, C. Walsh et al., 2018a, ApJ, 855, 62
- [4] S. Notsu et al., 2018b, in prep.
- [5] A. Isella, G. Guidi, L. Testi et al., 2016. Phys. Rev. Lett., 117. 251101

## Searching for Methylamine in star-forming regions using ALMA archival data

H. Minamoto,<sup>1</sup> Y. Oya,<sup>2</sup> H. Nomura,<sup>1</sup> and T. Hirota<sup>3</sup>

<sup>1</sup>*Department of Earth and Planetary Sciences, Tokyo Institute of Technology, Japan*

<sup>2</sup>*Department of Physics, The University of Tokyo, Japan*

<sup>3</sup>*National Astronomical Observatory of Japan, Japan*

Methylamine ( $\text{CH}_3\text{NH}_2$ ) is the simplest amine and thought to be a potential interstellar precursor of the amino acid glycine. It is confirmed by the experimental work that the reaction of methylamine with  $\text{CO}_2$  in water ice yields glycine under UV irradiation [1]. In terms of exploration in the Solar system, this molecule has been detected in two comets. However, in molecular clouds, a robust detection of methylamine has been reported only for Sgr B2(N) [2] so far, while a variety of complex organic molecules have been detected by radio observations. To search for methylamine, we focused on the Orion Kleinmann–Low nebula (hereafter Orion KL) and IRAS 16293-2422 (IRAS 16293), which are known as examples of the most prolific sources of line emission of a variety of complex organic molecules.

We used the ALMA Cycle2 archival data toward Orion KL (#2013.1.00533.S) and Cycle1 archival data toward IRAS 16293 (#2012.1.00712.S) in Band 6. In Orion KL, we found several candidate features of methylamine lines in Hot Core (Figure 1; left panel). We evaluated its column density and rotational temperature to be  $< 4.4 \times 10^{14} \text{ cm}^{-2}$  and  $> 109 \text{ K}$ , respectively, by preparing the rotation diagram (Figure 1; right panel). While in IRAS 16293, we cannot obtain a rotation diagram properly because of the line confusion.

We compare the results for several sources including the above two sources, considering their different chemical condition.

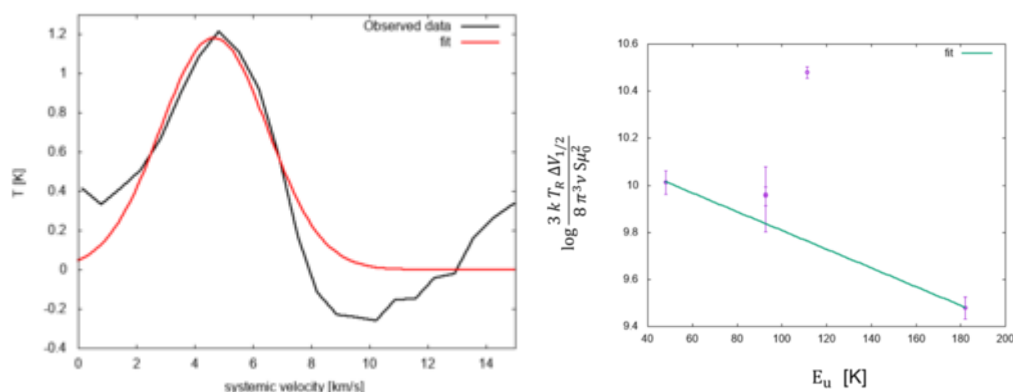


Figure 1: (*left panel*) Observed spectra of methylamine (black) and the result of the Gaussian fitting for it (red) in Orion KL (*right panel*) Rotation diagram of methylamine in Orion KL. The error bars represents  $\pm 3\sigma$  for each data.

### References

- [1] P. D. Holtom, C. J. Bennett, & Y. Osamura et al. 2005, ApJ, 626, 940.
- [2] D. T. Halfen, V. V. Ilyushin, & L. M. Ziurys, 2013, ApJ 767, 66.

**Mission Concept Study for the 2020 US Astrophysics Decadal Survey:  
The Latest Study Status of the Mid-infrared Spectrometer and Camera (MISC)  
for the Origins Space Telescope (OST)**

Itsuki Sakon,<sup>1</sup> Thomas L. Roellig<sup>2</sup>, Kimberly Ennico<sup>2</sup>, Taro Matsuo<sup>3</sup>, Tomoyasu Yamamuro<sup>4</sup>,  
Yuji Ikeda<sup>5</sup>, and the MISC Instrument Study Team

<sup>1</sup> *Department of Astronomy, Graduate School of Science, University of Tokyo,  
7-3-1 Hongo, Bunkyo-ku, Tokyo 113-0033, Japan*

<sup>2</sup> *NASA Ames Research Center, Moffett Field, CA 94035, USA*

<sup>3</sup> *Department of Earth and Space Science, Graduate School of Science, Osaka University, 1-1,  
Machikaneyamacho, Toyonaka, Osaka 560-0043, Japan*

<sup>4</sup> *Optocraft, 3-16-8-101, Higashi Hashimoto, Midori-ku, Sagami-hara,  
Kanagawa 252-0144, Japan*

<sup>5</sup> *Photocoding, 460-102 Iwakura-Nakamachi, Sakyo-ku, Kyoto 606-0025, Japan*

The Origins Space Telescope (OST; Meixner et al. 2018; Leisawitz et al. 2018) is one of the four mission concepts studied for the 2020 US astrophysics decadal survey. The OST has two mission concepts; Mission concept 1 is composed of a cryogenically cooled 9.1 m off-axis telescope and five instruments covering wavelengths from 5 to 660 $\mu$ m, while Mission Concept 2 of a cryogenically cooled 5.9 m on-axis telescope with JWST-sized collecting area and four instruments covering wavelengths from 5 to 660 $\mu$ m. The Mid-infrared Spectrometer and Camera (MISC; Sakon et al. 2018) is one of the instruments studied both for the Origins Space Telescope (OST) Mission Concept 1 and 2 (cf., OSS, Bradford et al. 2018; FIP, Staguhn et al. 2018; HERO, Wiedner et al. 2018). The mid-infrared transit spectrometer (TRA) is the primary function of the MISC instrument and is base-lined for the Concept 2 study. The MISC TRA employs the densified pupil spectroscopic design (Matsuo et al. 2016) to achieve <5 ppm of spectro-photometric stability and covers 2.8-20  $\mu$ m with R=50-300. The highest ever spectro-photometric stability achieved by MISC TRA enables to detect bio-signatures (e.g., ozone, water, and methane) in habitable worlds in both primary and secondary transits of exoplanets and makes the OST a powerful tool to bring a revolutionary progress in exoplanet sciences. The mid-infrared wide-field imaging and low-resolution spectroscopic function of the MISC instrument, which provides the OST not just with a focal plane guiding function but also with a powerful tool to diagnose the physical and chemical condition of the ISM using dust features, molecules lines and atomic and ionic lines, is also presented to the Decadal Review as an up-scoped version of the MISC instrument. In this presentation, I will give a summary of the latest study status of the MISC instrument for the OST.

## References

- [1] Bradford, C. M., et al., “The Origins Survey Spectrometer (OSS): a far-IR discovery machine for the Origins Space Telescope”, Proc. SPIE, 10698, in press (2018)
- [2] Leisawitz, D. T., et al. “The Origins Space telescope: mission concept overview”, Proc. SPIE, 10698, in press (2018)
- [3] Matsuo, T., et al. “A New Concept for Spectrophotometry of Exoplanets with Space-borne Telescopes”, ApJ, 823, 139 (2016)
- [4] Meixner, M., et al. “Overview of the Origins Space telescope: science drivers to observatory requirements”, Proc. SPIE, 10698, in press (2018)
- [5] Sakon, I., et al. “Mid-Infrared Spectrometer and Camera (MISC) for the Origins Space Telescope”, Proc. SPIE, 10698, in press (2018)
- [6] Staguhn, J. G., et al. “Origins Space telescope: the far infrared imager and polarimeter FIP”, Proc. SPIE, 10698, in press (2018)
- [7] Wiedner, M. C., et al. “HERO: heterodyn receiver for the Origins Space telescope”, Proc. SPIE, 10698, in press (2018)

## Observations of the $^{13}\text{CO}/\text{C}^{18}\text{O}$ isotope ratios toward the Galactic Center

A. Ubagai,<sup>1</sup> T. Oyama,<sup>1</sup> M. Araki,<sup>1</sup> S. Takano,<sup>2</sup> Y. Minami,<sup>1</sup> A. Ohsugi,<sup>1</sup>  
H. Ozaki,<sup>3</sup> Y. Sumiyoshi,<sup>3</sup> N. Kuze,<sup>4</sup> and K. Tsukiyama<sup>1</sup>

<sup>1</sup>Department of Chemistry, Tokyo University of Science, Japan

<sup>2</sup>Department of Physics, College of Engineering, Nihon University, Japan

<sup>3</sup>Division of Pure and Applied Science, Graduate School of Science and Technology,  
Gunma University, Japan

<sup>4</sup>Department of Materials and Life Sciences, Sophia University, Japan

Isotope ratios are one of the most powerful probes for chemical evolution of space. Generally, isotope ratios are measured *via* abundances of isotope molecules. To investigate chemical evolution of molecular clouds, isotopic species of CO are representative tracers due to its ubiquitousness and richness. However, ratios of  $^{13}\text{CO}/\text{CO}$  and  $\text{C}^{18}\text{O}/\text{CO}$  are difficult to measure because of optical thickness of CO. Thus, a ratio of  $^{13}\text{CO}/\text{C}^{18}\text{O}$  is an effective probe. For the Galactic Center region, the ratio was reported to be 10–15 by using FCRAO 14 m radio telescope in 1986 [1]. In this work, we observed intensities of emission lines of the  $J = 1-0$  transition of CO toward Sgr B2(N) using Nobeyama 45 m Radio Telescope to measure the isotopic ratios precisely. The observational position of  $\Delta\alpha = 57''$  and  $\Delta\delta = -5.6''$  from the Sgr B2(N) core was used to prevent overlapping with absorption lines, and then only emission lines were detected. The isotope ratios were derived to be 5.9–17.5 toward Galactic Center. As a result, we found that the ratios in this work can be comparable with that of the previous work [1].

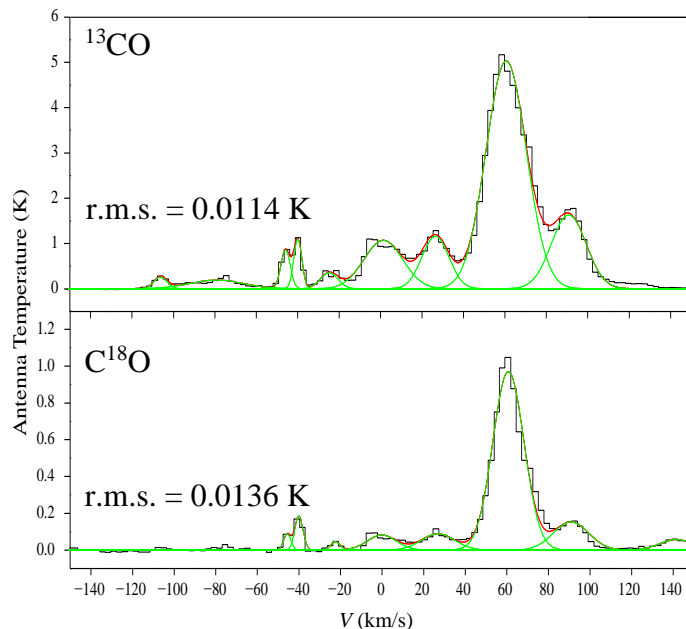


Table 1. Isotope Ratios of Individual Components

	$V$ (km/s)	$^{13}\text{CO}/\text{C}^{18}\text{O}$
	-46	$12.6 \pm 7.8$
3kpc expanding ring	-40	$5.9 \pm 2.6$
	-24	$15.0 \pm 9.3$
Galactic center	0	$17.5 \pm 3.9$
Scutum/Crux arm	25	$10.5 \pm 2.2$
Galactic center SgrB2(M)	61	$6.4 \pm 0.1$
unassigned	91	$10.6 \pm 0.9$

Figure 1: Observed  $J = 1-0$  rotational transitions of  $^{13}\text{CO}$  and  $\text{C}^{18}\text{O}$ . The green lines show individual velocity components, and the red line is a sum of them.

### Reference

- [1] D. K. Taylor & R. L. Dickman, 1986, BAAS 18, 1026.

## The Molecular Distributions in the Outflow of L1527

T. Fujita,<sup>1</sup> Y. Oya,<sup>1</sup> N. Sakai<sup>2</sup>, and S. Yamamoto<sup>1</sup>

<sup>1</sup>*Department of Physics, The University of Tokyo, Japan*

<sup>2</sup>*RIKEN Cluster for Pioneering Research, Japan*

We observed the CS ( $J=3-2$ ), H<sub>2</sub>CO ( $2_{1,1}-1_{1,0}$ ), c-C<sub>3</sub>H<sub>2</sub> ( $2_{2,0}-1_{1,1}$ ), and SO ( $3_4-2_3$ ) lines toward the low-mass protostellar core L1527 in Taurus. L1527 has an almost edge-on envelope/disk structure extending along the north-south direction and a bipolar outflow blowing along the east-west direction [1,2]. In this observation, we utilize the advantage of a relatively large field of view in Band 4, and delineated the extended outflow.

The CS emission clearly shows the outflow extending along the east-west direction (Fig. 1). The edges of the outflow are prominent. This distribution can be approximated by a parabola whose axis is tilted from the east-west direction by 6° (P.A.96°). To investigate the velocity structure of the outflow, we prepared position-velocity (PV) diagrams along the line perpendicular to the outflow axis (Fig. 2). In Fig. 2, an elliptic feature is seen, which likely traces the outflow cavity wall. Also, this elliptic feature is found to expand as an increasing distance from the protostar. This represents the expanding motion of the outflow.

On the other hand, the c-C<sub>3</sub>H<sub>2</sub> line mainly traces a component extending along the north-south direction, which likely represents the envelope gas (Fig. 3). The H<sub>2</sub>CO line traces both the outflow and the envelope. In the outflow, the H<sub>2</sub>CO and CS distributions are similar to each other. Meanwhile, the SO emission shows some blobs on the parabolic shape. The intensity of SO blobs does not always correlate with those of H<sub>2</sub>CO and CS. Hence, the SO blobs seem to trace local shocks in the outflow. Such a local shock can heat dust grains, which may lead to evaporation of SO. This would be related to the previous report that SO evaporates near the centrifugal barrier of the envelope due to an accretion shock [1].

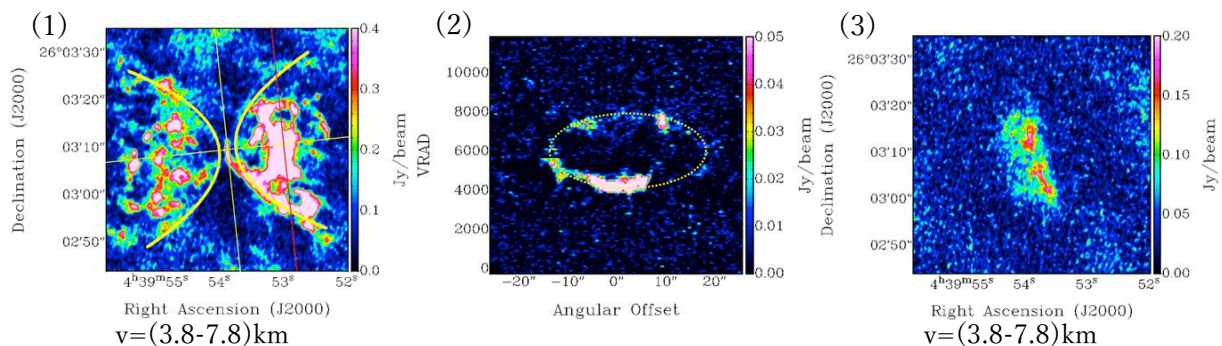


Figure: (1) The moment 0 map of the CS ( $J=3-2$ ) line. (2) The PV diagram of the CS line. The position axis is prepared along the red line shown in Fig. (1). (3) The moment 0 map of the c-C<sub>3</sub>H<sub>2</sub> ( $2_{2,0}-1_{1,1}$ ) line.

### References

- [1] N. Sakai et al., 2014, *Nature*, 507, 78.
- [2] Y. Aso et al., 2017, *ApJ*, 849, 56.

## Exploring molecular-cloud formation in the Pipe Nebula with the OH 18 cm transition

Y. Ebisawa,<sup>1</sup> N. Sakai,<sup>2</sup> K. M. Menten<sup>3</sup>, and S. Yamamoto<sup>1</sup>

<sup>1</sup>*Department of physics, The University of Tokyo, Japan*

<sup>2</sup>*RIKEN, Japan*

<sup>3</sup>*Max-Planck-Institute for Radio Astronomy, Germany*

The Pipe nebula is a nearby ( $\sim 145$  pc) massive molecular cloud with a low star-forming activity. It shows a characteristic filamentary structure from west (B59 region) to east (Bowl region) according to the  $^{13}\text{CO}$  (1-0) and  $\text{C}^{18}\text{O}$  (1-0) observations ([1] Onishi et al. 1999) (cyan contours in Fig. 1). Another filament from north to south is seen in the integrated intensity map of the  $^{12}\text{CO}$  (1-0) in the red-shifted velocities (6-10 km/s) ([1] Onishi et al. 1999) (red contours in Fig. 1). These filaments are overlapped in the bowl region, and collisions between them are considered to be important to understand the formation of the cloud ([2] Frau et al. 2015). In addition, the heating effect from the nearby B2 IV star,  $\theta$ -Ophiuchi, is also studied to understand the origin of the cloud ([3] Gritschneider & Lin 2012)

In order to examine these scenarios, we study the temperature structure of the Pipe nebula from observations of the four hyperfine structure components of the OH 18 cm transition (1.612, 1.665, 1.667 and 1.720 GHz) with the Green Bank Telescope (yellow circles in Fig. 1). This transition can be used as a good thermometer for molecular clouds, according to our recent study ([4] Ebisawa et al. 2015). As a result, we find no heating effect from the  $\theta$ -Ophiuchi. On the other hand, the temperature is found to be higher in the interface of the two filaments ( $\sim 110$  K), which might result from a heating effect by the filament collisions. This result demonstrates a unique power of the OH 18 cm transition in studies of molecular cloud formation.

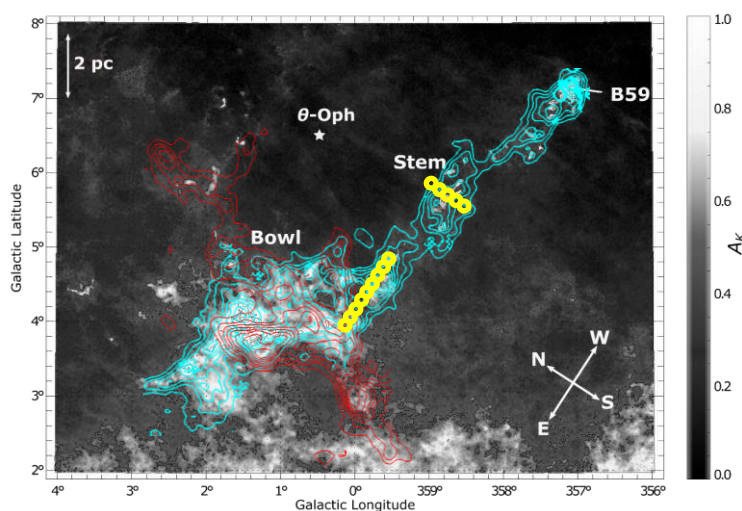


Figure 1: The visual extinction ( $A_k$ ) map (gray, [5] Lombardi et al. 2006) overlaid with the integrated intensity maps of  $^{13}\text{CO}$  (cyan contours) and  $^{12}\text{CO}$  (red contours) ([1] Onishi et al. 1999).

### References

- [1] T. Onishi, A. Kawamura, R. Abe et al. 1999, PASJ, 51, 871,
- [2] P. Frau, J. M. Giart, F. O. Alves et al. 2015, A&A, 574, L6,
- [3] M. Gritschneider & D. N. C. Lin 2012, ApJ, 754, L13,
- [4] Y. Ebisawa, H. Inokuma, N. Sakai et al. 2015, ApJ, 815, 13,
- [5] M. Lombardi, J. Alves and C. J. Lada 2006, A&A, 454, 781



## Mapping observations of deuterated species toward the low-mass protostar L1527 with ALMA

K. Yoshida,<sup>1,2</sup> N. Sakai,<sup>2</sup> and S. Yamamoto<sup>1</sup>

<sup>1</sup>*Department of physics, The University of Tokyo, Japan*

<sup>2</sup>*Star and Planet Formation Laboratory, RIKEN Cluster for Pioneering Research (CPR), Japan*

We observed formaldehyde ( $\text{H}_2\text{CO}$ ) and its deuterated species (HDCO and  $\text{D}_2\text{CO}$ ) toward the Class 0 low-mass protostar L1527 with ALMA. The distributions of  $\text{H}_2\text{CO}$  and the deuterated isotopologues are found to be clearly different from each other. The emission of  $\text{H}_2\text{CO}$  is strong around the protostar ( $r < 250$  au), as previously reported [1]. On the other hand, the deuterated species mainly reside in the outer envelope ( $r \sim 1000$  au). It has been thought that  $\text{H}_2\text{CO}$  is efficiently produced on dust grains and released into the gas phase in the warm region near the protostar. This process is indeed the case for  $\text{H}_2\text{CO}$ , because its distribution is concentrated in the vicinity of the protostar, where the temperature is higher than the desorption temperature of  $\sim 40$  K [2]. On the other hand, the deuterated species are likely produced in the gas phase and/or released from dust grains via non-thermal processes, because the kinetic temperature derived from the different  $K$  transitions of  $\text{D}_2\text{CO}$  is as low as 20 K.

The D/H ratio in the outer envelope is derived to be high ( $\text{HDCO}/\text{H}_2\text{CO} \sim 0.8$ ). The high D/H ratio in the outer envelope is confirmed also for the CCD/CCH case, based on our recent ALMA observations. On the other hand, the D/H ratios are found to be low in the vicinity of the protostar ( $\sim$  a few percent). Hence, the decrease in the deuterium fractionation is confirmed along the protostellar envelope within a 1000 au scale.

Figure 1: The integrated intensity maps of the  $\text{H}_2\text{CO}$  ( $5_{15}-4_{14}$ ),  $\text{D}_2\text{CO}$  ( $4_{04}-3_{03}$  and  $4_{23}-3_{22}$ ), and HDCO ( $4_{13}-3_{12}$ ) lines obtained with the ALMA ACA array.

### References

- [1] N. Sakai et al., 2014, ApJL, 791, 38
- [2] J. J. Tobin et al., 2013, ApJ 771, 48

## Development of Terahertz Superconductive HEB Mixers and Its Application to Molecular Spectroscopy

M. Takegahara,<sup>1</sup> Y. Ebisawa,<sup>1</sup> Y. Watanabe,<sup>2</sup> N. Sakai,<sup>3</sup> Y. Oya,<sup>1</sup> and S. Yamamoto<sup>1</sup>

<sup>1</sup>Department of Physics, The University of Tokyo, Japan

<sup>2</sup>Department of Physics, University of Tsukuba, Japan

<sup>3</sup>RIKEN Cluster for Pioneering Research, Japan

Observations of abundances of fundamental atoms and molecules as well as their distribution are very important for exploring the chemical evolution in star-forming regions. Since some of them have emission lines in the THz band, we are developing a superconductive HEB (Hot Electron Bolometer) mixer as a heterodyne device to observe those lines. In fabrication of the HEB mixer, AlN is applied as a buffer layer, since it is known to help improvement of the critical temperature for the NbTiN superconducting film. But its effect on the performance of the HEB Mixers was unknown. Hence, we prepared the HEB mixers with and without the AlN buffer layer, and compared their performances. As a result, the noise temperature of the mixers with AlN is found to be improved by 0.32 dB on average compared with ones without buffer layer.

Then, we employed the fabricated HEB mixer for spectroscopic studies in the 0.9 THz band in the laboratory. A 10.8 nm-thick NbTiN film is used as the superconducting material of the HEB mixer, and the width of the superconducting microbridge is 0.2  $\mu\text{m}$ . A 20 nm-thick AlN buffer layer is applied. This HEB mixer is mounted on the ALMA type cartridge receiver of the emission spectrometer (SUMIRE) at RIKEN (Figure 1). With this spectrometer, we observed the HDO ( $1_{11}-0_{00}$ : 893.638666 GHz), HDO ( $2_{02}-1_{01}$ : 919.310885 GHz), D<sub>2</sub>O ( $2_{12}-1_{01}$ ; 897.947107 GHz) and methanol (894.614183 GHz) lines. Examples of the observed spectra are shown in Figure 2. In this experiment, we notice that the lines show some unexpected and strange line shapes. A reason for such a feature is now under consideration.

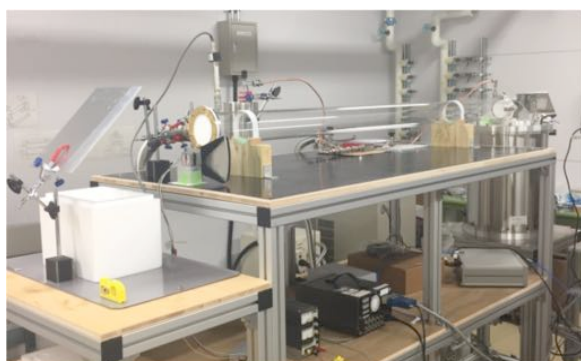
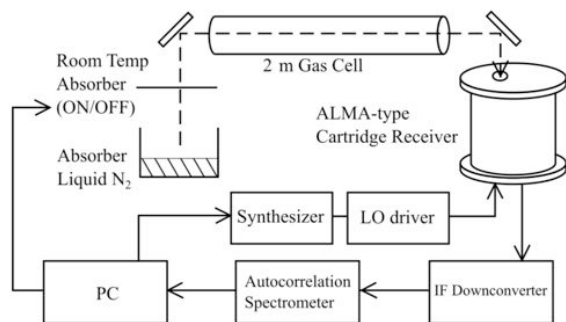


Figure1: Emission spectrometer at RIKEN (SUMIRE)

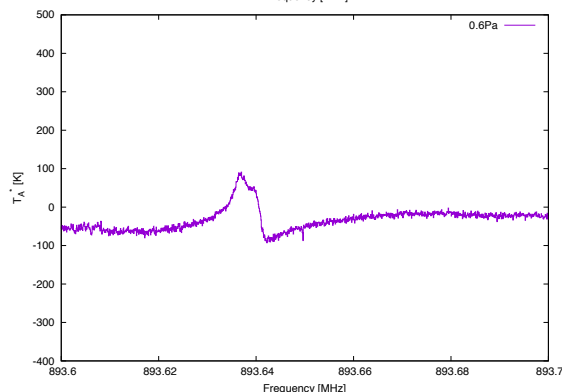
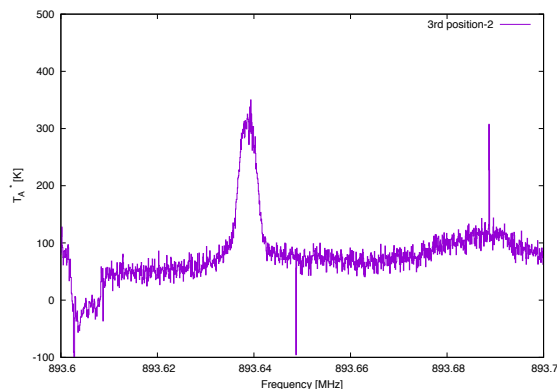


Figure 2: Spectra of the HDO ( $1_{11}-0_{00}$ ) transition

## The Co-evolution of Disks and Stars in Embedded Stages

Y. Okoda,<sup>1</sup> Y. Oya,<sup>1</sup> N. Sakai,<sup>2</sup> Y. Watanabe,<sup>3,4</sup> J. K. Jørgensen,<sup>5</sup> E. van Dishoeck,<sup>6</sup>  
and S. Yamamoto<sup>1</sup>

<sup>1</sup>*Department of Physics, The University of Tokyo, Japan*

<sup>2</sup>*RIKEN Cluster for Pioneering Research, Japan*

<sup>3</sup>*Department of Physics, The University of Tsukuba, Japan*

<sup>4</sup>*Tomonaga Center for the History of the Universe, Faculty of Pure and Applied Sciences,  
University of Tsukuba, Japan*

<sup>5</sup>*Centre for Star and Planet Formation, Niels Bohr Institute, Natural History Museum of  
Denmark, Denmark*

<sup>6</sup>*Leiden Observatory, Leiden University, Leiden, The Netherlands Max-Planck Institut für  
Extrsterrestrische Physik (MPE), Germany*

When a disk structure is formed around a newly born star is an important issue for astrophysics. We are tackling this problem from an astrochemical point of view by using ALMA.

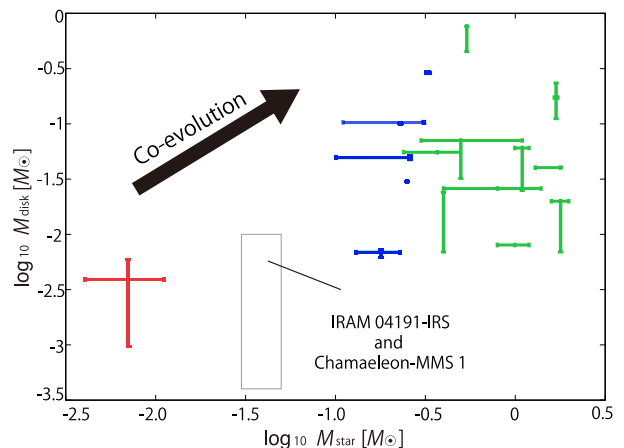
IRAS 15398–3359 is the low-mass Class 0 protostellar source located in the Lupus 1 molecular cloud at a distance of 155 pc. We have observed the CCH and SO emission toward this source at a 0."2 angular resolution ( $\sim 30$  au). The CCH emission traces the infalling-rotating envelope extended along the northwest-southeast axis, while the SO emission has a compact distribution around the protostar within 40 au. The velocity structure of the SO emission indicates a rotating disk structure around the protostar. We evaluate the protostellar mass to be  $0.007 M_{\odot}$  assuming the Keplerian rotation. Thus, this source is found to be a very young protostar. Nevertheless, the rotating disk structure has already been formed around it. This result suggests that the disk structure can be formed in the earlier stage than ever expected [1].

We have searched for other sources like IRAS 15398–3359 to investigate disk formation at the youngest stages of protostellar evolution. Based on the analyses of the ALMA archival data of the  $C^{18}O$ , SO, and  $^{13}CO$  emission, the protostellar masses of L328-IRS, IRAM 04191-IRS, and Chamaeleon-MMS 1 are roughly estimated to be  $0.2 M_{\odot}$ ,  $0.05 M_{\odot}$ , and  $0.03 M_{\odot}$ , respectively. Although L328-IRS is a very low luminosity object (VeLLO) [2], the protostellar mass is much higher than that of IRAS 15398–3359. Instead of the low luminosity, we find that a narrow spectral line width can be an effective indicator to find very-low-mass protostars. Figure 1 shows the relation between the protostellar masses and the disk masses of the sources at the infant stages. It likely suggests co-evolution of disks and protostars.

Figure 1: Comparison between the protostellar masses and the disk masses. The red marks with error bars represent IRAS 15398–3359. The blue and green marks show the protostars of  $T_{\text{bol}} < 70$  K (Class 0) and  $T_{\text{bol}} > 70$  K (Class I), respectively [3]. IRAM 04191-IRS and Chamaeleon-MMS 1 would be plotted in the slash range.

### References

[1] Okoda, Y et al. 2018, ApJL, 864, L25; [2] Lee, C. W., Kim, M., Kin, G., Saito, M., et al. 2013, ApJ, 777, 50; [3] Alves et al. (2017); Chou et al. (2014); Lee et al. (2017), (2018); Sakai et al. (2014a); Tobin et al. (2012), (2015); Yen et al. (2015), (2017)



## The FUGIN Hot Core Survey — The survey method and the initial results for L=10-20deg

K. Sato<sup>1,2</sup>, T. Hasegawa,<sup>2</sup> T. Umemoto<sup>2</sup>, H. Saito<sup>4</sup>, N. Kuno<sup>4</sup>, M. Seta<sup>5</sup>, S. Sakamoto<sup>2</sup> and the FUGIN project team

<sup>1</sup>*Department of Astronomy, the University of Tokyo, Japan*

<sup>2</sup>*National Astronomical Observatory of Japan, Japan*

<sup>4</sup>*Department of Physics, University of Tsukuba*

<sup>5</sup>*Department of Physics, Kwansai Gakuin University*

We are conducting an unbiased survey of hot cores based on the CH<sub>3</sub>CN (6<sub>K</sub> – 5<sub>K</sub>, K = 0, 1, 2, 3) and HNCO (5<sub>0,5</sub> – 4<sub>0,4</sub>) lines included in the spectral coverage of the FUGIN Galactic survey of the <sup>12</sup>CO, <sup>13</sup>CO and C<sup>18</sup>O (1 – 0) lines with the Nobeyama 45-m telescope [1]. As the sensitivity of the observations has been set for the CO lines, the S/N ratio for the CH<sub>3</sub>CN and HNCO lines are limited. We stack the five lines (four CH<sub>3</sub>CN and one HNCO) to improve the S/N ratio and search for emission guided by the C<sup>18</sup>O emission strength and velocity. For the source candidates picked in this way, we further make separate pointed observations of a set of hot core/dense gas probes (C<sup>34</sup>S, SO, OCS, HC<sub>3</sub>N, and CH<sub>3</sub>OH thermal/maser lines in addition to CH<sub>3</sub>CN and HNCO lines) to confirm their existence and characterize the detected sources.

In this paper, we report the initial result for L=10-20 deg. >From the FUGIN data, we picked 64 source candidates for the confirmation observations. In the confirmation observations with the Nobeyama 45m telescope in May 2018, we made 3 by 3 maps with 50'' grid spacing centered on each candidate sources, so that we can estimate the spatial extent of the sources. From the observations, we identified 25 “hot cores” as well as 23 “dense clouds” as defined below:

- **Hot Cores:** Two or more hot core lines detected with compact (< 50'') distribution.
- **Dense Clouds:** Two or more lines detected among the hot core/dense gas probes.

Figure 1 shows the distribution of the identified sources. They are typically at 2-5 kpc from the sun. Many of the “hot cores” correspond to the ATLASGAL-based clumps [2], but there are a few new sources. From the intensity ratios of the observed lines, we see a diversity of the physical and chemical conditions among the identified sources. Further characterizations of the sources are presented in a separate paper (T. Hasegawa et al., this meeting).

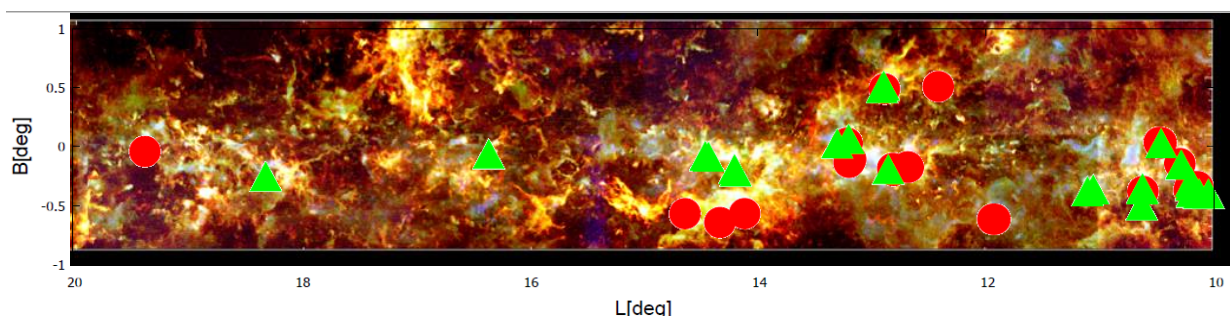


Figure 1: The location of the identified hot cores (red dot) and dense clouds (green triangles) on the FUGIN CO image.

### References

- [1] T. Umemoto et al., 2017, PASJ 69, 78.
- [2] J. S. Urquhart et al., 2018, MNRAS 473, 1059.

**The FUGIN Hot Core Survey – The environment and chemistry  
of the regions of massive star formation**

T. Hasegawa,<sup>1</sup> K. Sato,<sup>1,2</sup> T. Umemoto<sup>1</sup>, N. Kuno<sup>3</sup>, H. Saito<sup>3</sup>, M. Seta<sup>4</sup>, S. Sakamoto<sup>1</sup>  
and the FUGIN project team

<sup>1</sup>*National Astronomical Observatory of Japan*

<sup>2</sup>*Department of Astronomy, The University of Tokyo, Japan*

<sup>3</sup>*Division of Physics, The University of Tsukuba, Japan*

<sup>4</sup>*Department of Physics, Kwansai Gakuin University, Japan*

We are conducting an unbiased survey of hot cores based on the CH<sub>3</sub>CN ( $6_K - 5_K$ ,  $K = 0, 1, 2, 3$ ) and HNCO ( $5_{0,5} - 4_{0,4}$ ) lines included in the spectral coverage of the FUGIN Galactic survey of the <sup>12</sup>CO, <sup>13</sup>CO and C<sup>18</sup>O ( $1 - 0$ ) lines with the Nobeyama 45-m telescope [1]. As the sensitivity of the observations has been set for the CO lines, the S/N ratio for the CH<sub>3</sub>CN and HNCO lines are limited. We stack the five lines (four CH<sub>3</sub>CN and one HNCO) to improve the S/N ratio and search for emission guided by the C<sup>18</sup>O emission strength and velocity. For the source candidates picked in this way, we further make separate pointed observations of a set of hot core lines (C<sup>34</sup>S, SO, OCS, HC<sub>3</sub>N, and CH<sub>3</sub>OH thermal/maser lines in addition to CH<sub>3</sub>CN and HNCO lines) to confirm their existence and characterize the detected sources.

We have applied this method to L=10 – 20 deg part of the FUGIN survey (it covers up to L=50 deg), and identified 25 hot cores (Sato et al., this meeting). In this paper, we present the initial findings for these sources. Many of the hot cores are embedded in regions of vigorous star forming activities, and are under a strong influence of feedbacks from preceding generation of massive stars. For the sources cross-matched with the ATLAGAL-based clumps with clump mass and bolometric luminosity estimates [2], the values of  $\log(L_{\text{bol}}/M_{\odot})$  range from 0.55 to 2.1 and suggests that they are in a range of evolutionary stages centered at the hot core stage [3]. The intensity ratios of the observed lines show a diversity of chemical abundances. We try a principal component analysis of the line intensity ratios  $I(X)/I(\text{C}^{34}\text{S})$  ( $X = \text{SO}, \text{OCS}, \text{HC}_3\text{N}, \text{HNCO}, \text{CH}_3\text{OH thermal/maser}, \text{and CH}_3\text{CN}$ ) for hot cores with stronger C<sup>34</sup>S emission. The first principal component (PC1) has almost uniform loadings in the same sign for all the ratios, and its correlation with  $\log(L_{\text{bol}}/M_{\odot})$  suggests that C<sup>34</sup>S gets stronger as the core evolves. The loading pattern of the second principal component (PC2) indicates two outstanding groups in the opposite direction; HNCO and CH<sub>3</sub>OH (thermal) on one side, and SO and CH<sub>3</sub>OH (maser) on the other. This variation between “HNCO and CH<sub>3</sub>OH (thermal)-rich” cores and “SO and CH<sub>3</sub>OH (maser)-rich” cores does not appear to correlate with the evolutionary stages of the cores, and may arise from other factors such as the environment (in the past and current) and/or the elemental abundances.

#### References

- [1] T. Umemoto et al., 2017, PASJ 69, 78.
- [2] J. S. Urquhart et al., 2018, MNRAS 473, 1059.
- [3] A. Gianetti et al., 2017, A&A 603, A33.

**Multi-Molecular Line Observation toward NGC 3627 with ALMA**

Y. Watanabe<sup>1</sup>, Y. Nishimura<sup>2</sup>, K. Sorai<sup>3</sup>, N. Kuno<sup>1</sup>, N. Sakai<sup>4</sup>, and Y. Yamamoto<sup>5</sup>

*<sup>1</sup>Division of Physics, University of Tsukuba, Japan*

*<sup>2</sup>Institute of Astronomy, The University of Tokyo, Japan*

*<sup>3</sup>Department of Physics, Hokkaido University, Japan*

*<sup>4</sup>RIKEN, Japan*

*<sup>5</sup>Department of Physics, The University of Tokyo, Japan*

Understanding of cloud-scale chemical compositions is important for studies on galactic-scale physical conditions and gas dynamics in external galaxies. It will also constitute a fundamental base for astrochemical studies of AGNs and starbursts. With this motivation, we have conducted a spectral line survey toward the spiral arm regions of nearby galaxies and mapping spectral line surveys toward the Galactic molecular clouds. With these observations, we have revealed chemical compositions of molecular gas at a scale from 1 kpc to 10 pc (Watanabe et al. 2014, 2016, 2017, Nishimura et al. 2017). In this study, we focus on effects of galaxy-scale gas dynamics on the chemical compositions of molecular gas in the barred spiral galaxy, because shocks are predicted in the bar by theoretical studies. Shock tracers such as SiO and CH<sub>3</sub>OH are reported in the bar of IC 342 (Meier & Turner 2005, Usero et al. 2006), and the results are discussed in relation to shocks in the bar. We have recently observed the bar, bar-end and spiral arm regions of NGC 3627 with ALMA (cycle-3) in the 3 mm band at a spatial resolution of  $\sim 100$  pc. In this observation, we find no significant enhancement of CH<sub>3</sub>OH in the bar. On the other hand, CH<sub>3</sub>OH abundance is enhanced from the spiral arm to the bar-end. In this region, we find a signature that two molecular clouds are thought to be colliding to each other in a position-velocity diagram. Therefore, the CH<sub>3</sub>OH would be evaporated from dust mantle by shock induced by the collision. Moreover, CCH and CN is found to be enhanced in the vicinity of star forming regions. These molecules are efficiently produced in the photodissociation region. From this observation, we thought that the molecular cloud scale chemical compositions reflect gas dynamics and environment in the galactic disk.

**References**

- [1] Meier & Turner 2005, ApJ, 618, 259
- [2] Nishimura et al. 2017, ApJ, 848, 17
- [3] Usero et al. 2006, A&A, 448, 457
- [4] Watanabe et al. 2014, ApJ, 788, 4
- [5] Watanabe et al. 2016, ApJ, 819, 144
- [6] Watanabe et al. 2017, ApJ, 845, 116

## A Search for Chemical Evolutional Indicators in High-Mass Star-Forming Regions

K. Taniguchi,<sup>1</sup> M. Saito,<sup>2,3</sup> T. K. Sridharan<sup>4</sup> and T. Minamidani<sup>3,5</sup>

<sup>1</sup>*Departments of Astronomy and Chemistry, University of Virginia, USA*

<sup>2</sup>*TMT-J Project, National Astronomical Observatory of Japan, Japan*

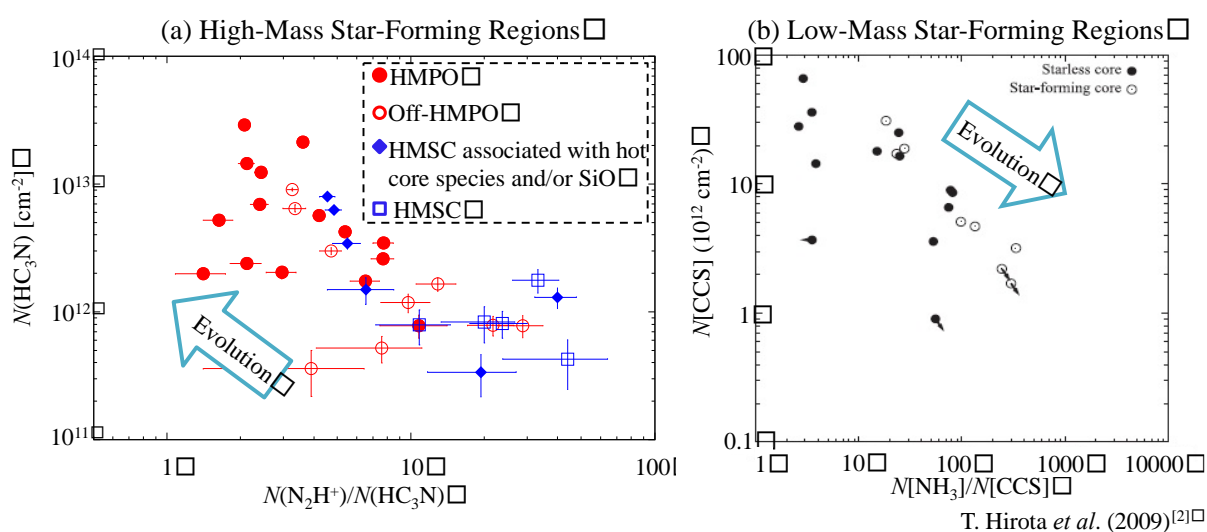
<sup>3</sup>*Department of Astronomical Science, SOKENDAI, Japan*

<sup>4</sup>*Harvard-Smithsonian Center for Astrophysics, USA*

<sup>5</sup>*Nobeyama Radio Observatory, National Astronomical Observatory of Japan, Japan*

Carbon-chain molecules have been known as good chemical evolutional indicators in low-mass star-forming regions (e.g., [1],[2]). They are abundant in young starless cores and decrease in star-forming cores. On the other hand, chemical evolutional indicators have not been clearly established in high-mass star-forming regions, nevertheless there were many attempts (e.g., [3]).

We have carried out survey observations of  $\text{HC}_3\text{N}$ ,  $\text{HC}_5\text{N}$ ,  $\text{CCS}$ , *cyclic*- $\text{C}_3\text{H}_2$ , and  $\text{N}_2\text{H}^+$  toward 17 high-mass starless cores (HMSCs)<sup>[4]</sup> and 28 high-mass protostellar objects (HMPOs)<sup>[5]</sup> using the Nobeyama 45-m radio telescope. The main purpose of this survey project is to find good chemical evolutional indicators, which enable us to find the very early stage of high-mass protostars containing the initial conditions of massive star formation. We investigated several molecular combinations and found that the  $N(\text{N}_2\text{H}^+)/N(\text{HC}_3\text{N})$  ratio is a good candidate for chemical evolutional indicators in high-mass star-forming regions. Figure 1 (a) shows the relationship between the column density ratio of  $N(\text{N}_2\text{H}^+)/N(\text{HC}_3\text{N})$  and the  $\text{HC}_3\text{N}$  column density in HMSCs and HMPOs. The ratio decreases from HMSC to HMPO. Surprisingly, this tendency is opposite to that in low-mass star-forming regions as shown Figure 1 (b). One possible explanation for the difference between high-mass and low-mass star-forming regions is the higher temperature in high-mass star-forming regions;  $\text{CH}_4$  and/or  $\text{C}_2\text{H}_2$  evaporated from grain mantles form  $\text{HC}_3\text{N}$ , whereas  $\text{N}_2\text{H}^+$  is destroyed by  $\text{CO}$  molecules liberated from dust.



T. Hirota *et al.* (2009)<sup>[2]</sup>

Figure 1: Chemical evolutional indicators in (a) high-mass star-forming regions and (b) low-mass star-forming regions. (a) Off-HMPO means that the center positions of the telescope were off from the 1.2 mm dust continuum emission peaks.

In addition, HMSCs, which were classified based on the mid-infrared ( $8.3 \mu\text{m}$ ) observations, associated with  $\text{CH}_3\text{OH}$ ,  $\text{CH}_3\text{CN}$ , and/or  $\text{SiO}$  are plotted between HMSCs and HMPOs. This suggests that we can find very-early-stage high-mass protostars embedded within dense cores, using the  $N(\text{N}_2\text{H}^+)/N(\text{HC}_3\text{N})$  ratio.

We compare the detection rates of carbon-chain molecules between HMPOs and low-mass protostars<sup>[6]</sup>. The detection rates of cyanopolyynes in HMPOs (93% for  $\text{HC}_3\text{N}$  and 50% for  $\text{HC}_5\text{N}$ <sup>[7]</sup>) are higher than those in low-mass protostars (75% and 31%, respectively), whereas CCS has been more frequently detected in low-mass protostars (88%) compared to HMPOs (46%). These results imply that carbon-chain chemistry around protostars is different between high-mass and low-mass protostars.

## References

- [1] T. Suzuki, S. Yamamoto, M. Ohishi et al., 1992, ApJ, 392, 551.
- [2] T. Hirota, M. Ohishi, and S. Yamamoto, 2009, ApJ, 699, 585.
- [3] T. Sakai, N. Sakai, K. Kamegai et al., 2008, ApJ, 678, 1049.
- [4] T. K. Sridharan, H. Beuther, M. Saito, F. Wyrowski, and P. Schilke, 2005, ApJ, 634, L57.
- [5] T. K. Sridharan, H. Beuther, P. Schilke, K. M. Menten, and F. Wyrowski, 2002, ApJ, 566, 931.
- [6] C. J. Law, K. I. Oberg, J. B. Bergner and D. Graninger, 2018, ApJ, 863, 88.
- [7] K. Taniguchi, M. Saito, T. K. Sridharan, and T. Minamidani, 2018, ApJ, 854, 133.



## Vibrational temperatures of HC<sub>3</sub>N in Sagittarius B2(N)

A. Ohsugi,<sup>1</sup> T. Oyama,<sup>1</sup> M. Araki,<sup>1</sup> S. Takano,<sup>2</sup> A. Ubagai,<sup>1</sup>  
Y. Minami,<sup>1</sup> H. Ozaki,<sup>3</sup> Y. Sumiyoshi,<sup>3</sup> N. Kuze,<sup>4</sup> and K. Tsukiyama<sup>1</sup>

<sup>1</sup> Department of Chemistry, Tokyo University of Science, Japan

<sup>2</sup> Department of Physics, College of Engineering, Nihon University, Japan

<sup>3</sup> Division of Pure and Applied Science, Graduate School of Science and Technology,  
Gunma University, Japan

<sup>4</sup> Department of Materials and Life Sciences, Sophia University, Japan

Sagittarius (Sgr) B2(N) having complicated cores is one of the most famous massive star-forming regions. Investigation of its core structures is a crucial step to understand the formation process of those regions. As a previous work, Belloche *et al.* observed the rotational lines of various vibrational states for HC<sub>3</sub>N in the 80-267 GHz region and divided them into four velocity components of 51, 63, 72 and 78 km/s [1]. The assumed rotational temperatures of 200-230 K could reproduce intensities of the observed lines in their analysis. In the present work, we observed the  $J = 12-11$  transitions of the vibrational states of  $v_6 = 1$ ,  $v_7 = 1$  and  $v_6 = v_7 = 1$  with Nobeyama 45 m radio telescope. The vibrational temperatures of HC<sub>3</sub>N in the 108.9-110.5 GHz region for individual velocity components were derived independently by using the rotation diagram of these components, as shown in Fig.1. The vibrational temperatures of 255-417 K obtained, as shown in Table 1, were higher than the assumed rotational temperatures in the previous work [1]. These higher temperatures are thought to be due to radiative pumping.

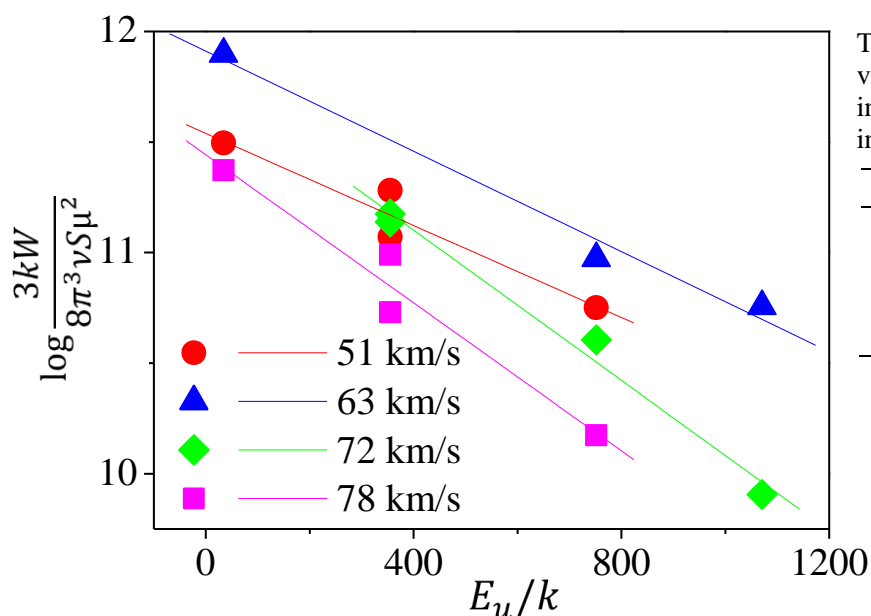


Table 1: The determined vibrational temperatures of individual components in Sgr B2(N).

$V$ (km/s)	$T_{\text{vib}}$ (K)
51	$417 \pm 83$
63	$383 \pm 48$
72	$255 \pm 22$
78	$259 \pm 40$

Figure 1: The rotation diagram of four velocity components for HC<sub>3</sub>N in Sgr B2(N).

### References

- [1] A. Belloche, H. S. P. Müller, K. M. Menten, P. Schilke & C. Comito, 2013, A&A 559, A47.

## Determination of the $^{13}\text{C}$ isotopic ratios of $\text{HC}_3\text{N}$ in the low-mass star-forming region L483

T. Oyama,<sup>1</sup> M. Araki,<sup>1</sup> Y. Minami,<sup>1</sup> H. Ozaki,<sup>2</sup> S. Takano,<sup>3</sup> A. Ohsugi,<sup>1</sup>  
A. Ubagai,<sup>1</sup> Y. Sumiyoshi,<sup>2</sup> N. Kuze<sup>4</sup> and K. Tsukiyama<sup>1</sup>

<sup>1</sup>*Department of Chemistry, Tokyo University of science, Japan*

<sup>2</sup>*Division of Pure and Applied Science, Graduate School of Science and Technology,  
Gunma University, Japan*

<sup>3</sup>*Department of Physics, College of Engineering, Nihon University, Japan*

<sup>4</sup>*Department of Materials and Life Sciences, Sophia University, Japan*

Linear carbon-chain molecules are characteristic species in interstellar medium. Studies of formation mechanisms for those molecules are crucial steps to reveal chemical evolutions in interstellar medium. Recently, warm carbon-chain chemistry (WCCC) has received attention as a formation mechanism of these molecules in low-mass star-forming regions [1]. L483 is one of these regions [2] and a WCCC candidate source [3]. Although several carbon-chain species were detected in L483 [4, 5], its  $^{13}\text{C}$  isotopomers were not observed. Isotopic ratios of carbon-chain molecules reflect their formation mechanism. In the present study, we have observed the  $J = 10-9$  transitions for  $\text{HC}_3\text{N}$  and its  $^{13}\text{C}$  isotopomers toward L483 with Nobeyama 45 m radio telescope in March 29-31, 2018. The beam width was 19.0-20.3", and the main beam efficiency was 0.54. The on-source integration time was 5 hours. Figure 1 shows the observed spectra of the  $J = 10-9$  transition for the  $^{13}\text{C}$  isotopomers. The column density and rotational temperature of  $\text{HC}_3\text{N}$  were determined to be  $1.9 \times 10^{13} \text{ cm}^{-2}$  and 10.9 K, respectively. In limited S/N ratios, the ratios of the  $^{13}\text{C}$  isotopomers were derived to be  $N[\text{H}^{13}\text{CCCN}] : N[\text{HC}^{13}\text{CCN}] : N[\text{HCC}^{13}\text{CN}] = 2.9(5) \times 10^{11} : 6.1(9) \times 10^{11} : 3.6(5) \times 10^{11} = 1 : 2.1(3) : 1.2(2)$  in 1-sigma error, where the rotational temperatures were fixed to that of  $\text{HC}_3\text{N}$ . The column densities of  $\text{H}^{13}\text{CCCN}$  and  $\text{HC}^{13}\text{CCN}$  are almost equivalent in various sources, which indicate that  $\text{HC}_3\text{N}$  is produced from a precursor with two equivalent carbon atoms as follows:  $\text{HCCH} + \text{CN} \rightarrow \text{HCCCN} + \text{H}$  [6]. On the other hand, the possible in-equivalent ratios in this work might be a result of a reaction with a precursor having two inequivalent carbon atoms as follows:  $\text{CCH} + \text{HNC} \rightarrow \text{HCCCN} + \text{H}$ . In future work, to improve the limited S/N ratios, we are planning to observe  $\text{HC}_3\text{N}$  by using Green bank telescope.

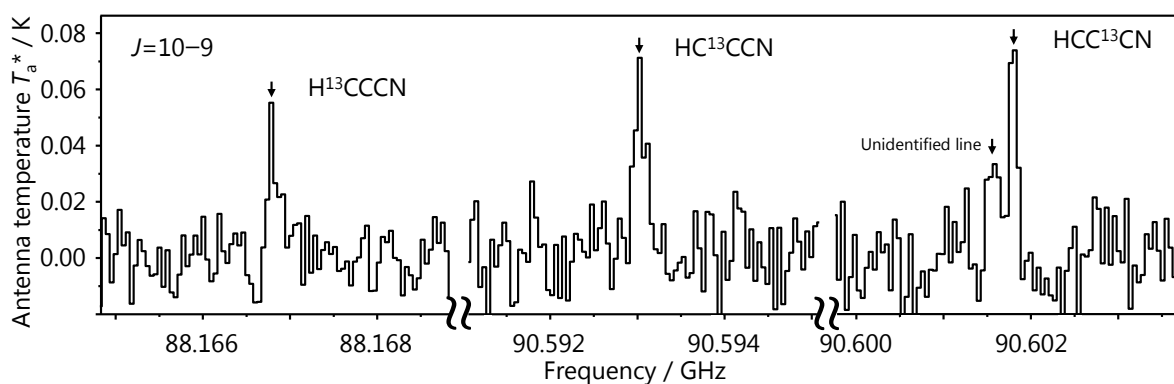


Figure 1: Observed lines of the  $^{13}\text{C}$  isotopomers of  $\text{HC}_3\text{N}$ .

### References

- [1] N. Sakai & S. Yamamoto, 2013, *Chem. Rev.* 113, 8981. [2] M. Agúndez *et al.*, 2008, *A&A* 478, L19. [3] T. Hirota, N. Sakai & S. Yamamoto, 2010, *ApJ* 720, 1370. [4] T. Hirota, M. Ohishi & S. Yamamoto, 2009, *ApJ* 699, 585. [5] Y. Oya *et al.*, 2017, *ApJ* 837, 174. [6] S. Takano *et al.*, 1998, *A&A*. 329, 1156.

## Analysis of the column densities of C<sub>4</sub>H using the revised dipole moment

T. Oyama,<sup>1</sup> H. Ozaki,<sup>2</sup> M. Araki,<sup>1</sup> Y. Sumiyoshi,<sup>2</sup> S. Takano,<sup>3</sup> A. Ohsugi,<sup>1</sup>  
A. Ubagai,<sup>1</sup> Y. Minami,<sup>1</sup> N. Kuze<sup>4</sup> and K. Tsukiyama<sup>1</sup>

<sup>1</sup>Department of Chemistry, Tokyo University of Science, Japan

<sup>2</sup>Division of Pure and Applied Science, Graduate School of Science and Technology,  
Gunma University, Japan

<sup>3</sup>Department of Physics, College of Engineering, Nihon University, Japan

<sup>4</sup>Department of Materials and Life Sciences, Sophia University, Japan

A series of C<sub>n</sub>H molecules are the simplest linear carbon chains. They are crucial for not only traces of young clouds but also benchmarks of chemical reaction network calculations. However, their abundances occasionally show anomaly. For example, observed column densities of C<sub>4</sub>H in various sources are one order of magnitude higher than theoretically estimated values. Herbst *et al.* suggested that these excesses of C<sub>4</sub>H come from the theoretically determined dipole moment of C<sub>4</sub>H [1]. Based on the simple theory, the <sup>2</sup>Σ<sup>+</sup> ground state of this molecule has the small dipole moment of 0.87 D [2]. However, the mixing of wavefunctions between the ground state and the low-lying <sup>2</sup>Π excited state having the large dipole moment of 4.4 D occurs, giving a higher dipole moment to the ground state. By using a higher dipole moment, a smaller column density is derived *via* observed line intensities. In the present study, we re-calculated the dipole moment of C<sub>4</sub>H by quantum chemical calculations including the mixing. The calculations were carried out by the multi-reference configuration interaction (MRCI) level of *ab initio* theory using the aug-cc-pVQZ basis set. The new dipole moment was derived to be 2.366 D, which is three times higher than the value of 0.87 D used so far. Reported lines of C<sub>4</sub>H were analyzed to revise column densities by using the new dipole moment. Revised column densities are one order of magnitude lower than those in the previous works, as listed in Table 1. The column densities of C<sub>n</sub>H molecules in IRC+10216 are described in Figure 1. Using the revised column density of C<sub>4</sub>H, abundances of the C<sub>n</sub>H series show a linearity. Trends of the other sources listed in Table 1 are also similar. These trends might be results of sequential formation of C<sub>n</sub>H molecules in the sources.

Table 1: The column densities of C<sub>4</sub>H.

Objects	Previous work		Re-analysis	
	<i>N</i> / cm <sup>-2</sup>	<i>T</i> / K	<i>N</i> / cm <sup>-2</sup>	<i>T</i> / K
L483 <sup>a</sup>	6.9E+13	10	1.4(2)E+13	7.9(8)
TMC-1 CP <sup>b</sup>	2.9E+14	6.7	4.2E+13	6.7
Barnard 1 <sup>a</sup>	2.5E+14	5	3.4E+13	5
L134N <sup>a</sup>	6.1E+13	5	8.3E+12	5
Horsehead <sup>a</sup>	3.0E+13	15	4.1E+12	15
Orion Bar <sup>a</sup>	2.5E+13	15	3.2E+12	15
L1527 <sup>c</sup>	1.0E+14	14.3	2.37(8)E+13	14.5(9)
Lupus-1A <sup>d</sup>	5.0E+14	7.3	6.7E+13	7.3
IRC+10216 <sup>e</sup>	3.0E+15	35	4.1E+14	35

<sup>a</sup> Ref. 3. <sup>b</sup> Ref. 4. <sup>c</sup> Ref. 5. <sup>d</sup> Ref. 6. <sup>e</sup> Ref. 7.

### References

[1] E. Herbst & Y. Osamura, 2008, ApJ 679, 1670.

[2] D. E. Woon, 1995, Chem. Phys. Lett. 244, 1995. [3] M. Agúndez *et al.*, 2008, A&A 478, L19. [4] N. Sakai *et al.*, 2008, ApJ 672, 371. [5] M. Araki *et al.*, 2012, ApJ 744, 163. [6] N. Sakai *et al.*, 2010, ApJL 718, L49. [7] J. Cernicharo, M. Guélin & C. Kahane, 2000, A&ASS 142, 181.

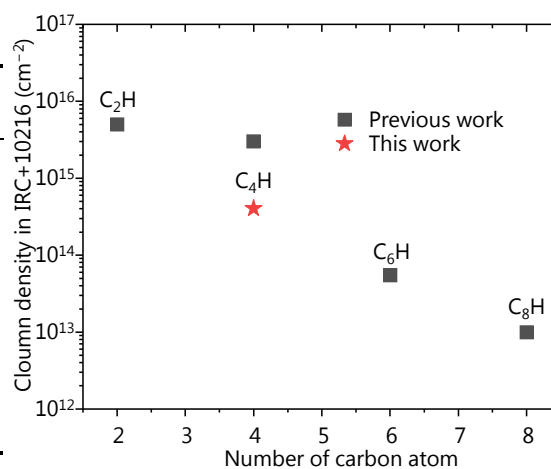


Figure 1: The column densities of C<sub>n</sub>H molecules in IRC+10216.

## The Molecular Abundance of the Circumnuclear Disk Surrounding an Active Galactic Nucleus in the Seyfert 2 Galaxy NGC 1068

T. Nakajima,<sup>1</sup> S. Takano,<sup>2</sup> T. Tosaki,<sup>3</sup> K. Kohno,<sup>4</sup> N. Harada,<sup>5</sup> E. Herbst,<sup>6</sup>  
Y. Tamura,<sup>7</sup> T. Izumi,<sup>8</sup> and A. Taniguchi<sup>7</sup>

<sup>1</sup> Institute for Space-Earth Environmental Research/Nagoya University, Japan

<sup>2</sup> Department of Physics, General Studies, College of Engineering/Nihon University, Japan

<sup>3</sup> Department of Geoscience/Joetsu University of Education, Japan

<sup>4</sup> Institute of Astronomy, Graduate School of Science/The University of Tokyo, Japan

<sup>5</sup> Academia Sinica Institute of Astronomy and Astrophysics, Taiwan

<sup>6</sup> Department of Chemistry/University of Virginia, USA

<sup>7</sup> Division of Particle and Astrophysical Science, Graduate School of Science/Nagoya University, Japan

<sup>8</sup> National Astronomical Observatory of Japan, Japan

The chemical properties have been expected to be powerful astrophysical tools for the study of galaxies, because the molecular line observations of different galaxies allow us to study the effects of these different physical properties/activities on the molecular medium. We carried out the line survey toward one of the nearest active galactic nucleus (AGN) Seyfert 2 galaxy NGC 1068 with the Nobeyama 45-m telescope [1][2][3]. Moreover, our ALMA cycle-0 (P.I., S. Takano; [4][5]), cycle-1 (P.I., S. Takano) and cycle-2 (P.I., T. Tosaki; [6] and T. Nakajima) observations in NGC 1068 were also carried out, and we have obtained the high-resolution images of molecular distribution in the circumnuclear disk (CND) (Fig.1) based on the line survey observation in the 3-mm band (Fig.2). In this presentation, we will report the results of this “imaging line survey observation” in NGC 1068 with ALMA.

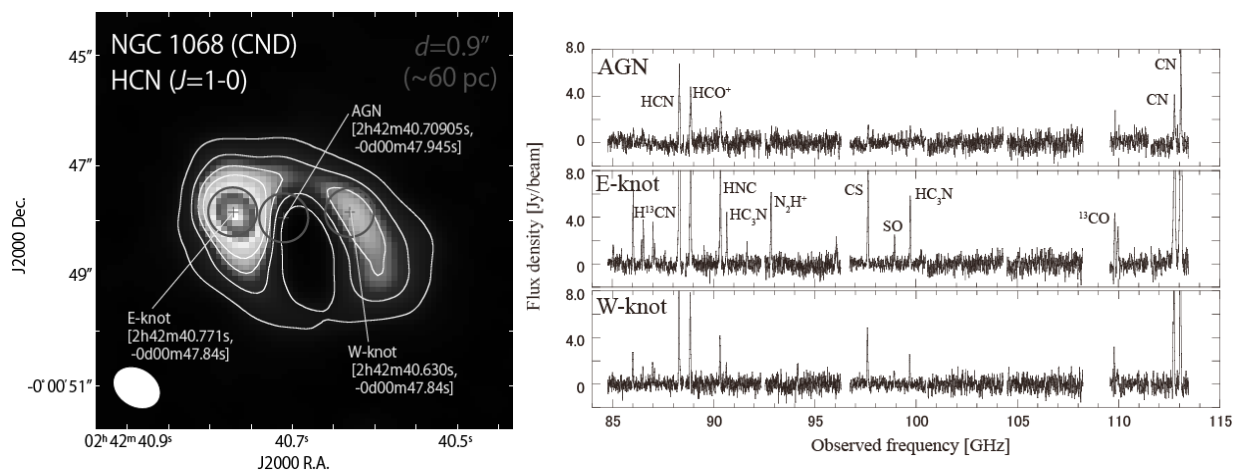


Figure 1(left): Beam sizes and positions of ALMA on the molecular distribution of HCN in the CND. Figure 2 (right): Line survey spectra toward the AGN position, E-knot, and W-knot in the 3-mm band.

### References

- [1] T. Nakajima, S. Takano, K. Kohno, & H. Inoue, 2011, ApJL 728, 38
- [2] T. Nakajima, S. Takano, K. Kohno, N. Harada, & E. Herbst, 2018, PASJ 70, 7
- [3] S. Takano, T. Nakajima, & K. Kohno, 2018, submitted to PASJ
- [4] S. Takano, T. Nakajima, K. Kohno, N. Harada, E. Herbst, et al., 2014, PASJ 66, 75
- [5] T. Nakajima, S. Takano, K. Kohno, N. Harada, E. Herbst, et al., 2015, PASJ 67, 8
- [6] T. Tosaki, K. Kohno, N. Harada, T. Tsukagoshi, K. Tanaka et al., 2017, PASJ 69, 18

## Chemical Change Associated with Envelope-Disk Transition in Massive Star Formation

Y. Zhang,<sup>1</sup> J. C. Tan,<sup>2,3</sup> N. Sakai,<sup>1</sup> K. Tanaka,<sup>4,5</sup> J. M. De Buizer<sup>6</sup>,  
M. Liu,<sup>3</sup> M. T. Beltrán,<sup>7</sup> D. Mardones,<sup>8</sup> and G. Garay<sup>8</sup>

<sup>1</sup>*RIKEN, Japan*

<sup>2</sup>*Chalmers University of Technology, Sweden*

<sup>3</sup>*University of Virginia, USA*

<sup>4</sup>*Osaka University, Japan*

<sup>5</sup>*NAOJ, Japan*

<sup>6</sup>*SOFIA-USRA, USA*

<sup>7</sup>*INAF, Italy*

<sup>8</sup>*Universidad de Chile, Chile*

We report ALMA observation of the massive protostellar source G339.88-1.26. We discovered a highly collimated SiO outflow extending from the 1.3 mm continuum peak, which connects to a slightly wider but still highly collimated CO outflow. Rotational features perpendicular to the outflow axis are detected in many molecular lines, especially in SiO, SO<sub>2</sub>, and H<sub>2</sub>S. The highest rotation velocity detected in SiO is up to  $\sim 25$  km s<sup>-1</sup>. On the other hand, in SO<sub>2</sub> and H<sub>2</sub>S, rotational features are seen within similar radii but only reach a velocity up to  $\sim 15$  km s<sup>-1</sup>. The peaks of the emissions of H<sub>2</sub>CO, CH<sub>3</sub>OH and other complex organic molecules (COMs) are offset from the central source. They appear to be dominant in the more extended region, probably tracing the outer envelope, as well as the outflow cavity walls. One possibility to understand these features is that the SO<sub>2</sub> and H<sub>2</sub>S are tracing the inner envelope and/or the centrifugal barrier, where the warm temperature or the accretion shock may have released them to the gas phase from the dust grain mantle. On the other hand, the accretion shock, internal shock, or the strong radiation field may also have destroyed some fraction of the dust grain to release SiO which will remain in gas phase in the innermost part of the disk and therefore reach higher rotational velocities. Such strong radiation or shocks also reduce COMs in the inner envelope. These results indicate that the picture of transition from a rotating/infalling envelope to a Keplerian disk through the centrifugal barrier accompanied by change of chemical composition may be also valid in at least this high-mass source.

### References

## Spatially resolved chemical compositions of a prestellar core

S. Ohashi,<sup>1</sup> and N. Sakai,<sup>1</sup>

<sup>1</sup>*RIKEN Cluster for pioneering research, Japan*

We present ALMA and ACA observations with Band 3 and 6 toward the prestellar core, TUKH122 located in the Orion A cloud. The Band 3 observations have been performed with 3 mm dust continuum,  $\text{N}_2\text{H}^+$  (1 - 0) and  $\text{CH}_3\text{OH}$  ( $J_K=2_K-1_K$ ) molecular lines using ALMA 12-m array and ACA. The Band 6 observations have been performed with 1.2 mm dust continuum,  $\text{N}_2\text{D}^+$  (3 - 2), and  $\text{DCO}^+$  (3 - 2) molecular lines using only ACA. From dust continuum observations, we identify several condensations aligned along the parent filamentary structure. The separation of these condensations is  $\sim 0.035$  pc, consistent with the thermal Jeans length at a density of  $4.4 \times 10^5 \text{ cm}^{-3}$ . This density is similar to the central part of the core. The spatial distributions of  $\text{N}_2\text{H}^+$ ,  $\text{N}_2\text{D}^+$ , and  $\text{DCO}^+$  are similar to that of dust continuum. However, an  $\text{N}_2\text{D}^+$  hole is recognized in the dust peak position, which may suggest that the ionization degree may become lower with increasing density. On the other hand, the  $\text{CH}_3\text{OH}$  emission shows a large shell-like distribution and surrounds these condensations, suggesting that the  $\text{CH}_3\text{OH}$  molecule formed on dust grains is released into the gas phase by nonthermal desorption such as photoevaporation caused by cosmic-ray-induced UV radiation.

### References

- [1] Ohashi, S., Sanhueza, P., Sakai, N., et al. 2018, ApJ, 856, 147